Check for updates

*ChemistrySelect*

ChemistrySelect
Chemistry Europe
European Chemical Societies Publishing

REVIEW

# Conductive Biomaterials in Skin Tissue Engineering: From Bioelectrical Cues to Wound Healing Applications

Zeynep SÜNBÜL | Cem Bülent ÜSTÜNDAĞ | Esma AHLATCIOĞLU ÖZEROL

Department of Bioengineering, Faculty of Chemical and Metallurgical Engineering, Yildiz Technical University, Istanbul, Turkey

**Correspondence:** Esma AHLATCIOĞLU ÖZEROL (eahlatci@yildiz.edu.tr)

**Received:** 2 April 2026 | **Revised:** 10 September 2026 | **Accepted:** 22 October 2026

**Keywords:** biomaterials | carbon materials | conductive polymers | metallic materials | skin tissue engineering

## ABSTRACT

Skin tissue engineering (STE) has emerged as a promising strategy for repairing tissue loss caused by skin diseases and injuries. STE integrates cells, scaffolds, and bioactive factors, individually or in combination, to promote tissue regeneration. Natural and synthetic biomaterials are widely used to fabricate scaffolds, which provide three-dimensional (3D) frameworks guiding cellular behaviors such as adhesion, proliferation, and migration. Successful regeneration requires scaffold materials with biocompatibility, suitable mechanical properties, and a controllable biodegradation rate. Wound healing is a complex and dynamic biological process in which endogenous electrical signals play important roles in cell migration, proliferation, and tissue remodeling. Accordingly, conductive materials have attracted increasing attention in skin tissue engineering because they can transmit electrical cues and exhibit antibacterial and angiogenesis-promoting effects. These materials are often incorporated into natural or synthetic polymeric matrices to address limitations such as poor mechanical stability, excessive water solubility, or inadequate biodegradability. This review provides a comprehensive overview of conductive materials used in skin tissue engineering, categorized into conductive polymers, carbon-based materials, and metallic materials. The mechanisms by which conductive materials influence wound healing and their current and potential applications in skin tissue engineering are also critically discussed.

## 1 | Introduction

The skin, as the largest organ of the human body, performs essential physiological functions, including the maintenance of fluid balance, thermoregulation, and protection against external physical, chemical, and biological insults. Acting as the primary interface between the body and the external environment, it is highly vulnerable to injury and infection, thereby necessitating effective and timely wound management strategies [1]. Wound healing is an intricate and dynamic biological process that involves a tightly regulated sequence of events, including hemostasis, inflammation, proliferation, and remodeling. This process is governed by a complex interplay of biochemical signals, as well as mechanical and electrical cues within the wound microenvironment [2]. Although the skin possesses an inherent capacity for self-regeneration mediated by resident stem and progenitor cells [1], this capability is often inadequate in cases of extensive burns, severe trauma, and chronic non-healing wounds, which remain a significant clinical challenge [3]. Traditional wound care approaches, such as gauze and bandage-based dressings, primarily function as passive protective barriers that prevent external contamination and maintain a basic level of moisture. However, these conventional systems lack the ability to actively modulate the wound microenvironment or promote cellular activities essential for effective tissue regeneration [4]. In response to these limitations, skin tissue engineering (STE) has emerged as a promising and rapidly advancing field aimed at developing functional biomimetic systems for enhanced

All rights reserved, including rights for text and data mining and training of artificial intelligence technologies or similar technologies.
© 2026 Wiley-VCH GmbH

wound healing. STE strategies typically involve the integration of cells, biomaterials, and bioactive molecules-either individually or synergistically-to facilitate tissue regeneration and restore skin functionality. Within this framework, both natural and synthetic biomaterials, such as collagen, chitosan, and polyvinyl alcohol, have been extensively explored for the fabrication of scaffolds and advanced wound dressings. These scaffolds serve as three-dimensional architectures that not only provide structural support but also deliver biochemical and biophysical cues that regulate key cellular processes, including adhesion, proliferation, migration, and differentiation, thereby promoting tissue repair and regeneration [5, 6].

Recent studies have highlighted the critical role of endogenous electrical fields generated at wound sites in directing cell migration, particularly that of dermal fibroblasts, and in accelerating the overall healing process [2]. This phenomenon has led to increasing interest in the development of electroactive biomaterials capable of mimicking the native bioelectrical environment of the skin. In this context, conductive materials have gained considerable attention due to their ability to transmit electrical stimuli, enhance cell–material interactions, and promote tissue regeneration. Furthermore, many conductive materials exhibit intrinsic antibacterial properties, which are highly advantageous for preventing infection and improving healing outcomes in compromised wound environments [7]. Conductive materials used in skin tissue engineering can be broadly classified into three categories: (i) conductive polymers, such as polythiophene, polyaniline (PANI), polypyrrole (PPy), and poly(3,4-ethylenedioxythiophene) (PEDOT); (ii) carbon-based materials, including graphene, graphene oxide, reduced graphene oxide, and fullerene; and (iii) metallic materials, such as gold, silver, and copper. These materials are commonly integrated with natural or synthetic polymeric matrices to fabricate electroactive scaffolds and wound dressings with enhanced biological performance.

This review provides a comprehensive overview of recent advances in the application of conductive materials for wound healing and skin tissue engineering. The conductive materials are systematically categorized into polymers, carbon-based materials, and metallic materials, and recent studies are critically discussed with respect to fabrication methods, biological performance, and therapeutic outcomes.

## 2 | Skin Tissue Engineering

The skin, as the largest organ of the human body, functions as a critical barrier between the internal environment and external surroundings, providing protection against physical, chemical, and biological threats [8]. Structurally, the skin is composed of three distinct layers. The outermost layer, the epidermis, serves as the primary protective barrier against external damage. Beneath this lies the dermis, which provides structural support and plays a central role in wound repair through its rich composition of extracellular matrix (ECM) and cellular components. The innermost layer, the hypodermis, consists mainly of adipose tissue and contributes to thermoregulation, energy storage, and mechanical cushioning [9]. Despite its essential functions, the skin is highly susceptible to damage caused by injuries such as wounds, burns, and chronic conditions, including diabetes mellitus. Skin loss not only impairs physiological functions but also significantly diminishes the patient's quality of life [10]. Wound healing is a complex and well-orchestrated biological process that proceeds through four overlapping stages: hemostasis, inflammation, proliferation, and remodeling. This process is regulated by various biological factors, including biochemical signals, as well as mechanical and electrical cues present within the wound microenvironment [2, 11]. Conventional wound dressings are generally passive and inert, serving primarily as protective barriers against microbial contamination and external damage, while offering limited support for active tissue regeneration. Commonly used materials, such as gauze and bandages, provide basic wound coverage but exhibit minimal capacity to promote cellular activities involved in healing [4]. In contrast, skin tissue engineering approaches focus on the development of advanced biomaterial-based scaffolds designed to actively facilitate wound healing. These scaffolds may be used alone or in combination with cells and growth factors to enhance regenerative outcomes. An ideal scaffold should provide adequate mechanical support, promote cell adhesion and proliferation, and exhibit controlled biodegradability, allowing it to degrade and be safely resorbed following tissue regeneration [10].

### 2.1 | Cell Sources in Skin Tissue Engineering

Cells constitute a key component of STE applications, as they are directly involved in tissue regeneration and functional restoration. Various cell types have been utilized in STE, including endothelial cells, dermal fibroblasts, keratinocytes, pericytes, human endometrial stem cells, adipose-derived stem cells, umbilical cord-derived mesenchymal stem cells, and bone marrow-derived stem cells. Each cell type contributes to different aspects of the healing process, such as angiogenesis, ECM production, and immunomodulation. However, among these, keratinocytes and dermal fibroblasts are the most widely used cell types in skin tissue engineering due to their essential roles in epidermal regeneration and dermal matrix formation, respectively [12].

#### 2.1.1 | Keratinocytes

Keratinocytes constitute the predominant cell population within the epidermis and play a central role in maintaining skin homeostasis. These cells are critically involved in the formation and maintenance of the epidermal barrier through the synthesis and accumulation of keratin proteins, which provide structural integrity and mechanical resilience to the skin. In addition to their structural function, keratinocytes contribute significantly to tissue regeneration processes by regulating cellular proliferation, differentiation, and migration during epidermal renewal [13]. Beyond their role as a physical barrier, keratinocytes actively participate in cutaneous immune responses, functioning as key regulators of skin immunity. Upon injury or exposure to external stimuli, keratinocytes secrete a diverse array of cytokines, chemokines, and antimicrobial peptides, thereby orchestrating the activation and recruitment of various immune cells, including Langerhans cells, macrophages, and T lymphocytes. This immunomodulatory activity not only facilitates the initial inflammatory response but also supports subsequent stages of wound healing by promoting tissue repair and preventing



23656549, 2026, 45, Downloaded from https://chemistry-europe.onlinelibrary.wiley.com/doi/10.1002/slct.75081 by Esma AHLATCIOLU ÖZEROL - Yildiz Technical University , Wiley Online Library on [25/11/2026]. See the Terms and Conditions (https://onlinelibrary.wiley.com/terms-and-conditions) on Wiley Online Library for rules of use; OA articles are governed by the applicable Creative Commons License

infection. Therefore, keratinocytes are increasingly recognized as multifunctional cells that integrate structural, regenerative, and immunological functions, making them a critical component in the design and development of advanced skin tissue engineering strategies [14].

#### 2.1.2 | Fibroblasts

Fibroblasts are mesenchymal cells that play a pivotal role in tissue homeostasis, repair, and regeneration. They are primarily responsible for the formation and maintenance of soft connective tissues through the synthesis, deposition, and remodeling of ECM components, including collagen, elastin, and glycosaminoglycans. Beyond their structural function, fibroblasts actively regulate the cellular microenvironment by secreting a wide range of signaling molecules, such as cytokines and growth factors. Among these, epidermal growth factor (EGF) is particularly important, as it promotes keratinocyte proliferation and migration during the wound healing process.

Furthermore, fibroblasts exhibit dynamic interactions with various cell types, enabling them to coordinate complex biological processes involved in tissue repair. Their crosstalk with immune cells, endothelial cells, and stem cells contributes to the regulation of inflammation, angiogenesis, and cellular differentiation. Notably, fibroblasts can modulate stem cell behavior through paracrine signaling, thereby enhancing regenerative outcomes. Due to these multifunctional properties, fibroblasts are considered key mediators in wound healing and are extensively utilized in skin tissue engineering applications [15, 16].

### 2.2 | Skin Tissue Scaffold Production Methods

Scaffolds are a fundamental component of STE applications, as they provide a three-dimensional framework that supports cell attachment, proliferation, and differentiation, thereby facilitating tissue regeneration. They play a crucial role in promoting the repair of damaged tissues by enhancing essential cellular functions and mimicking the native ECM environment. An ideal scaffold should exhibit key properties such as biocompatibility, adequate mechanical strength, controlled biodegradability, and a well-defined porous architecture. In particular, pore size, pore distribution, and interconnectivity are critical parameters that significantly influence cell behavior, including migration, nutrient diffusion, and waste removal. Therefore, optimizing these structural features is essential for achieving effective tissue regeneration. The fabrication method has a direct impact on the morphological and functional properties of scaffolds, especially their pore characteristics. Consequently, selecting an appropriate production technique is of great importance. Commonly employed fabrication methods for skin tissue engineering scaffolds include electrospinning, 3D printing, freeze-drying, solvent casting, gas foaming, four-dimensional (4D), and microfluid-based printing each offering distinct advantages in terms of structural control and application-specific design [17]. The main fabrication strategies used for STE scaffolds, together with their structural characteristics, advantages, limitations, and effects on biological performance, are summarized in Table 1.

#### 2.2.1 | Electrospinning

Electrospinning is a widely employed technique in scaffold fabrication due to the ability of nanofibrous structures to closely resemble the architecture of native human tissue. In this technique, a polymer solution is subjected to a high-voltage electric field, resulting in the formation of continuous nanofibers that are subsequently deposited onto a grounded collector. The electrospinning process is governed by three primary categories of parameters: solution, process, and environmental factors. Solution parameters include viscosity, molecular weight, elasticity, and electrical conductivity. Notably, an increase in electrical conductivity generally leads to the production of finer nanofibers.

Process parameters encompass the applied voltage, the distance between the spinneret and the collector, and the flow rate of the polymer solution. In addition, environmental conditions such as ambient temperature and relative humidity play a critical role in determining fiber morphology and structural uniformity. Electrospun nanofibers are characterized by high mechanical strength, a large specific surface area, and an interconnected porous network. These distinctive features contribute significantly to enhanced cell adhesion, proliferation, and nutrient transport, thereby improving wound healing outcomes in skin tissue engineering applications [18, 19].

#### 2.2.2 | 3D Printing

3D printing has emerged as a highly promising and versatile technique in tissue engineering, and it is widely preferred for the fabrication of tissue scaffolds. This approach enables the production of complex and highly organized structures through a layer-by-layer deposition process, allowing precise control over scaffold architecture, including pore size, geometry, and interconnectivity. Such control is essential for replicating the native tissue microenvironment and enhancing cellular responses. Furthermore, advanced 3D printing technologies allow the incorporation of sensitive biological components, such as living cells and bioactive molecules, enabling the development of bio-functional constructs. A broad range of 3D printing techniques has been employed in biomedical applications, including fused deposition modeling (FDM), stereolithography apparatus (SLA), selective laser sintering (SLS), 3D plotting (bioprinting), inkjet printing, and laminated object manufacturing (LOM). Each technique offers distinct advantages in terms of resolution, material compatibility, and processing conditions. Beyond STE, 3D printing has been successfully utilized for the fabrication of scaffolds and constructs for various tissues and organs, including bone, cartilage, heart valves, and liver, highlighting its significant potential in regenerative medicine [20].

#### 2.2.3 | Freeze-Drying

Freeze-drying, also known as lyophilization, is a widely utilized fabrication technique for the production of 3D, porous, sheet-like tissue scaffolds. This method involves the freezing of a polymer solution, followed by the sublimation of ice under reduced pressure, resulting in a highly porous structure. The



23656549, 2026, 45, Downloaded from https://chemistry-europe.onlinelibrary.wiley.com/doi/10.1002/slct.75081 by Esma AHLATCIOLU ÖZEROL - Yildiz Technical University , Wiley Online Library on [25/11/2026]. See the Terms and Conditions (https://onlinelibrary.wiley.com/terms-and-conditions) on Wiley Online Library for rules of use; OA articles are governed by the applicable Creative Commons License

**TABLE 1** | Comparison of fabrication methods used for skin tissue engineering scaffolds.

| Fabrication Method | Structural characteristics | Advantages | Limitations | Effect on biological performance | Reference |
|---|---|---|---|---|---|
| Electrospinning | Nanofibers | High surface area, tunable fiber diameter and porosity, suitable for drug/NP incorporation, ECM-mimicking structure | Limited control over 3D thickness, solvent toxicity, relatively low mechanical strength in some systems, fiber uniformity can be challenging | Promotes cell adhesion, proliferation and migration, facilitates gas exchange and exudate management, enables controlled delivery of bioactive agents | [34, 35] |
| Freeze-drying | Sponge like structures | High porosity, suitable for hydrophilic/natural polymers, can incorporate bioactive molecules, suitable for 3D scaffolds | Time- and energy-intensive, shrinkage, limited control over pore uniformity, relatively weak mechanical properties | Facilitates cell infiltration, nutrient diffusion and tissue ingrowth, high porosity can support cell attachment and proliferation | [36, 37] |
| 3D printing | Controlled 3D architecture | Specific structures, precise control of pore size and geometry, multi-material fabrication, incorporation of cells/bioactive agents | Relatively high cost, limited printable materials, printing-induced cell stress, optimization of bioink rheology required | Enables controlled cell distribution and tissue-specific architecture, can enhance cell organization, proliferation and tissue regeneration, facilitates personalized wound dressings | [38, 39] |
| Solvent casting | 2D films/membranes | Simple, low-cost, easy processing, suitable for polymer blends and drug incorporation, large-area films can be produced | Limited control over 3D architecture and porosity, residual solvent risk, slow solvent evaporation, poor scalability for complex structures | Provides a protective and moist wound environment, can support cell viability when biocompatible polymers/solvents are used, enables local drug delivery | [36, 40] |
| Gas foaming | 3D foam | Solvent-free or low-solvent processing, high porosity, relatively simple and inexpensive | Poor pore interconnectivity, limited control of pore size, relatively weak mechanical properties, nonporous outer surface may form | High porosity can facilitate nutrient/gas diffusion and cell infiltration; however, poor pore interconnectivity may restrict cellular penetration | [40, 41] |
| 4D printing | Dynamic, stimulus-responsive 3D structures capable of changing shape/function over time | Time-dependent and programmable structures, stimuli-responsive behavior, personalized and adaptive systems, controlled drug release | Complex material design, limited long-term stability, relatively low technological maturity, difficult clinical translation | Enables adaptive interaction with the wound environment, can provide on-demand drug/antimicrobial release, may enhance tissue integration and regeneration | [42], [26] |
| Microfluidic—Based Fabrication | Micro-/nano-scale fibers, particles, droplets or hydrogel structures, highly uniform architecture | Excellent control over size, morphology and composition, low reagent consumption, reproducible fabrication, enables complex multifunctional systems | Complex device design, relatively low throughput, channel clogging, scale-up and standardization challenges | Enables controlled drug delivery, tunable release, cell encapsulation and localized therapeutic effects, can support angiogenesis, immune modulation and tissue integration | [43, 44] |

pore architecture of the scaffold is largely determined by factors such as the freezing rate and the geometry of the mold, allowing for a certain degree of structural control. In addition to scaffold fabrication, freeze-drying is also employed in the encapsulation of bioactive agents, such as nanoparticles, due to its ability to preserve structural integrity and bioactivity. However, despite these advantages, the technique has certain limitations. It is compatible with a relatively limited range of polymers and often requires the use of organic solvents, which may be toxic and necessitate careful removal to ensure biocompatibility [21–23].



23656549, 2026, 45, Downloaded from https://chemistry-europe.onlinelibrary.wiley.com/doi/10.1002/slct.75081 by Esma AHLATCIOLU ÖZEROL - Yildiz Technical University , Wiley Online Library on [25/11/2026]. See the Terms and Conditions (https://onlinelibrary.wiley.com/terms-and-conditions) on Wiley Online Library for rules of use; OA articles are governed by the applicable Creative Commons License

### 2.2.4 | Solvent Casting

Solvent casting is a simple and widely employed fabrication technique in both tissue engineering and food packaging applications. In this method, the polymer is first dissolved in an appropriate solvent, and the resulting solution is cast into a mold with the desired geometry, followed by solvent evaporation to form a solid structure. To introduce porosity, solvent casting is often combined with the salt leaching technique, enabling the fabrication of thin films with a porous architecture. During the casting process, water-soluble porogens such as inorganic salts (e.g., NaCl) or organic particles (e.g., sucrose) are incorporated into the polymer solution. After solidification, these particles are leached out, leaving behind pores within the scaffold structure. However, a key limitation of this method is that the resulting pores may exhibit poor interconnectivity, which can hinder cell migration, nutrient diffusion, and overall tissue integration. Therefore, while solvent casting is advantageous due to its simplicity and cost-effectiveness, further modifications are often required to improve pore connectivity and biological performance [21].

### 2.2.5 | Gas Foaming

Gas foaming is a widely used technique for the fabrication of highly porous scaffolds in tissue engineering applications. In this method, gases acting as pore-forming agents are incorporated into the polymer matrix, and pore generation is achieved through gas expansion, typically induced by increasing temperature or reducing pressure. This process results in scaffolds with high porosity and relatively uniform pore distribution, which are advantageous for facilitating nutrient transport and tissue ingrowth. Carbon dioxide ($CO_2$) is the most commonly utilized porogen in gas foaming due to its inert, nontoxic, and non-flammable nature, making it suitable for biomedical applications. In addition to $CO_2$, chemical foaming agents such as hydrogen peroxide ($H_2O_2$) can also be employed, where gas formation occurs through decomposition reactions. Despite its advantages, gas foaming may present limitations in controlling pore interconnectivity and achieving precise structural architecture, which are critical factors for effective cell migration and tissue regeneration [24, 25].

### 2.2.6 | Emerging Manufacturing Paradigms

Recent advances in tissue engineering have driven the development of emerging manufacturing paradigms that enable the fabrication of conductive biomaterials with enhanced structural precision, functional complexity, and stimuli-responsive behavior. Unlike conventional fabrication techniques, these advanced approaches provide greater control over scaffold architecture, material distribution, and dynamic performance, thereby facilitating the design of biomimetic wound dressings that more closely replicate the native skin microenvironment. Among these technologies, microfluidic-based fabrication and four-dimensional (4D) printing have attracted increasing attention due to their ability to precisely manipulate material composition and create adaptive constructs capable of responding to environmental stimuli. Although their application in conductive skin tissue engineering is still in its early stages, these innovative manufacturing strategies are expected to play a pivotal role in the development of next-generation smart wound dressings with improved therapeutic efficacy [26].

**2.2.6.1 | Microfluidic-Based Fabrication.** Microfluidic-based production has emerged as a powerful fabrication strategy for developing advanced biomaterials with precise control over size, morphology, composition, and functionality. By manipulating minute volumes of fluids within microscale channels, microfluidic systems enable highly reproducible synthesis under well-defined conditions while minimizing reagent consumption and production variability. Compared with conventional fabrication methods, microfluidics offers superior control over mass transfer, mixing efficiency, and reaction kinetics, making it particularly suitable for the production of complex biomaterials for biomedical applications [27].

In tissue engineering and regenerative medicine, microfluidic technology has been widely employed for the fabrication of nanoparticles, microspheres, hydrogel microgels, fibers, and cell-laden bioinks with uniform physicochemical properties. The precise control over material architecture facilitates the development of scaffolds that closely mimic the native ECM, thereby enhancing cell attachment, proliferation, differentiation, and tissue regeneration. Moreover, microfluidic systems enable the encapsulation of therapeutic agents, growth factors, and living cells with high efficiency, allowing the fabrication of multifunctional drug delivery systems and bioactive scaffolds [28].

Microfluidic platforms also provide significant opportunities for the preparation of conductive biomaterials by enabling precise control over material composition, fiber dimensions, and microscale architecture. For example, PEDOT:PSS conductive microfibers have been fabricated using microfluidic spinning, with their diameter precisely regulated by controlling the flow rates of the spinning and sheath fluids [29]. Similarly, microfluidic systems have been used to integrate conductive materials such as graphene-based nanomaterials into biomaterial constructs, demonstrating their potential for electrically active tissue engineering. These characteristics are particularly promising for engineering electrically active tissues, including neural and cardiac tissues, where conductive biomaterials can provide electrical cues relevant to tissue regeneration [29, 30].

Despite these advantages, the large-scale manufacturing of microfluidic-produced biomaterials remains challenging due to relatively low production throughput, device fabrication complexity, and the need for specialized equipment. Nevertheless, recent developments in parallelized microfluidic platforms, automated manufacturing systems, and integrated bio-fabrication technologies are significantly improving production capacity and scalability. Consequently, microfluidic-based production is expected to play an increasingly important role in the fabrication of personalized, multifunctional, and conductive biomaterials for next-generation biomedical applications [27].

**2.2.6.2 | Four-Dimensional (4D) Printing.** 4D printing is an emerging manufacturing technology that extends conventional 3D printing by incorporating time as the fourth dimension. Unlike static 3D-printed constructs, 4D-printed structures are



23656549, 2026, 45, Downloaded from https://chemistry-europe.onlinelibrary.wiley.com/doi/10.1002/slct.75081 by Esma AHLATCIOLU ÖZEROL - Yildiz Technical University , Wiley Online Library on [25/11/2026]. See the Terms and Conditions (https://onlinelibrary.wiley.com/terms-and-conditions) on Wiley Online Library for rules of use; OA articles are governed by the applicable Creative Commons License

fabricated from stimuli-responsive materials capable of undergoing predetermined changes in shape, mechanical properties, or functionality when exposed to external stimuli such as temperature, pH, moisture, light, electric or magnetic fields, and biochemical signals. This dynamic behavior enables the fabrication of adaptive biomedical devices that can respond to physiological conditions in real time [31].

In biomedical engineering, 4D printing has attracted considerable attention for the development of next-generation tissue engineering scaffolds, drug delivery systems, biosensors, and wound dressings. Smart biomaterials, including shape–memory polymers, hydrogels, and conductive composites, can be programmed to alter their architecture or release therapeutic agents in response to the local microenvironment. For example, 4D-printed scaffolds can dynamically adjust their morphology to better mimic native ECM remodeling, thereby promoting cell adhesion, proliferation, and tissue regeneration. Similarly, stimuli-responsive wound dressings can modulate drug release, maintain an optimal wound environment, and conform to irregular wound geometries, improving healing outcomes [32].

The integration of conductive biomaterials into 4D printing further expands its biomedical potential. Electrically conductive polymers and carbon-based nanomaterials, such as graphene and reduced graphene oxide (rGO), enable the fabrication of smart constructs that deliver electrical cues and exhibit stimulus-responsive behavior. These multifunctional systems are particularly promising for electrically active tissues, including skin, nerve, and cardiac tissues, where electrical stimulation has been shown to regulate cell migration, angiogenesis, collagen deposition, and tissue remodeling [31].

Despite its significant potential, several challenges remain before the widespread clinical translation of 4D printing. In particular, material scalability, precise control of stimulus-induced shape transformation, mechanical stability, and stringent biocompatibility requirements remain important barriers to clinical application. In addition, the development of multifunctional and composite stimuli-responsive biomaterials with improved structural fidelity and physiological compatibility is needed to better reproduce the dynamic biomechanics of native tissues. The integration of biosensing functionalities may further enhance the ability of 4D-printed constructs to dynamically interact with and respond to the biological environment. Continued advances in smart biomaterials, multi-material bio-fabrication, and computational design are therefore expected to facilitate the development of adaptive and biomimetic constructs with greater translational potential. Consequently, 4D printing represents a promising platform for the fabrication of multifunctional and physiologically responsive biomaterials for regenerative medicine [33].

## 2.3 | Signaling Factors for Skin Tissue Engineering

Signaling factors constitute an important component of STE, playing a critical role in regulating cellular activities and enhancing tissue regeneration. Although their use is not mandatory in all applications, the incorporation of signaling molecules can significantly accelerate wound healing by promoting cell migration, proliferation, and differentiation. These factors are generally classified into biochemical, physicochemical, and physical categories. Among these, biochemical signaling factors-particularly growth factors-are of primary importance. Growth factors are biologically active polypeptides that interact with specific cell surface receptors, triggering intracellular signaling pathways that regulate key cellular processes. In STE, commonly utilized growth factors include epidermal growth factor (EGF), basic fibroblast growth factor (bFGF), transforming growth factor-beta (TGF-$\beta$3), platelet-derived growth factor (PDGF), and vascular endothelial growth factor (VEGF). EGF and VEGF are among the most extensively studied and applied growth factors in this field. EGF is known to enhance keratinocyte proliferation, migration, and re-epithelialization, thereby contributing to the restoration of the epidermal layer. In contrast, VEGF plays a crucial role in angiogenesis by promoting neovascularization, improving blood supply to the tissue, and supporting collagen deposition. Together, these growth factors significantly contribute to the acceleration and improvement of the wound healing process [12, 16].

## 2.4 | Materials for Skin Tissue Scaffolds Production

### 2.4.1 | Natural Materials

Natural polymers are widely preferred in skin tissue engineering due to their excellent biocompatibility and biodegradability. However, their relatively poor mechanical strength and rapid degradation often limit their direct use in biomedical applications. Therefore, natural polymers are frequently combined with synthetic polymers to enhance their mechanical properties, structural stability, and overall performance in tissue engineering scaffolds. Furthermore, the incorporation of conductive materials into these polymeric systems has emerged as an effective strategy to introduce additional properties, such as electrical conductivity, antibacterial activity, and improved cellular responses [45].

*Collagen* is a major component of the ECM and the most abundant structural protein in the human body [46]. Collagen plays a critical role in the wound healing process by supporting cell attachment, promoting fibroblast proliferation, and facilitating the formation of new ECM during tissue regeneration. Therefore, collagen-based biomaterials are widely used in wound dressing applications. Owing to its excellent biocompatibility, biodegradability, flexibility, and good moisture retention capacity, collagen is frequently employed in STE as a scaffold material that mimics the natural microenvironment of skin tissue [47]. Recently, collagen has also been combined with conductive nanomaterials, such as graphene, carbon nanotubes, and metallic nanoparticles, to develop electrically conductive scaffolds for advanced STE applications.

*Gelatin* is a natural polymer obtained through the partial hydrolysis of collagen and retains several bioactive sequences present in native collagen. Among these, the RGD (arginine–glycine–aspartic acid) cell-binding motif plays a crucial role in mediating cell–material interactions. The RGD sequence promotes cell adhesion and spreading by binding to integrin receptors located



23656549, 2026, 45, Downloaded from https://chemistry-europe.onlinelibrary.wiley.com/doi/10.1002/slct.75081 by Esma AHLATCIOLU ÖZEROL - Yildiz Technical University , Wiley Online Library on [25/11/2026]. See the Terms and Conditions (https://onlinelibrary.wiley.com/terms-and-conditions) on Wiley Online Library for rules of use; OA articles are governed by the applicable Creative Commons License

on the cell membrane, thereby facilitating the formation of focal adhesion complexes and cytoskeletal organization. This interaction significantly improves cellular attachment, proliferation, and differentiation on scaffold surfaces. Due to these biological properties, gelatin has been widely employed as a biomaterial in tissue engineering applications. It exhibits excellent biocompatibility and biodegradability, and its hydrophilic nature enables efficient nutrient and oxygen diffusion within 3D scaffold structures. In addition, gelatin can be easily processed into various forms such as hydrogels, nanofibers, films, and porous scaffolds, making it a versatile material for regenerative medicine [48, 49].

In the context of conductive STE, gelatin is frequently combined with conductive materials such as conductive polymers, carbon-based nanomaterials, or metallic nanoparticles to improve electrical signaling within the engineered tissue. When integrated with conductive components, gelatin-based scaffolds can provide both biological cues for cell adhesion and electrical cues that enhance cellular communication and tissue regeneration. Therefore, gelatin-based conductive scaffolds have attracted significant attention for applications in wound healing, skin regeneration, and bioelectronic skin interfaces, as they combine favorable biological properties with the ability to support electrical stimulation and signal transmission within engineered tissues [50].

*Hyaluronic acid (HA)* is a naturally occurring polysaccharide and a major component of the ECM, particularly in skin tissue. In skin tissue engineering, HA is widely utilized due to its remarkable biocompatibility, biodegradability, and ability to mimic the native ECM microenvironment. It promotes collagen synthesis, maintains a moist wound environment, and provides structural support for damaged tissues, thereby accelerating dermal regeneration and tissue remodeling. Furthermore, HA can regulate cell proliferation, migration, and angiogenesis during the wound healing process, which makes it highly beneficial for regenerative applications [51, 52]. Despite these advantages, HA alone exhibits relatively poor mechanical strength and structural stability, which may limit its use as a standalone scaffold material. To address this limitation, HA is frequently combined with other natural or synthetic polymers such as chitosan, gelatin, or polycaprolactone to improve its mechanical integrity and stability. In recent years, HA has also been incorporated with conductive materials, including conductive polymers, carbon-based nanomaterials, and metallic nanoparticles, to develop electrically active scaffolds. These hybrid systems aim to enhance cell–material interactions and facilitate electrical signal transmission, which is particularly important in conductive STE and advanced wound healing applications [53].

*Chitosan* is a linear, cationic polysaccharide derived from the partial deacetylation of chitin, which is commonly obtained from crustacean shells. Due to its structural similarity to glycosaminoglycans found in the ECM, chitosan has gained significant attention in tissue engineering applications, particularly in skin regeneration. It exhibits a range of beneficial biological properties, including antimicrobial, hemostatic, biodegradable, biocompatible, and nontoxic characteristics. These properties make chitosan highly suitable for wound healing applications, as it can prevent microbial infections while simultaneously supporting tissue regeneration. Chitosan-based materials can be fabricated through various techniques such as electrospinning, solvent casting, freeze-drying, and hydrogel formation to create porous scaffolds that mimic the natural ECM architecture. In addition, its high porosity and excellent water retention capacity help maintain a moist wound environment, which is critical for efficient healing. The positively charged amino groups of chitosan also promote interactions with negatively charged biological molecules, thereby enhancing cell adhesion and proliferation [54, 55].

Despite these advantages, pure chitosan exhibits limited mechanical strength and poor electrical conductivity, which restrict its application in electrically active tissue engineering. Therefore, chitosan is rarely used alone in advanced skin tissue engineering but is more commonly incorporated into hybrid biomaterial systems in the form of nanoparticles, nanocomposites, hydrogels, or composite scaffolds. These hybrid systems combine chitosan with other natural polymers, conductive polymers, or conductive nanomaterials to improve mechanical stability, electrical conductivity, drug delivery capability, and overall biological performance while preserving the inherent bioactivity of chitosan. Consequently, chitosan-based composites have emerged as promising platforms for the development of next-generation conductive wound dressings [56].

*Alginate* is a naturally derived linear anionic polysaccharide. Alginate has been extensively used in biomedical and regenerative medicine applications due to its excellent biocompatibility, biodegradability, and low toxicity. One of the key advantages of alginate in wound healing applications is its high hydrophilicity, which allows it to absorb large amounts of wound exudate and maintain a moist microenvironment that promotes tissue regeneration. In addition, alginate can easily form hydrogels through ionic crosslinking with divalent cations such as calcium ions, enabling the fabrication of 3D scaffolds that resemble the ECM. These hydrogels provide a supportive environment for cell attachment, proliferation, and migration. However, alginate lacks specific cell-binding motifs, which can limit direct cell adhesion on its surface. To overcome this limitation, alginate is often combined with bioactive polymers such as gelatin or collagen. In conductive STE, alginate has also been integrated with conductive nanomaterials and polymers to develop multifunctional scaffolds that combine moisture management, biological compatibility, and electrical conductivity to enhance wound healing outcomes [57, 58].

*Silk Fibroin* is a natural fibrous protein obtained from the cocoons of *Bombyx mori* silkworms and has attracted considerable interest as a biomaterial for tissue engineering applications. Silk fibroin exhibits several advantageous properties, including high biocompatibility, controllable biodegradability, excellent mechanical strength, and the ability to form diverse structures such as films, hydrogels, nanofibers, and porous scaffolds. These characteristics make it a promising biomaterial for wound healing and skin tissue engineering applications. In addition, silk fibroin demonstrates a high-water absorption capacity and can support the attachment and proliferation of various skin-related cells, including fibroblasts and keratinocytes. Its structural stability and ability to form mechanically robust scaffolds provide additional advantages compared to many other natural polymers. Furthermore, silk fibroin-based materials can be easily modified or combined with other polymers and conductive components



23656549, 2026, 45, Downloaded from https://chemistry-europe.onlinelibrary.wiley.com/doi/10.1002/slct.75081 by Esma AHLATCIOLU ÖZEROL - Yildiz Technical University , Wiley Online Library on [25/11/2026]. See the Terms and Conditions (https://onlinelibrary.wiley.com/terms-and-conditions) on Wiley Online Library for rules of use; OA articles are governed by the applicable Creative Commons License

to enhance their biological and electrical properties. Despite these advantages, silk fibroin may exhibit limitations in terms of elasticity and flexibility, which can affect its performance in dynamic skin environments. Therefore, composite systems incorporating silk fibroin with elastomeric or conductive materials are increasingly being explored to improve its functionality in STE [59, 60].

*Elastin* is a highly elastic and durable protein that plays a fundamental role in maintaining the mechanical resilience and flexibility of many tissues, including the skin dermis. In STE, elastin-based biomaterials are used to replicate the natural elasticity and mechanical behavior of native skin tissue. Elastin has been shown to promote the adhesion, proliferation, and migration of dermal fibroblasts, which are critical processes for effective wound healing and tissue regeneration. Additionally, elastin-based scaffolds can enhance cell–matrix interactions and improve the structural organization of regenerated tissue. Due to its excellent stretchability and durability, elastin is often incorporated into composite biomaterials to improve the mechanical performance of tissue-engineered scaffolds. Recent studies have also explored the integration of elastin with conductive polymers and nanomaterials to develop multifunctional scaffolds that combine mechanical flexibility with electrical conductivity. Such systems are particularly promising for conductive STE, where both biomechanical compatibility and electrical signaling play important roles in promoting tissue regeneration [61]. Elastin shows superior durability and stretchability. It enhances the adhesiveness, growth, and migration of dermal fibroblasts, making it suitable for use in STE applications [48, 62].

### 2.4.2 | Synthetic Materials

Synthetic materials are widely utilized in STE applications due to their cost-effectiveness, ease of fabrication, and tunable mechanical properties. These advantages make them attractive candidates for large-scale production and reproducible scaffold design. In particular, their structural stability and controllable degradation profiles allow for precise adaptation to specific biomedical requirements. However, despite these benefits, synthetic polymers generally exhibit limited biocompatibility and insufficient interaction with the native ECM. Their hydrophobic nature and lack of bioactive functional groups can hinder cell adhesion, proliferation, and differentiation. As a result, their standalone use may not be sufficient to achieve optimal skin regeneration, necessitating modification strategies or combination with natural polymers to enhance their biological performance [63].

*Polylactic acid (PLA)* is a biodegradable aliphatic polyester that has been widely employed in skin tissue engineering due to its excellent biocompatibility, favorable mechanical properties, and ease of processing [64]. Despite these advantages, PLA exhibits certain limitations, particularly its relatively slow degradation rate and inherent hydrophobicity, which may hinder cell attachment and tissue integration in some applications. To address these drawbacks, PLA is often modified through blending, copolymerization, or surface functionalization with other natural or synthetic polymers. Such modifications aim to improve its degradation profile, hydrophilicity, and biological performance. For instance, PLA has been combined with conductive polymers such as polypyrrole to impart electrical conductivity, which is particularly beneficial in applications where electrical stimulation can enhance cellular activities, including proliferation and differentiation [65]. Additionally, these composite systems can provide multifunctional properties, making them highly suitable for advanced wound healing and skin tissue engineering applications.

*Polyglycolic acid (PGA)* is a highly crystalline and mechanically robust aliphatic polyester that has been extensively utilized in biomedical applications. Despite its lack of intrinsic wound-healing activity, PGA is frequently employed in STE due to its superior mechanical properties. It is commonly combined with fibrin-based materials, such as fibrin glue, to enhance its biological performance and improve tissue integration [66]. Owing to its high crystallinity, PGA exhibits limited solubility in most organic solvents, which can restrict its processability [67]. Although PGA is biodegradable, its relatively rapid degradation rate may limit its long-term structural stability. Consequently, recent studies have focused on developing PGA-based composites and blends to tailor its degradation profile and improve its functional performance in tissue engineering applications [68].

*Polylactic-co-glycolic acid (PLGA)* is a copolymer composed of lactic acid and glycolic acid monomers, and it has been widely approved by the U.S. Food and Drug Administration (FDA) for various biomedical applications, including implantable devices [69]. PLGA is extensively utilized in STE due to its favorable properties, such as biocompatibility, bioresorbability, and controlled biodegradability. One of its key advantages is the ability to precisely modulate its degradation rate by adjusting the ratio of lactic acid to glycolic acid within the polymer structure, thereby enabling customization according to specific application requirements. However, PLGA inherently exhibits limited cell adhesion properties. To address this limitation, it is often blended with natural polymers, such as collagen, gelatin, or chitosan, which significantly enhance cellular attachment, proliferation, and overall biological performance [70].

*Polycaprolactone (PCL)* is a synthetic, semicrystalline aliphatic polyester widely utilized in wound dressing and skin tissue engineering applications due to its favorable physicochemical and biological properties. It is nontoxic, biodegradable, biocompatible, and exhibits excellent mechanical strength and flexibility, making it suitable for fabricating stable and durable scaffolds. One of the key advantages of PCL is its relatively slow and controllable degradation rate, which allows it to maintain structural integrity over extended periods, a desirable feature for long-term tissue regeneration processes [71, 72].

*Polyethylene glycol (PEG)* is an FDA-approved, hydrophilic polymer widely recognized for its nontoxic, non-immunogenic, and highly biocompatible nature. Owing to these properties, PEG has been extensively employed in a wide range of biomedical applications, particularly in STE and drug delivery systems. Its excellent water solubility, high permeability, and strong resistance to protein adsorption minimize nonspecific biological interactions, making it especially suitable for applications requiring controlled biological responses [73–75].



23656549, 2026, 45, Downloaded from https://chemistry-europe.onlinelibrary.wiley.com/doi/10.1002/slct.75081 by Esma AHLATCIOLU ÖZEROL - Yildiz Technical University , Wiley Online Library on [25/11/2026]. See the Terms and Conditions (https://onlinelibrary.wiley.com/terms-and-conditions) on Wiley Online Library for rules of use; OA articles are governed by the applicable Creative Commons License

*Polyurethane (PU)* is a versatile polymer widely used in biomedical applications due to its remarkable biocompatibility, elasticity, and biostability [76]. Despite these challenges, PU remains a promising material in wound dressing applications due to its ability to support cell adhesion, promote cell proliferation, and mimic the mechanical properties of soft tissues [77].

*Polyvinyl alcohol (PVA)* is a synthetic, water-soluble polymer that has gained significant attention in biomedical applications, particularly in wound dressing materials. It is known for its excellent biocompatibility, chemical resistance, film-forming ability, and capacity to support skin regeneration. Additionally, PVA exhibits high moisture absorption and retention capabilities, which help maintain an optimal wound healing environment [78, 79]. Another important advantage of PVA is its ability to improve the spinnability of polymer solutions when used in combination with other materials, making it highly suitable for electrospinning applications. Furthermore, PVA-based composites can be engineered to enhance mechanical properties, biological performance, and drug delivery capabilities, thereby broadening their applicability in tissue engineering [80].

### 2.4.3 | Conductive Materials for Skin Tissue Engineering

Conductive materials have emerged as a highly promising class of biomaterials in STE owing to their ability to modulate key biological processes involved in wound healing. This effect is primarily associated with their ability to provide an electrically active microenvironment that can interact with the endogenous bioelectrical signals present in native skin. Skin tissue exhibits endogenous electric fields that arise from transepithelial potential differences and are involved in regulating cellular activities such as migration, proliferation, and differentiation [81]. These bioelectrical cues provide directional signals for cells during tissue repair, and disruption of the endogenous electrical microenvironment following injury may impair coordinated cellular responses. Therefore, the incorporation of conductive materials into scaffold systems has attracted considerable attention as a strategy to mimic or restore the bioelectrical microenvironment of injured skin [82] (Figure 1).

Beyond providing structural support, conductive biomaterials can actively influence different stages of wound healing through bioelectrical signaling and cell–material interactions. Conductive matrices can facilitate the transmission of endogenous or externally applied electrical cues, which may influence membrane potential, ion distribution, cellular polarization, and downstream intracellular signaling pathways. These effects can regulate cell adhesion, spreading, migration, proliferation, and differentiation. In particular, electrically active scaffolds can provide directional cues that promote fibroblast migration and proliferation, thereby supporting collagen deposition and ECM remodeling. Similarly, electrical stimulation and conductive substrates can enhance keratinocyte migration and proliferation, contributing to re-epithelialization and wound closure. In addition, the physicochemical and electrical properties of conductive matrices can influence protein adsorption, cell adhesion, cytoskeletal organization, and cell–matrix interactions, thereby establishing a favorable interface between cells and the biomaterial [82, 83].

Conductive biomaterials can also contribute to angiogenesis, which is essential for restoring oxygen and nutrient supply to regenerating tissue. Electrical cues provided by conductive scaffolds can stimulate endothelial cell migration and proliferation and promote the expression of pro-angiogenic factors, thereby facilitating the formation of new blood vessels. Furthermore, conductive biomaterials may modulate the inflammatory phase of wound healing by influencing macrophage behavior. In particular, appropriate electrical and physicochemical cues can promote macrophage polarization toward a pro-regenerative M2 phenotype while reducing excessive pro-inflammatory responses and cytokine production. This modulation may help establish a more favorable microenvironment for subsequent tissue regeneration and remodeling [84].

The regenerative effects of conductive biomaterials can be further enhanced through externally applied electrical stimulation. Electrical stimulation provides controlled biophysical cues that can regulate cellular signaling, migration, proliferation, and differentiation and may consequently accelerate tissue regeneration and functional recovery. Thus, conductive scaffolds can act not only as passive electrical conductors but also as active interfaces capable of converting electrical stimuli into cellular responses. These effects are particularly relevant to electrically stimulated tissue regeneration, where the combination of conductive materials and controlled electrical stimulation can enhance coordinated cellular behavior during wound repair [85].

Beyond their electroactive properties, many conductive materials exhibit additional biological functionalities, including antioxidant and antibacterial activities, which can help reduce oxidative stress and limit microbial colonization that may delay wound healing. Furthermore, conductive biomaterials have enabled the development of advanced therapeutic platforms, including electrically responsive drug delivery systems that provide localized and on-demand release of bioactive agents under external electrical stimulation. Many conductive nanomaterials also possess photothermal properties, enabling localized heat generation under near-infrared (NIR) irradiation, which may further support antimicrobial activity, cellular responses, and tissue regeneration [86]. Collectively, these multifunctional properties establish conductive biomaterials as promising candidates for next-generation STE, where their ability to regulate bioelectrical signaling, cell–material interactions, cellular behavior, angiogenesis, and inflammation can be exploited to promote more effective and functionally relevant tissue regeneration (Figure 2).

### 2.4.4 | Conductive Polymers in Skin Tissue Engineering

Conductive polymers have attracted considerable attention in tissue engineering applications due to their unique ability to transmit electrical signals, along with their generally favorable biocompatibility. Their electroactive nature enables the regulation of essential cellular behaviors, including adhesion, proliferation, and migration, which are fundamental processes for effective tissue regeneration. By providing electrical cues



23656549, 2026, 45, Downloaded from https://chemistry-europe.onlinelibrary.wiley.com/doi/10.1002/slct.75081 by Esma AHLATCIOLU ÖZEROL - Yildiz Technical University , Wiley Online Library on [25/11/2026]. See the Terms and Conditions (https://onlinelibrary.wiley.com/terms-and-conditions) on Wiley Online Library for rules of use; OA articles are governed by the applicable Creative Commons License

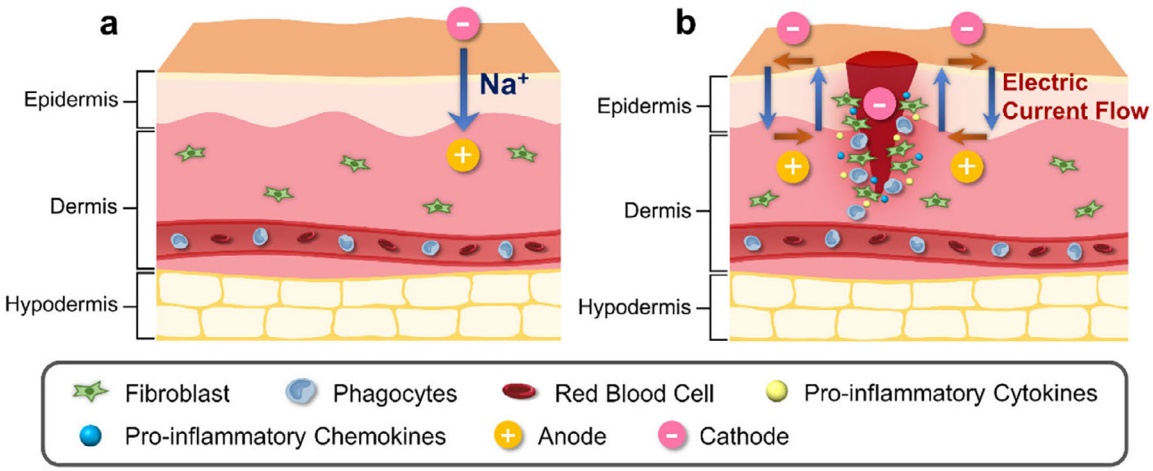


**FIGURE 1** | Schematic representation of bioelectrical signaling in normal and wounded skin. (a) In intact skin, asymmetric ionic fluxes regulated by the $Na^+/K^+$ pump generate a transepithelial electrical potential. (b) Injury disrupts this potential, creating an endogenous electric field that directs cell migration and modulates proliferation, phagocytosis, and inflammatory signaling during wound healing [87].

that mimic the native physiological environment, conductive polymers can actively influence cell–material interactions and enhance tissue repair outcomes. Despite these advantages, the practical application of conductive polymers in tissue engineering is limited by their inherent nonbiodegradable or poorly biodegradable nature. This characteristic may lead to long-term accumulation in the body, potentially causing adverse biological responses and limiting their clinical applicability. To overcome this limitation, conductive polymers are frequently blended or combined with biodegradable polymers, such as polyesters or natural biopolymers. These composite systems are designed to achieve a balance between electrical functionality and controlled biodegradability. Such hybrid structures not only retain the desirable electrical conductivity of the conductive component but also exhibit improved mechanical properties, enhanced processability, and better biological performance. Moreover, the incorporation of biodegradable matrices facilitates gradual degradation and replacement by newly formed tissue, making these composites more suitable for long-term tissue engineering applications [88]. Conductive polymers commonly investigated in tissue engineering applications include PANI, PPy, and PEDOT, which are widely recognized for their electroactive properties and potential to modulate cellular responses.

*Polyaniline (PANI)* is an electroactive polymer whose conjugated backbone enables efficient electron delocalization, thereby providing electrical conductivity. PANI can be synthesized through various polymerization techniques, including electrochemical polymerization, chemical oxidative polymerization, vapor-phase polymerization, photochemically initiated polymerization, enzyme-catalyzed polymerization, and polymerization involving electron acceptors. Furthermore, PANI is classified based on its oxidation state into three primary forms, namely leucoemeraldine, emeraldine, and pernigraniline, listed in order of increasing oxidation level. In terms of solubility, PANI is insoluble in common solvents such as water, acetone, and ethanol, whereas it can dissolve in polar aprotic solvents, including dimethylformamide (DMF), dimethyl sulfoxide (DMSO), and N-methyl-2-pyrrolidone (NMP) [89]. PANI has been widely explored in biomedical applications, such as cancer therapy, drug delivery, and tissue engineering, due to its electrical conductivity and good chemical stability [90]. However, its practical application is limited by several drawbacks, including poor biocompatibility, lack of biodegradability, intrinsic rigidity, and limited mechanical flexibility. Additionally, its poor processability further restricts its direct use in scaffold fabrication. To overcome these limitations, PANI is commonly combined with natural polymers or modified through chemical approaches to form composite materials with enhanced biological and mechanical properties [91, 92]. Although PANI is generally considered biocompatible, it has been reported to exhibit cytotoxic effects at higher concentrations [93].

*Polypyrrole (PPy)* is another widely studied conductive polymer in biomedical applications, primarily due to its relatively simple synthesis, good biocompatibility, and favorable electrical properties [94]. It is typically synthesized via electrochemical polymerization or chemical oxidative polymerization methods [95] PPy also exhibits strong photothermal properties, enabling the conversion of near-infrared (NIR) light into heat energy. This localized heating effect enhances blood circulation and stimulates fibroblast activity, thereby promoting angiogenesis and accelerating wound healing. In addition, PPy possesses inherent antibacterial properties, which are advantageous in preventing infections during tissue regeneration [49]. Despite these beneficial characteristics, PPy presents several limitations, including hydrophobicity, water insolubility, and relatively low environmental stability. Moreover, its nonbiodegradable nature remains a major concern for long-term biomedical applications [96, 95]. To address these issues, PPy is often modified or blended with other polymers to improve its physicochemical and biological performance. Furthermore, PPy can be fabricated in various nanostructured forms, such as nanoparticles, nanowires, nanosheets, and nanotubes, which further expand its applicability in tissue engineering [97].

*Polythiophene (PTh)* is a conductive polymer that has been extensively utilized in electronic and optoelectronic device applications due to its $\pi$-conjugated backbone structure. In recent years, however, its advantageous properties such as high electrical conductivity, chemical stability, environmental durability, and cost-effectiveness-have attracted increasing interest in the field



23656549, 2026, 45, Downloaded from https://chemistry-europe.onlinelibrary.wiley.com/doi/10.1002/slct.75081 by Esma AHLATCIOLU ÖZEROL - Yildiz Technical University , Wiley Online Library on [25/11/2026]. See the Terms and Conditions (https://onlinelibrary.wiley.com/terms-and-conditions) on Wiley Online Library for rules of use; OA articles are governed by the applicable Creative Commons License

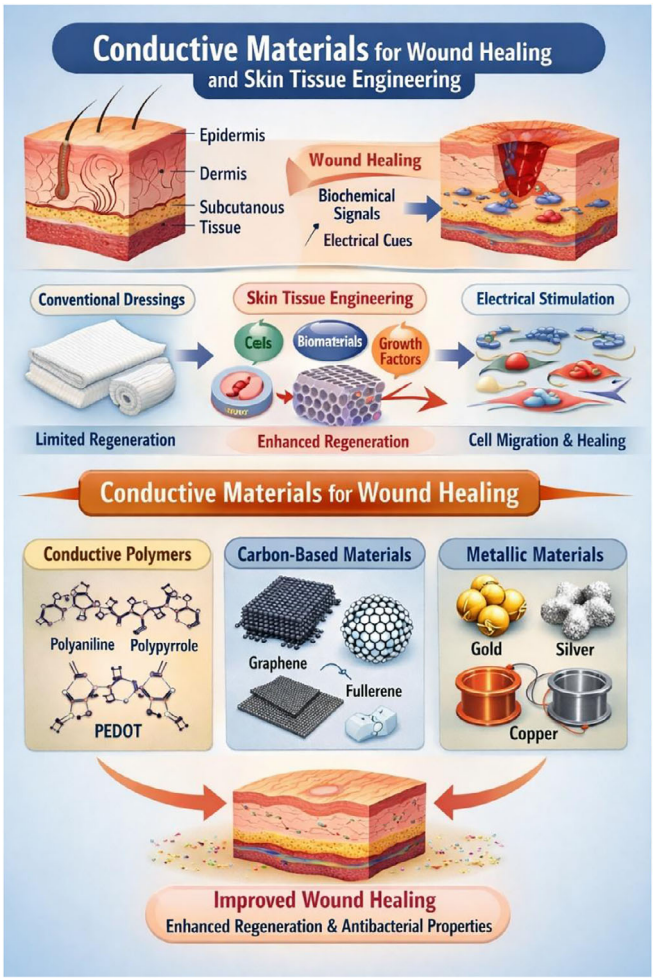


**FIGURE 2** | Conductive materials for wound healing and skin tissue engineering.

of biomedical applications [98]. The intrinsic conductivity of PTh enables effective electrical signal transmission, which is particularly important in electrically responsive tissues such as neural and cardiac systems. Notably, PTh has been reported to promote stem cell proliferation even under serum-free conditions, highlighting its promising role in tissue engineering and regenerative medicine [99]. This behavior is attributed not only to its electrical properties but also to its favorable surface characteristics, which can support cell adhesion, growth, and differentiation. In addition, the physicochemical properties of PTh can be tailored through functionalization or copolymerization, allowing further optimization for specific biological applications.

Furthermore, thiophene-based materials can be combined with a wide range of natural and synthetic polymers, as well as other biomaterials, to develop composite systems with enhanced performance. Such hybrid structures have demonstrated improved antimicrobial activity, which is critical for preventing infections in biomedical devices and wound healing applications. Moreover, these composites offer significant advantages in controlled drug delivery systems by enabling stimuli-responsive release profiles, particularly in response to electrical or environmental triggers [100]. PTh is commonly synthesized via electrochemical and chemical oxidative polymerization methods, both of which provide flexibility in controlling the morphology, molecular weight, and conductivity of the resulting polymer [101]. Overall, the combination of tunable electrical properties, biocompatibility, and structural versatility makes polythiophene a highly promising candidate for advanced biomedical applications, particularly in skin tissue engineering, biosensing, and drug delivery systems.

*Poly(3,4-ethylenedioxythiophene) (PEDOT)* is a derivative of polythiophene that has gained significant attention in STE due to its superior electrical conductivity, low electrical impedance, excellent chemical stability, and compatibility with biological systems [102, 103]. PEDOT also demonstrates a strong affinity for proteins and cell monolayers, which enhances its interaction with biological environments [104]. Among its various formulations, PEDOT:PSS (poly(3,4-ethylenedioxythiophene):poly(styrene sulfonate)) is the most widely used composite in tissue engineering applications. The wound healing potential of PEDOT:PSS has been investigated in various in vivo models, where it has been shown to enhance angiogenesis, thereby accelerating the wound healing process, although limited anti-inflammatory effects have been observed [105]. Despite these advantages, the inherent water insolubility of PEDOT presents a challenge for its application in biological systems. To address this limitation, several strategies have been developed, including in situ polymerization approaches. For instance, the incorporation of PEDOT into Hofmeister effect-assisted polydopamine-functionalized gelatin hydrogels (Gel–PDA/PEDOT) has resulted in the development of highly conductive and water-compatible materials. These advanced composite systems demonstrate significant potential as next-generation wound dressing materials [81].

### 2.4.5 | Carbon-Based Materials in Skin Tissue Engineering

Carbon-based nanomaterials have attracted significant attention in STE due to their exceptional physicochemical properties, including high chemical stability, superior elastic modulus, and lightweight structure. These materials, such as carbon nanotubes (CNTs), graphene, graphene oxide (GO), reduced graphene oxide (rGO), graphene quantum dots (GQDs), and fullerenes, have been widely utilized in various biomedical applications, including diagnosis, cancer therapy, drug delivery, and tissue engineering [106].

*Carbon nanotubes (CNTs)* are allotropes of carbon characterized by their cylindrical nanostructure and remarkable mechanical, thermal, and electrical properties. Due to these unique features, CNTs have been extensively applied in biomedical fields such as drug delivery, biosensing, and gene therapy. Structurally, CNTs are classified into single-walled (SWCNTs) and multi-walled (MWCNTs), and they may also exist in different morphological forms, such as toroidal and graphenated structures. CNTs are typically synthesized using arc discharge, laser ablation, and chemical vapor deposition (CVD) methods. Despite their outstanding properties, the potential toxicity of CNTs remains a major limitation for biomedical applications. Their toxicity is influenced by several factors, including size, length, structural type, and the presence of residual impurities. To address these concerns, various strategies have been developed, such as surface



23656549, 2026, 45, Downloaded from https://chemistry-europe.onlinelibrary.wiley.com/doi/10.1002/slct.75081 by Esma AHLATCIOLU ÖZEROL - Yildiz Technical University , Wiley Online Library on [25/11/2026]. See the Terms and Conditions (https://onlinelibrary.wiley.com/terms-and-conditions) on Wiley Online Library for rules of use; OA articles are governed by the applicable Creative Commons License

functionalization and incorporation into biocompatible matrices, which improve their dispersion in aqueous environments and reduce cytotoxic effects. Typically, CNTs are dispersed in a biocompatible matrix to mitigate their toxicity and enhance solubility in water [107, 108]. Owing to their high electrical and thermal conductivity, as well as their antibacterial, antioxidant, and adhesive properties, CNTs are widely considered promising candidates for STE applications [109].

*Graphene* is a two-dimensional (2D) carbon nanomaterial composed of a single layer of $sp^2$-hybridized carbon atoms arranged in a hexagonal lattice. It is recognized as one of the strongest known materials, offering exceptional mechanical strength, flexibility, and lightweight characteristics. In addition, graphene exhibits excellent electrical and thermal conductivity, making it highly suitable for biomedical applications [110]. Graphene can be synthesized through two primary approaches: top–down methods, such as mechanical, liquid-phase, and electrochemical exfoliation, and bottom–up methods, including epitaxial growth and CVD [111]. Due to its outstanding properties, graphene has been widely explored in applications such as biosensing, drug delivery, bioimaging, and tissue engineering. In the context of STE, graphene has been shown to enhance cell proliferation and accelerate tissue regeneration [112]. However, challenges such as difficulties in controlling size and morphology, high production costs, and poor solubility limit its broader application. To overcome these issues, graphene derivatives such as graphene oxide, reduced graphene oxide, and graphene quantum dots have been developed [113].

*Graphene Quantum Dots* (GQDs) are zero-dimensional carbon-based nanomaterials derived from graphene, CNTs, or fullerenes via both top–down and bottom–up synthesis strategies. Top-down approaches typically include hydrothermal, solvothermal, and ultrasonic methods, whereas bottom–up techniques involve precursor pyrolysis and fullerene decomposition [114]. Owing to their quantum confinement and edge effects, GQDs exhibit unique physicochemical properties such as strong and tunable fluorescence, high aqueous dispersibility, excellent biocompatibility, and low cytotoxicity. These characteristics make them highly attractive for a wide range of biomedical applications, including biosensing, bioimaging, drug delivery, and cancer diagnostics. In the context of STE, GQDs have gained increasing attention due to their nanoscale dimensions and favorable interactions with biological systems. Their ability to generate reactive oxygen species under specific conditions can be leveraged for antimicrobial purposes, which is particularly beneficial in wound healing applications. Moreover, GQDs can be incorporated into polymeric scaffolds to enhance cellular responses, including cell adhesion and proliferation, while also enabling fluorescence-based tracking of cells and tissue regeneration processes [115]. Their multifunctional nature further supports the development of smart and stimuli-responsive wound dressings.

*Graphene oxide (GO)*, an oxidized derivative of graphene, has emerged as a highly versatile material with significant potential in biomedical applications, particularly in tissue engineering and wound healing. GO is commonly synthesized using oxidation-based methods such as Brodie's, Staudenmaier's, and Hummers' methods, which introduce abundant oxygen-containing functional groups (e.g., hydroxyl, carboxyl, and epoxy groups) onto its surface. These functional groups not only enhance its hydrophilicity but also facilitate strong interactions with biomolecules, polymers, and cells. In STE applications, GO has been shown to significantly improve key cellular functions, including cell adhesion, proliferation, and differentiation [116]. Its high surface area and rich functionalization enable efficient drug loading and sustained release, making it an excellent candidate for wound dressing systems with controlled therapeutic delivery. Additionally, GO exhibits strong mechanical properties, contributing to the structural integrity of scaffolds, and demonstrates inherent antibacterial activity, which helps reduce the risk of infection in wound sites. Importantly, GO has also been reported to enhance hemostatic performance, promote protein adsorption, and support accelerated tissue regeneration and cell differentiation in skin-related applications [117, 118, 119].

*Reduced graphene oxide (rGO)*, obtained through the partial removal of oxygen-containing groups from GO, exhibits significantly improved electrical conductivity, making it particularly suitable for applications involving electrically active tissues and electroactive scaffolds. While chemical reduction remains the most commonly employed method, it often involves toxic reducing agents such as hydrazine derivatives, raising concerns regarding biocompatibility. To overcome these limitations, alternative reduction strategies including thermal, microwave-assisted, and photochemical methods have been developed. More recently, green synthesis approaches utilizing plant extracts have attracted considerable interest as sustainable and environmentally friendly alternatives [117, 120]. From a biomedical perspective, rGO combines enhanced electrical conductivity with favorable mechanical properties and notable antibacterial activity. In STE, rGO-based materials have demonstrated the ability to promote angiogenesis, stimulate cell proliferation, and enhance overall wound healing performance [121]. Its conductive nature also enables the development of electroactive wound dressings that can respond to external electrical stimuli, thereby further accelerating tissue repair processes. When incorporated into composite scaffolds, rGO can significantly improve both the electrical and biological performance of the system, making it a highly promising material for advanced skin regeneration strategies.

*Fullerenes* are spherical, zero-dimensional carbon nanostructures composed entirely of carbon atoms arranged in a closed-cage configuration. They are often referred to as "radical sponges" due to their strong free radical scavenging ability [122], and it is also called "radical sponge". $C_{60}$, $C_{70}$, and $C_{80}$ are the most common types of fullerenes, and $C_{60}$ is the most frequently used type of fullerene in biomedical applications, and it is also called buckminsterfullerene. Fullerene is produced via laser irradiation, plasma, and chemical reduction techniques. It is used in numerous applications, such as solar cells, sensors, and the delivery of drugs or genes, combining with polymers to make fullerene soluble in aqueous solutions [123]. Fullerenes have been explored in a wide range of applications, including solar cells, sensors, and drug and gene delivery systems. To improve their solubility in aqueous environments, they are often functionalized or combined with polymers. In biomedical contexts, fullerenes exhibit notable anti-inflammatory, antiviral, and antibacterial properties [124]. Their excellent biocompatibility and diverse biological activities make them promising candidates for wound healing and STE applications [125].



23656549, 2026, 45, Downloaded from https://chemistry-europe.onlinelibrary.wiley.com/doi/10.1002/slct.75081 by Esma AHLATCIOLU ÖZEROL - Yildiz Technical University , Wiley Online Library on [25/11/2026]. See the Terms and Conditions (https://onlinelibrary.wiley.com/terms-and-conditions) on Wiley Online Library for rules of use; OA articles are governed by the applicable Creative Commons License

### 2.4.6 | Metallic Materials in Skin Tissue Engineering

Metallic materials have been utilized as antimicrobial agents for centuries, and their antibacterial properties have been extensively investigated in biomedical research. In recent years, metallic materials have gained significant attention as potential alternatives to conventional antibiotics, particularly due to their ability to combat antibiotic-resistant bacteria. These materials exert their antimicrobial effects by disrupting bacterial cell membranes, generating reactive oxygen species, and interfering with essential cellular components and metabolic pathways [126]. In wound dressing applications, metallic materials are predominantly employed in the form of nanoparticles for two primary purposes: serving as carriers for drug or bioactive molecule delivery and directly enhancing wound healing through their intrinsic physicochemical properties. Metal nanoparticles, such as gold (Au), silver (Ag), and copper (Cu), exhibit remarkable antimicrobial activity and have been shown to significantly promote tissue regeneration and wound repair [127].

*Gold nanoparticles* (AuNPs) are widely utilized in biomedical applications, including drug delivery, cancer therapy, bioimaging, and diagnostics, due to their unique physicochemical characteristics. These include high surface area, ease of surface functionalization, excellent optical properties, and strong photothermal effects. Additionally, AuNPs exhibit antibacterial activity and can be engineered for targeted therapeutic applications. However, one of the major challenges associated with AuNPs is their tendency to aggregate, which may reduce their effectiveness and alter their biological interactions. To address this issue, ultrasmall gold nanoparticles are often preferred, as they demonstrate improved cellular uptake and faster intracellular degradation [128, 129]. AuNPs can be synthesized in a wide variety of shapes, including spherical, rod-like, prismatic, hexagonal, cubic, star-shaped, bipyramidal, and branched structures, each exhibiting distinct physicochemical and biological properties [130]. They typically employ chemical reduction methods that utilize organic or inorganic stabilizing agents. Additionally, Turkevich, Brust–Schiffrin, electrochemical, laser ablation, and vacuum sputtering methods are used for the production of gold nanoparticles [131].

*Silver* has been used in medical applications since ancient times, with historical evidence indicating its use in wound treatment in civilizations such as ancient Egypt and Macedonia. In modern biomedical applications, silver is primarily utilized in the form of nanoparticles or nanowires, which exhibit enhanced physicochemical and biological properties. Silver nanoparticles (AgNPs) possess a broad spectrum of biological activities, including antibacterial, antifungal, antiviral, anti-inflammatory, antioxidative, and antitumor effects. These properties make them particularly effective as antimicrobial agents in wound dressing applications [132]. Silver nanoparticles can be synthesized in various shapes, such as spherical and cubic forms, using chemical, physical, photochemical, and biological (green synthesis) methods [133]. Among these, green synthesis has gained considerable attention due to its environmentally friendly nature and the avoidance of toxic reagents typically used in conventional synthesis processes. This approach not only enhances biocompatibility but also improves the suitability of AgNPs for biomedical applications [137].

*Copper* has also been widely employed as an antimicrobial agent for an extended period and has recently gained attention in nanomaterial-based biomedical applications due to its cost-effectiveness and favorable biological properties. Compared to gold and silver, copper-based nanomaterials are generally more economical and can exhibit comparable antimicrobial activity with lower overall cost. Copper nanoparticles can be synthesized through both top–down and bottom–up approaches. Top-down methods include techniques such as laser ablation, ball milling, nanolithography, and magnetron sputtering, whereas bottom–up approaches involve electrochemical synthesis, microwave-assisted synthesis, hydrothermal or solvothermal methods, sol–gel processes, and biosynthesis techniques [135]. In skin tissue engineering applications, copper plays a crucial role in promoting wound healing by stimulating endothelial cell proliferation and enhancing angiogenesis. Additionally, copper-based nanomaterials exhibit strong antioxidant activity and contribute to improved mechanical strength and porosity of scaffold systems. These combined properties make copper a promising candidate for incorporation into advanced wound dressing materials and tissue engineering constructs [136].

### 2.4.7 | Hybrid Conductive Biomaterials for Biomedical Applications

In addition to conductive hydrogels and conductive bioinks, hybrid conductive biomaterials have attracted increasing attention because they enable the combination of electrical functionality with the biological and physicochemical properties of complementary components. In these systems, conductive nanoparticles, including graphene-based nanomaterials, CNTs, metallic nanoparticles, and other nanoscale conductive components, are frequently incorporated into polymeric matrices to improve electrical conductivity, mechanical properties, and biological performance. Beyond nanoparticle-based systems, multifunctional nanocomposites and bioactive delivery systems have also been investigated to combine electrical functionality with enhanced therapeutic effects. The incorporation of these components can facilitate cell–material interactions, controlled delivery of bioactive agents, antimicrobial activity, and electrically responsive cellular behavior, thereby expanding the potential applications of conductive biomaterials in tissue engineering and regenerative medicine [137, 121]. Thus, hybrid conductive platforms offer a versatile strategy for integrating electrical and biochemical cues to achieve enhanced therapeutic and regenerative outcomes.

### 2.4.8 | Comparative Considerations of Conductive Material Classes

Conductive biomaterials can be broadly categorized into conductive polymers, carbon-based materials, and metallic materials, each exhibiting distinct advantages and limitations for biomedical applications [137]. Conductive polymers, such as polypyrrole, polyaniline, and PEDOT:PSS, generally provide tunable electrical conductivity, good flexibility, and relatively favorable cytocompatibility; however, their limited biodegradability and the potential toxicity of their degradation products may restrict their long-term clinical use [138]. Carbon-based materials, including



23656549, 2026, 45, Downloaded from https://chemistry-europe.onlinelibrary.wiley.com/doi/10.1002/slct.75081 by Esma AHLATCIOLU ÖZEROL - Yildiz Technical University , Wiley Online Library on [25/11/2026]. See the Terms and Conditions (https://onlinelibrary.wiley.com/terms-and-conditions) on Wiley Online Library for rules of use; OA articles are governed by the applicable Creative Commons License

graphene, GO, rGO, and CNTs, generally exhibit high electrical conductivity and can enhance the mechanical properties and antibacterial activity of polymeric matrices. Nevertheless, their limited biodegradability, aggregation tendency, and dose- and material-dependent cytotoxicity remain important concerns for biomedical applications [121, 139]. In contrast, metallic materials, such as gold, silver, and copper, typically exhibit superior electrical conductivity and, particularly in the case of silver-based materials, pronounced antibacterial activity. However, their limited biodegradability, potential ion-mediated cytotoxicity, and relatively high stiffness compared with soft biological tissues can constrain their integration into regenerative biomaterials [140]. From a mechanical perspective, conductive polymers offer greater flexibility, whereas carbon-based and metallic materials can provide enhanced reinforcement and electrical performance when incorporated into polymeric matrices. Overall, although metallic materials offer high conductivity and established clinical relevance for certain bulk applications, conductive polymers and carbon-based materials may provide greater versatility for flexible and tissue-interfacing biomedical systems. Therefore, the selection of a conductive material should consider not only its electrical performance but also biodegradability, cytocompatibility, toxicity, antibacterial activity, mechanical compatibility, and clinical translation potential. Thus, material selection should be application-dependent rather than conductivity-driven. Conductive polymers may be preferable when flexibility and conformal tissue interfacing are prioritized, whereas carbon-based materials may provide a favorable balance between electrical and mechanical reinforcement. Metallic nanomaterials can offer superior conductivity and antibacterial activity but require careful control of concentration and ion release because of potential cytotoxicity and long-term accumulation. The conductive materials comparison used in skin tissue engineering and wound healing are summarized in Table 2.

## 3 | Overview of Conductive Materials in Skin Tissue Engineering

### 3.1 | Conductive Polymers

Rajasekaran et al. investigated a PANI-based electroactive fibrous scaffold by incorporating 0.3 wt% PANI into silk fibroin-loaded PCL fibers using HFIP-based solvent systems with and without formic acid. The resulting BpS (pH 9) and EpS (pH 3) fibers exhibited distinct surface morphologies and physicochemical properties depending on the solvent environment. Notably, the BpS fibers demonstrated superior mechanical stability and cellular compatibility compared with the EpS fibers, with human placenta-derived mesenchymal stem cells exhibiting significantly higher proliferation on the BpS substrate. In a full-thickness wound model, the electroactive BpS scaffold promoted more effective wound healing and complete wound closure compared with the EpS and Tegaderm-treated groups. Furthermore, the BpS-treated wounds exhibited differential regulation of wound-healing-related genes, including increased expression of IL-1$\beta$, IFN-$\gamma$, collagen III, and EGF at day 7 and TGF-$\beta$1, collagen I, and FGF at day 14, indicating enhanced extracellular matrix remodeling and tissue regeneration. These findings demonstrate that incorporation of PANI into SF/PCL fibers can provide a mechanically stable and electroactive wound dressing with favorable cellular compatibility and enhanced wound-healing performance [91].

Liu et al. developed a light-responsive PANI-Cur composite nanofibrous wound dressing by electrospinning. Hydrogen bonding and electrostatic interactions between polyaniline (PANI) and curcumin (Cur) enhanced light absorption and promoted interfacial electron separation and transfer. Under light irradiation, the PANI-Cur nanofibers exhibited strong antibacterial activity against *Staphylococcus aureus* (99.77%) and *Escherichia coli* (98.45%). In vivo experiments further demonstrated accelerated wound healing in a mouse skin injury model, highlighting the potential of PANI-Cur nanofibers as smart conductive wound dressings with light-responsive antibacterial and wound-healing properties [153].

Najafian et al. developed ECM-mimetic electrically conductive nanofibrous scaffolds composed of polyaniline-grafted tragacanth gum (TG-g-PANI) and PVA for skin tissue engineering applications. The fabricated scaffolds demonstrated suitable physicochemical properties, cytocompatibility, and hemocompatibility, while supporting the adhesion and proliferation of L929 fibroblasts. Both conductive formulations exhibited favorable blood compatibility, with hemolysis rates below 2%, and showed HSA protein adsorption. Among the tested formulations, the scaffold containing 20 wt% TG-g-PANI (S3) exhibited higher electrical conductivity, biodegradation, and fibroblast proliferation than the 30 wt% formulation (S4), together with superior physicochemical properties and structural uniformity. These findings indicate that the optimized TG-g-PANI/PVA scaffold, particularly S3, represents a promising conductive platform for skin tissue engineering [154].

Pang et al. developed a methacrylate-functionalized polyaniline nanoparticle (Me-PANI NPs)@PAM hydrogel, in which the modified PANI nanoparticles served as chemical crosslinking points within a polyacrylamide (PAM) network. The PANI nanoparticles provided NIR-triggered photothermal antibacterial activity, enabling controllable bacterial inhibition by adjusting the irradiation time. In addition, energy dissipation by the nanoparticles under mechanical deformation imparted high flexibility to the hydrogel, which exhibited a maximum stretching ratio of 400%. The hydrogel also demonstrated high water absorption capacity and good biocompatibility, supporting its potential as a mechanically flexible and photothermally responsive wound dressing for infection control and skin wound healing [155].

Javid et al. developed electroconductive nanofibrous scaffolds based on poly(vinyl alcohol)-grafted polyaniline (PVA-g-PANI) and neat PVA using an electrospinning technique for skin tissue engineering applications. PVA-g-PANI was synthesized by grafting aniline onto a phenylamine-functionalized PVA macromonomer through oxidative polymerization and subsequently co-electrospun with PVA at different ratios. Increasing the PVA-g-PANI content from 0 to 30 wt% increased the scaffold surface wettability, with contact angle values ranging from 55.7° to 105.1°, while progressively decreasing the biodegradation rate due to the low biodegradability of PANI. All scaffolds except the 30 wt% PVA-g-PANI formulation exhibited good hemocompatibility, with hemolysis rates below 2%. Among the investigated formulations, scaffolds containing 15 and 20 wt% PVA-g-PANI (S3



23656549, 2026, 45, Downloaded from https://chemistry-europe.onlinelibrary.wiley.com/doi/10.1002/slct.75081 by Esma AHLATCIOLU ÖZEROL - Yildiz Technical University , Wiley Online Library on [25/11/2026]. See the Terms and Conditions (https://onlinelibrary.wiley.com/terms-and-conditions) on Wiley Online Library for rules of use; OA articles are governed by the applicable Creative Commons License

**TABLE 2** | Comparison of conductive biomaterials for skin tissue engineering and wound healing.

| Conductive biomaterial | Fabrication methods | Conductivity value (S/cm) | Biological performance | Degradation characteristics | Advantages | Limits | Wound healing applications | Reference |
|---|---|---|---|---|---|---|---|---|
| Polyaniline (PANI) | Chemical oxidative polymerization, electrochemical method | $\sim 10^{-2} - 10$ | Promotes fibroblast proliferation and angiogenesis | Poor biodegradability | High conductivity, low cost, easy synthesis | Low solubility and processability, limited biodegradability | Nanofibrous skin tissue scaffolds | [90, 141] |
| Polypyrrole (PPy) | Chemical oxidative polymerization, Electrochemical method | $\sim 10^{-7} - 10^{2}$ | Enhanced cell adhesion, growth, and proliferation | Poor biodegradability | Good biocompatibility, excellent photothermal conversion efficiency and electrical conductivity | Poor mechanical and processing properties | Film, drug delivery, nanoparticle, nanofiber | [97, 142, 143] |
| PEDOT:PSS | Oxidative polymerization | $\sim 10^{-4} - 10^{3}$ | Promotes cell proliferation and angiogenesis | Poor biodegradability | High conductivity and stability | Brittle and rigid | Hydrogel, nanofiber | [105, 144], [145] |
| Graphene | Mechanical exfoliation method, CVD | $\sim 10^{2} - 10^{3}$ | Improved cellular internalization and therapeutic delivery | Poor biodegradability | Biocompatibility, stability, targeted drug delivery | High production cost, scalability limitation, potential cytotoxicity | Conductive scaffolds | [43, 113, 146, 147] |
| Graphene Oxide (GO) | Hummer's method, Tour method | $\sim 10^{-8}$ | Improve cell attachment and adhesion, enhance cell proliferation | Limited biodegradability | Hydrophilicity, flexibility | Low conductivity | Hydrogel, nanocomposites, drug delivery | [116, 117] |
| Reduced Graphene Oxide (rGO) | Chemical reduction, green reduction | $\sim 10^{-5}$ | Angiogenic potential, antibacterial | Slow biodegradation | Mechanical strength, electrical conductivity | Aggregation | Electroactive wound dressings | [121, 139] |
| Carbon nanotubes | Electric-arc discharge, laser ablation, CVD | $\sim 10^{4} - 10^{5}$ | Supports cell adhesion | Nonbiodegradable | Chemical inertness, high tensile strength, biocompatibility | High impurity | Microneedles, hydrogel, nanofibers | [148, 149, 150] |
| Gold nanoparticle (AuNp) | Electrochemical, physical, biological, chemical | $\sim 10^{-8} - 10^{2}$ | Promotes fibroblast proliferation and migration, enhances angiogenesis | Nonbiodegradable | High surface area, tunability, strong biocompatibility. | High cost, accumulation in organs | Conductive wound dressings, biosensors | [151, 152] |
| Silver nanoparticle (AgNp) | Chemical reduction, green synthesis, photochemical synthesis, electrochemical synthesis, microwave-assisted synthesis | $\sim 10^{-8} - 10^{2}$ | Antibacterial, promotes wound closure | Nonbiodegradable | High conductivity, relatively low cost, easy synthesis | Cytotoxicity at high concentrations, oxidative stress, uncontrolled $Ag^{+}$ release, | Antibacterial wound dressings | [90, 126, 132, 141] |



23655549, 2026, 45, Downloaded from https://chemistry-europe.onlinelibrary.wiley.com/doi/10.1002/slct.75081 by Esma AHL.ATCIOLU ÖZEROL - Yildiz Technical University , Wiley Online Library on [25/11/2026]. See the Terms and Conditions (https://onlinelibrary.wiley.com/terms-and-conditions) on Wiley Online Library for rules of use; OA articles are governed by the applicable Creative Commons License

and S4) demonstrated the most favorable overall physicochemical and biological properties, indicating their potential for skin tissue engineering applications [156].

Shah et al. developed NiSe nanoparticle ointment and NiSe-incorporated PANI/PEO nanofibers for wound healing applications. NiSe nanoparticles were synthesized using a hydrothermal method, while NiSe-incorporated PANI/PEO fibers were fabricated by electrospinning. The resulting fibers exhibited a bead-free morphology with an average diameter of 330 nm, while the NiSe nanoparticles showed an average crystallite size of 6.2 nm. Compared with NiSe nanoparticles, the NiSe-incorporated PANI/PEO fibers demonstrated enhanced antibacterial and antioxidant activities with lower toxicity. Notably, the NiSe/PANI/PEO fibers achieved a wound healing rate of 95.6% ± 0.25%, compared with 89.5% ± 1.18% for NiSe nanoparticles. Histopathological analysis and IL-6 evaluation further confirmed effective wound recovery and tissue regeneration, highlighting the potential of NiSe-incorporated PANI/PEO nanofibers for wound healing applications [157].

Kheirabadi et al. developed poly(vinyl alcohol)/tragacanth gum/polyaniline (PVA/TG/PANI) nanofibrous membranes through co-electrospinning of PVA/TG and PVA/PANI solutions for STE applications. The resulting nanofibers exhibited a uniform morphology with an average fiber diameter of 176.45 ± 29 nm, together with hydrophilic characteristics, tunable swelling behavior, and suitable mechanical strength and flexibility. The PVA/TG/PANI membranes demonstrated high cytocompatibility, with the highest cell viability reaching 91.94% in HDF-4 cells, and significantly enhanced antibacterial activity against *E. coli* and *S. aureus* compared with PVA/TG and PVA/PANI membranes. The membranes also exhibited an enhanced antibiofilm effect, particularly against *S. aureus*, and promoted cell migration in a scratch assay. However, the study was limited to in vitro evaluations, and the mechanisms underlying the enhanced antibacterial activity were not directly investigated. Overall, the findings suggest that PANI/TG-containing nanofibrous membranes combine cytocompatibility, antibacterial activity, hydrophilicity, and suitable mechanical properties, making them promising candidates for skin tissue engineering and wound healing applications [158].

Switha et al. developed a PANI-PVA-chitosan nanoparticle (CNP) bionanocomposite for skin tissue engineering applications. CNPs were synthesized using a cost-effective ionic gelation method and exhibited a spherical morphology with particle sizes below 47 nm. Incorporation of CNPs into the PANI-PVA matrix improved the thermal stability, mechanical properties, swelling behavior, and porosity of the resulting bionanocomposite. The material exhibited antibacterial activity against both Gram-positive and Gram-negative bacteria, with inhibition zones of 13 mm for *Enterococcus faecalis*, 10.9 mm for *Staphylococcus aureus*, 15 mm for *Salmonella typhi*, and 17 mm for *Escherichia coli*. Furthermore, the bio-nanocomposite showed a hemolysis rate below 2%, indicating good hemocompatibility. These findings demonstrate the potential of PANI-PVA-CNPs as an electroactive and antibacterial biomaterial for skin tissue regeneration [143].

Wu et al. developed a Lactera (LAC)-PPy microcomposite (MC) that combines NIR-triggered photothermal mild hyperthermia with the anti-inflammatory and regenerative properties of LAC for burn wound healing. PPy was synthesized using a microwave-assisted method and integrated with LAC to generate a bioactive photothermal microenvironment under NIR irradiation. The treatment promoted CD31-mediated angiogenesis, CD34-associated follicle activation, heat shock protein (HSP) expression, and M2 macrophage polarization, while modulating oxidative stress and inflammation. Immunofluorescence analysis confirmed the upregulation of these regenerative markers, accompanied by accelerated wound healing and improved skin structure. These findings highlight the potential of LAC-PPy MC as a non-invasive, NIR-responsive platform for burn and complex wound treatment [159].

Chu et al. developed a polypyrrole (Ppy)-composited PVA/PEG/HA hybrid hydrogel with enhanced mechanical and photothermal properties for the treatment of diabetic foot ulcers. Under NIR irradiation, the Ppy-containing hydrogel generated localized heat that effectively eliminated bacteria and promoted macrophage phagocytosis and M1 activation, thereby enhancing bacterial clearance. Following infection control, macrophages transitioned toward the M2 phenotype, contributing to inflammation resolution and tissue regeneration. Furthermore, genes associated with keratinization, keratinocyte differentiation, and skin barrier formation were upregulated, accompanied by enhanced collagen and VEGF expression. These findings demonstrate that the Ppy-based hydrogel can simultaneously address bacterial infection and impaired tissue regeneration, highlighting its potential as a photothermal conductive dressing for chronic diabetic wounds [160].

Zarei et al. developed conductive electrospun nanofibrous scaffolds based on chitosan, collagen, polyethylene oxide (PEO), and different concentrations of PPy (5–25 wt%) for tissue engineering applications. Increasing PPy content reduced the average fiber diameter and significantly enhanced the electrical conductivity of the scaffolds, reaching $164.274 \times 10^{-3}$ S/m. The PPy nanoparticles were uniformly distributed within the nanofibers, while the scaffolds exhibited suitable mechanical properties and in vitro degradability. Among the tested formulations, the scaffold containing 10 wt% PPy demonstrated superior cell adhesion, growth, and proliferation. These findings highlight the potential of PPy-containing conductive nanofibers for skin and other electrically active tissues, including nerve and cardiac tissue engineering [161].

Ma et al. developed a conductive polypyrrole@keratin nanofiber membrane (PPy@KNM) using electrospinning followed by in situ chemical polymerization of pyrrole monomers for electrically stimulated wound healing. PPy was successfully deposited onto the keratin nanofiber membrane, and the highest conductivity and tensile strength were achieved using 0.6 M oxidant and 0.5 M p-toluenesulfonic acid (p-TSA) dopant. The resulting PPy@KNM exhibited good biocompatibility and no cytotoxicity in vitro. Moreover, electrical stimulation at an optimal current intensity of 80 μA for 5 min/day significantly promoted cell growth and proliferation. These findings demonstrate the potential of PPy@KNM as a conductive wound dressing capable of enhancing wound healing through electrically stimulated cellular responses [142].



23656549, 2026, 45, Downloaded from https://chemistry-europe.onlinelibrary.wiley.com/doi/10.1002/slct.75081 by Esma AHLATCIOLU ÖZEROL - Yildiz Technical University , Wiley Online Library on [25/11/2026]. See the Terms and Conditions (https://onlinelibrary.wiley.com/terms-and-conditions) on Wiley Online Library for rules of use; OA articles are governed by the applicable Creative Commons License

Wang et al. developed an antibiotic-free capacitive antibacterial dressing composed of polypyrrole-wrapped carbon cloth (PPy-CC) electrodes and a bacterial cellulose (BC) hydrogel separator for electrically stimulated wound treatment. Under a low-voltage electrical stimulation of 1 V for 10 min, the dressing achieved bactericidal efficiencies of up to 99.97% and 99.99% against multidrug-resistant (MDR) bacteria. The high electrical capacity and rechargeability of the system enabled repeated charging and sustained antibacterial activity. In vivo experiments further demonstrated effective inhibition of wound infection and accelerated wound recovery in infected full-thickness mouse wounds. These findings highlight the potential of PPy-CC/BC capacitive dressings as a biosafe, antibiotic-free, and electrically stimulated strategy for treating infected wounds [162].

Zhou et al. developed an innovative photo-electronic wound dressing that is responsive to both visible light and electrical stimulation. This dual-responsive system represents the first of its kind and was designed to actively promote and accelerate the wound healing process. The researchers synthesized a composite by integrating polythiophene with selenoviologens, which exhibit redox activity and photo-responsiveness. These functional materials were incorporated into a flexible polyacrylamide (PAAm) hydrogel matrix, providing a biocompatible and mechanically stable platform for wound applications. The resulting hydrogel-based dressing was designed as a flexible and wearable device capable of being activated under visible light and low-level electrical input. In vivo experiments demonstrated that the synergistic effect of photothermal and electrical stimulation significantly enhanced tissue regeneration. Notably, the application of this dual-mode stimulation reduced the wound healing time from 15 days to just 7 days, highlighting the device's potential to improve clinical outcomes in wound care by accelerating the natural repair mechanisms [163].

Najafian et al. developed electroactive nanofibrous scaffolds based on polythiophene-grafted tragacanth gum (TG-g-PTh) and PVA for STE. The TG-g-PTh/PVA scaffolds were fabricated by co-electrospinning, resulting in 3D interconnected porous structures. TG-g-PTh exhibited an electrical conductivity of $1.0 \times 10^{-3}$ S/cm, while incorporation of the conductive polymer improved fibroblast adhesion and proliferation. Among the investigated formulations, the scaffold containing 7 wt% TG-g-PTh (S4) demonstrated the most favorable cytocompatibility and cell proliferation. The scaffolds also exhibited acceptable swelling, biodegradation, protein adsorption, and hemocompatibility, with hemolysis rates below 3%. The enhanced cellular response was attributed partly to the conductive substrate facilitating cell–cell and cell–matrix interactions [164].

Chai et al. developed a 3D-printed conductive composite dressing based on a PVA/κ-carrageenan network containing PEDOT:PSS as the conductive component and (+)-catechin-loaded mesoporous ZnO (CmZnO) as an antibacterial and anti-inflammatory agent. The dressing was fabricated using extrusion-based 3D printing and exhibited suitable electrical conductivity, blood clotting capacity, and tissue adhesiveness. The composite demonstrated antibacterial activities of 92.9% against *S. aureus* and 95.6% against *E. coli*. Under optimal electrical stimulation, the dressing enhanced wound healing in a full-thickness skin defect model by increasing CD31 expression and reducing the inflammatory marker IL-6. These findings highlight the potential of 3D-printed PEDOT:PSS-based composite dressings for combining electrical stimulation, antibacterial activity, hemostasis, and inflammation modulation in wound healing [165].

Lari et al. developed a conductive PEDOT:PSS/nHA/CS/PCL biocomposite scaffold using lyophilization technique for tissue engineering applications. The incorporation of biodegradable PCL improved the mechanical properties of the scaffold but reduced its electrical conductivity from $9.72 \times 10^{-8}$ S/cm for PEDOT:PSS/nHA/CS to $3.55 \times 10^{-8}$ S/cm for the PEDOT:PSS/nHA/CS/PCL scaffold. The resulting scaffold exhibited a randomly distributed porous structure with 66% porosity, while PCL incorporation increased the contact angle and decreased swelling and pore size. In vitro evaluation using human skin fibroblasts (HSFs) demonstrated 85% cell viability, with cells remaining attached to the scaffold surface after 7 days. Despite the reduction in conductivity, the PCL-containing scaffold maintained electrical activity that may support cell–scaffold interactions through enhanced intracellular signaling. Overall, the PEDOT:PSS/nHA/CS/PCL scaffold showed suitable biocompatibility and non-toxicity, indicating its potential for STE applications [166].

Hu et al. developed a multifunctional conductive PVA/PEDOT:PSS/green tea-derived carbon dots (GCDs) hydrogel (PPPCD) using a repeated freeze-thaw method for skin wound healing. PEDOT:PSS provided electrical conductivity, while GCDs contributed antioxidant, antibacterial, and anti-inflammatory properties. The PPPCD hydrogel exhibited an electrical conductivity of $2.097 \times 10^{-3}$ S/cm, which was higher than that of the PPP hydrogel ($1.274 \times 10^{-3}$ S/cm) due to the formation of additional conductive pathways by GCDs. The hydrogel showed excellent biocompatibility, effective ROS-scavenging capacity, and enhanced cell migration. In vivo, PPPCD promoted angiogenesis and epidermal regeneration while alleviating excessive inflammation, thereby accelerating wound healing. Notably, the electroactive hydrogel could transmit intrinsic electrical signals to the wound site and promote cellular stimulation without requiring external electrical stimulation. These findings highlight the potential of PVA/PEDOT:PSS/GCD hydrogels as multifunctional conductive wound dressings integrating electrical, antioxidant, antibacterial, and anti-inflammatory functions [167].

Lee et al. developed a conductive hydrogel with a grooved topography to enhance wound healing in dermal fibroblast cells. They utilized GelMA, a chemically modified form of gelatin, which offers photo-crosslinking ability under ultraviolet (UV) light along with excellent biocompatibility and mechanical properties. To impart electrical conductivity, they incorporated PEDOT:PSS into the hydrogel system. Initially, GelMA was synthesized using type B gelatin. It was then dissolved in phosphate-buffered saline (PBS), and PEDOT:PSS was added at varying concentrations. The scaffolds were fabricated using digital light processing (DLP) 3D printing technology. Human dermal fibroblast (HDF) was seeded onto the surface of the scaffolds. Both in vitro and in vivo experiments were conducted, in vitro studies performed on human dermal fibroblasts, and in vivo studies performed on rabbits. To evaluate the effect of electrical stimulation, the scaffolds were subjected to daily stimulation sessions (5 min per



23656549, 2026, 45, Downloaded from https://chemistry-europe.onlinelibrary.wiley.com/doi/10.1002/slct.75081 by Esma AHLATCIOLU ÖZEROL - Yildiz Technical University , Wiley Online Library on [25/11/2026]. See the Terms and Conditions (https://onlinelibrary.wiley.com/terms-and-conditions) on Wiley Online Library for rules of use; OA articles are governed by the applicable Creative Commons License

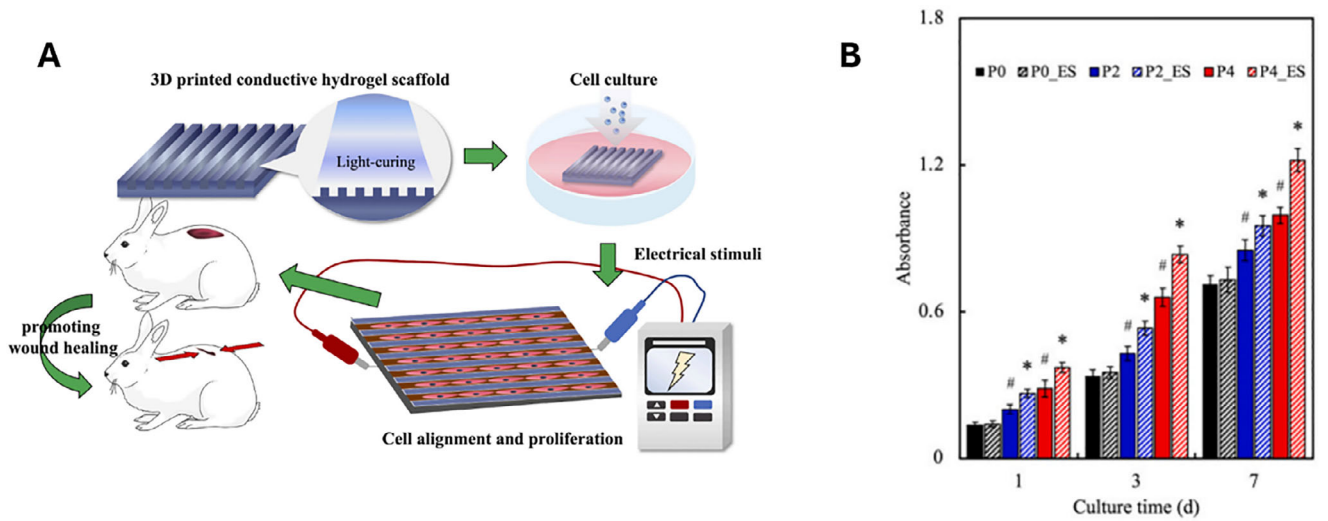


**FIGURE 3** | (A) Schematic representation of the production of conductive hydrogel for skin tissue engineering. (B) Proliferation rate of human dermal fibroblast cells cultured on the GelMa/PEDOT:PSS hydrogel scaffolds with electrical stimulation over time [168].

day at 10 mA, 100 μs pulse width, and 20 Hz frequency). The results demonstrated that scaffolds receiving electrical stimulation significantly enhanced cell proliferation compared to those without stimulation. Among the tested formulations, the GelMA hydrogel containing 0.04% PEDOT:PSS exhibited the highest biocompatibility [168]. (Figure 3)

Alves et al. developed electrospun PEDOT-based meshes for skin regeneration applications. In their study, PEDOT was synthesized via an alternative in situ chemical polymerization approach using hyaluronic acid as a dopant. The resulting CS/GEL/PEDOT electrospun nanofibrous meshes exhibited promising properties as conductive scaffolds, making them suitable for electro-stimulated wound dressing applications in STE. The results demonstrated that the incorporation of the conductive polymer increased the electrical conductivity, solution density, and fiber diameter, which in turn significantly affected the porosity, water uptake capacity, solubility, and biodegradability of the meshes. Importantly, these modifications were achieved without compromising the water vapor permeability, which remained within a suitable range for wound dressing applications. Overall, the study emphasizes the fabrication and characterization of CS/GEL nanofibers incorporated with HA-doped PEDOT as a novel strategy to obtain conductive nanofibrous structures [169].

Heo et al. developed a wireless closed-loop smart wound dressing incorporating conductive PEDOT hydrogel electrodes for continuous wound monitoring and on-demand electrical stimulation. The flexible bioelectronic system enabled real-time monitoring of wound temperature and skin impedance while delivering electrical stimulation according to changes in the wound microenvironment. The switchable adhesive hydrogel electrodes minimized secondary tissue damage during dressing removal and ensured stable skin contact. In preclinical wound models, the smart dressing significantly accelerated wound closure and enhanced dermal remodeling by promoting pro-regenerative gene expression, demonstrating its potential as an advanced platform for integrated wound monitoring and therapy [170].

Sani et al. developed a flexible and stretchable wearable bioelectronic wound patch incorporating PEDOT:PSS-modified electrochemical sensors for continuous and wireless monitoring of the wound microenvironment. PEDOT:PSS was electrodeposited as a conductive transducer layer beneath an ion-selective membrane to enhance electron transfer and improve the sensitivity and stability of electrochemical signal transduction. The multiplexed sensor array enabled real-time monitoring of metabolic and inflammatory biomarkers, while the integrated platform combined controlled antimicrobial and anti-inflammatory therapy with electrical stimulation to accelerate chronic wound healing. These findings highlight the potential of PEDOT:PSS-based wearable bioelectronics for intelligent wound monitoring and personalized wound management [171]

Liu et al. developed a sodium alginate–calcium–PEDOT:PSS (SCPPC) hydrogel dressing that integrates ionic and electronic conductivity with electrical stimulation for advanced wound management. Through dynamic ionic crosslinking, the hydrogel achieved a skin-like electrical conductivity of 0.0026 S $cm^{-1}$, while maintaining excellent injectability, conformability, self-healing ability, and mechanical stability. The optimized SCPPC hydrogel exhibited a compressive stress of 21.3 ± 1.5 kPa and a modulus of 20.8 ± 1.8 kPa, together with approximately 90% recovery after mechanical strain. When combined with electrical stimulation, the ES + SCPPC dressing achieved 96.46% ± 0.14% wound closure within 10 days, outperforming the corresponding control dressings. Histological analyses indicated that the conductive hydrogel and electrical stimulation synergistically promoted angiogenesis, macrophage polarization, re-epithelialization, collagen deposition, and cell proliferation. In addition to its therapeutic effects, the hydrogel exhibited high strain sensitivity, enabling real-time wound and joint-motion monitoring. Overall, the study demonstrates that PEDOT:PSS-based conductive hydrogels can integrate bioelectrical stimulation, wound healing, conformal dressing, self-healing, and real-time monitoring within a single multifunctional platform, highlighting their potential as next-generation smart wound dressings [172] (Figure 4 and Table 3).



23656549, 2026, 45, Downloaded from https://chemistry-europe.onlinelibrary.wiley.com/doi/10.1002/slct.75081 by Esma AHLATCIOLU ÖZEROL - Yildiz Technical University , Wiley Online Library on [25/11/2026]. See the Terms and Conditions (https://onlinelibrary.wiley.com/terms-and-conditions) on Wiley Online Library for rules of use; OA articles are governed by the applicable Creative Commons License

**TABLE 3** | Recent conductive polymer-based biomaterials for skin tissue engineering and wound healing.

| Material | Fabrication method | Processing parameters | Electrical conductivity | Mechanical properties | Biodegradation | Biological performance | Applications | References |
|---|---|---|---|---|---|---|---|---|
| PANi/SF/PCL (BpS) | Electrospinning | 0.3 wt% PANi, SF/PCL in HFIP, pH 9, basic solvent system | 36 ± 6.1 mS/cm | Young's modulus: 33.4 ± 4 MPa, tensile strength: 1.95 ± 0.16 MPa | ~58% weight loss at 16 weeks | Enhanced hPMSC proliferation, promoted angiogenesis, collagen deposition, re-epithelialization, and accelerated wound closure. | Full-thickness wound dressing, skin tissue regeneration | [91] |
| PANi/SF/PCL (EpS) | electrospinning | 0.3 wt% PANi, SF/PCL in HFIP + FA, pH 3, acidic solvent system | 55.2 ± 4.8 mS/cm | Young's modulus: 5 ± 0.24 MPa, tensile strength: 0.44 ± 0.04 MPa | ~82% weight loss at 16 weeks | Lower cellular proliferation than BpS, prolonged inflammatory response and comparatively inferior wound healing performance | Full-thickness wound dressing, skin tissue regeneration | [91] |
| PANI/curcumin/PAN | Electrospinning | PANI/Cur composite, P0.1C0.25 formulation, light irradiation for activation | Not reported | Not reported | Not reported | 99.77% ± 0.10% *S. aureus* and 98.45% ± 0.27% *E. coli* inhibition, accelerated wound healing in mice | Smart antibacterial wound dressing, protective fabric | [153] |
| TG-g-PANI/PVA (S3) | Electrospinning | 20:80 wt% TG-g-PANI/PVA, total concentration 18 wt% | $1.07 \times 10^{-5}$ S/cm | Young's modulus: 118 ± 8 MPa, tensile strength: 11.4 ± 0.93 MPa, elongation: 58 ± 4% | Degradation after 15 days, higher degradation than S4 | Good L929 fibroblast proliferation and cytocompatibility, 121.6% viability at 72 h, hemocompatible | Skin tissue engineering | [154] |
| TG-g-PANI/PVA (S4) | Electrospinning | 30:70 wt% TG-g-PANI/PVA, total concentration 18 wt% | $0.83 \times 10^{-5}$ S/cm | Young's modulus: 98 ± 4 MPa, tensile strength: 9.7 ± 0.87 MPa, elongation: 47 ± 3% | Degradation after 15 days, lower degradation than S3 | Good L929 fibroblast proliferation and cytocompatibility, 114.3% viability at 72 h, hemocompatible | Skin tissue engineering | [154] |
| Me-PANI NPs@PAM hydrogel | In situ polymerization / chemical crosslinking | Me-PANI NPs used as chemical cross-linking points, NIR irradiation for photothermal activation | Not reported | Maximum stretching ratio: 400% | Not reported | Good biocompatibility, controllable antibacterial activity against Gram-positive bacteria under NIR irradiation, high water absorption | Antibacterial wound dressing, skin regeneration | [155] |
| PVA-g-PANI/PVA (S3) | Electrospinning | 15 wt% PVA-g-PANI | $9.1 \times 10^{-6}$ S/cm | Young's modulus: 194 ± 11 MPa, tensile strength: 27 ± 2 MPa, elongation: 68 ± 6% | 49.1% (14 days) | Good hemocompatibility, favorable biological properties | Skin tissue engineering | [156] |

(Continues)



23655549, 2026, 45, Downloaded from https://chemistry-europe.onlinelibrary.wiley.com/doi/10.1002/slct.75081 by Esma AHL.ATCIOLU ÖZEROL - Yildiz Technical University , Wiley Online Library on [25/11/2026]. See the Terms and Conditions (https://onlinelibrary.wiley.com/terms-and-conditions) on Wiley Online Library for rules of use; OA articles are governed by the applicable Creative Commons License

**TABLE 3** | (Continued)

| Material | Fabrication method | Processing parameters | Electrical conductivity | Mechanical properties | Biodegradation | Biological performance | Applications | References |
|---|---|---|---|---|---|---|---|---|
| PVA-g-PANI/PVA (S4) | Electrospinning | 20 wt% PVA-g-PANI | $2.7 \times 10^{-5}$ S/cm | Young's modulus: 127 ± 5 MPa, tensile strength: 15 ± 1.8 MPa, elongation: 51 ± 4% | 44.7% (14 days) | Good hemocompatibility, favorable biological properties | Skin tissue engineering | [156] |
| NiSe/PANI/PEO nanofibers | Electrospinning | Average fiber diameter: 330 nm | Not reported | Not reported | Not reported | Enhanced antibacterial and antioxidant activity, lower toxicity and 95.6 ± 0.25% wound healing rate. | Wound healing | [157] |
| PVA/TG/PANI nanofibrous membrane | Co-electrospinning | Co-electrospinning of PVA/TG and PVA/PANI solutions, average fiber diameter: 176.45 ± 29 nm | Not reported | Suitable mechanical strength and flexibility, Young's modulus of selected TG-containing membranes: 3.65–3.75 MPa | 40.27% ± 1% weight loss at 28 days | 91.94% HDF-4 cell viability, enhanced antibacterial and antibiofilm activity, promoted cell migration | Skin tissue engineering, wound healing | [158] |
| PANI-PVA-CNPs | Ionic gelation for CNP synthesis, incorporation into PANI-PVA matrix | 1%–3% CNPs, CNP size < 47 nm | Not Reported | Tensile strength: 43.98–48.36 MPa, Young's modulus: 720.21–894.46 MPa, elongation: 42–33.41% | Delayed degradation, PANI-PVA showed 30–45% weight loss over 10–50 days | Antibacterial activity against Gram-positive and Gram-negative bacteria, hemolysis <2% | Skin tissue engineering, wound healing | [143] |
| LAC-PPy microcomposite | Microwave-assisted polymerization | Microwave treatment, optimum treatment time: **5.5 min**, NIR irradiation for photothermal activation | Not reported | Not reported | Not reported | High biocompatibility, NIR-triggered accelerated wound healing, enhanced CD31/CD34 expression, reduced ROS, increased HSP expression and M2 macrophage polarization | Burn wound healing, complex wound treatment | [159] |
| PEG/PVA/HA/PPy | Freeze-thaw | NIR irradiation for photothermal activation | Not reported | Enhanced mechanical properties | Not reported | Enhanced bacterial clearance, promoted macrophage polarization, inflammation resolution, collagen deposition and VEGF expression, accelerated wound healing | Diabetic foot ulcer, chronic wound healing | [160] |

(Continues)



23655549, 2026, 45, Downloaded from https://chemistry-europe.onlinelibrary.wiley.com/doi/10.1002/slct.75081 by Esma AHL.ATCIOLU ÖZEROL - Yildiz Technical University , Wiley Online Library on [25/11/2026]. See the Terms and Conditions (https://onlinelibrary.wiley.com/terms-and-conditions) on Wiley Online Library for rules of use; OA articles are governed by the applicable Creative Commons License

**TABLE 3** | (Continued)

| Material | Fabrication method | Processing parameters | Electrical conductivity | Mechanical properties | Biodegradation | Biological performance | Applications | References |
|---|---|---|---|---|---|---|---|---|
| PPy/chitosan/collagen/PEO nanofibers | Electrospinning | 5–25 wt% PPy | Up to 164.274 × $10^{-3}$ S/m | Young's modulus: 0.78–1.79 MPa, tensile strength: 2.4–4.6 MPa, elongation: 2.4–4.2% for PPCC5–15 | ~26–28% weight loss after 3 weeks for PPCC10–15 | Good biocompatibility, PPCC10 showed superior cell adhesion, growth and proliferation | Skin, nerve and cardiac tissue engineering | [161] |
| PPy@keratin nanofiber membrane (PPy@KNM) | Electrospinning followed by in situ chemical polymerization | 0.6 M $FeCl_3$ oxidant + 0.5 M p-TSA dopant, electrical stimulation: 80 μA, 5 min/day | 1.46 S/cm | Tensile strength: 5.16 ± 0.68 MPa, elongation at break: lowest among tested formulations | Not reported | Good biocompatibility, no cytotoxicity, electrical stimulation enhanced cell growth and proliferation | Electrically stimulated wound healing | [86] |
| PPy-CC/BC capacitive dressing | PPy-wrapped carbon cloth electrodes + bacterial cellulose hydrogel separator | 1 V, 10 min electrical stimulation | Not reported | Not reported | Not reported | 99.97%–99.99% bactericidal efficiency against MDR bacteria, inhibited wound infection and accelerated wound healing | Infected wound treatment | [162] |
| $SeV^{2+}$-PTh/PAAm hydrogel | Solvent-casting | Visible light + low-level electrical stimulation | 1.77 mS/cm (parent hydrogel: 0.54 mS/cm) | Flexible and mechanically stable | Not reported | Dual photothermal/electrical stimulation reduced wound healing time from 15 to 7 days, enhanced tissue regeneration | Smart wound dressing | [163] |
| TG-g-PTh/PVA (S4) | Co-electrospinning | 7 wt% TG-g-PTh | 1.0 × $10^{-3}$ S/cm (TG-g-PTh) | Not reported | Degradation after 15 days, PTh incorporation reduced degradation rate | Enhanced fibroblast adhesion and proliferation, favorable cytocompatibility, hemolysis <3% | Skin tissue engineering | [164] |
| PEDOT:PSS/PVA/κ-carrageenan/CmZnO composite | 3D extrusion | Optimal electrical stimulation, (+)-catechin-loaded mesoporous ZnO | Suitable conductivity, numerical value not reported | Suitable tissue adhesiveness | Not reported | 92.9% *S. aureus* and 95.6% *E. coli* antibacterial activity, enhanced CD31 expression and reduced IL-6 | Conductive wound dressing, full-thickness skin wound healing | [165] |
| PEDOT:PSS/nHA/CS/PCL biocomposite scaffold | Freeze-drying | 66% porosity | 3.55 × $10^{-8}$ S/cm | Improved mechanical properties with PCL incorporation | Not reported | 85% HSF cell viability, cell attachment after 7 days, non-toxic | Skin tissue engineering | [166] |

(Continues)



23655549, 2026, 45, Downloaded from https://chemistry-europe.onlinelibrary.wiley.com/doi/10.1002/slct.75081 by Esma AHL.ATCIOLU ÖZEROL - Yildiz Technical University , Wiley Online Library on [25/11/2026]. See the Terms and Conditions (https://onlinelibrary.wiley.com/terms-and-conditions) on Wiley Online Library for rules of use; OA articles are governed by the applicable Creative Commons License

**TABLE 3** | (Continued)

| Material | Fabrication method | Processing parameters | Electrical conductivity | Mechanical properties | Biodegradation | Biological performance | Applications | References |
|---|---|---|---|---|---|---|---|---|
| PVA/PEDOT:PSS/GCD hydrogel (PPPCD) | Repeated freeze-thaw | PEDOT:PSS:PVA = 2:1 volume ratio | $2.097 \times 10^{-3}$ S/cm | Compressive strength >35 kPa | Not reported | Excellent biocompatibility, enhanced cell migration, angiogenesis and epidermal regeneration, reduced inflammation, ROS scavenging | Conductive wound dressing, skin wound healing | [167] |
| GelMA/PEDOT:PSS hydrogel | DLP 3 D Printing | 0.04% PEDOT:PSS, 10 mA, 100 μs, 20 Hz, 5 min/day electrical stimulation, grooved surface | Excellent, numerical value not reported | Enhanced mechanical strength and swelling | Gradual degradation, higher PEDOT:PSS content accelerated degradation, with P4 showing ~47.9% residual weight after 28 days | Enhanced HDF proliferation, directional migration and orientation, full-thickness skin regeneration under electrical stimulation | Skin wound healing, tissue engineering | [168] |
| CS/GEL/PEDOT electrospun mesh | Electrospinning, in situ chemical polymerization of PEDOT using hyaluronic acid as dopant | PEDOT incorporation into CS/GEL nanofibers | 2306.00 ± 11.40 μS (solution conductivity) | Young's modulus: 0.12 ± 0.05 MPa, tensile strength: 0.83 ± 0.45 MPa, elongation: 9.58 ± 4.25% | 68.69% ± 3.50% hydrolytic degradation at 28 days, enzymatic degradation 76.48 ± 4.71% at 14 days | Suitable water vapor permeability and water uptake properties suitable for wound dressing regeneration | Conductive wound dressing, skin tissue engineering | [169] |
| PEDOT:PSS-modified electrochemical sensor patch | Electrodeposition of PEDOT:PSS | Wireless, multiplexed sensor array | Not reported | Flexible and stretchable | Not reported | Real-time monitoring of metabolic/inflammatory biomarkers, integrated antimicrobial and anti-inflammatory therapy, accelerated chronic wound healing | Wearable smart wound monitoring and personalized therapy | [171] |
| SCPPC hydrogel (sodium alginate–calcium–PEDOT:PSS) | Dynamic ionic cross-linking | Electrical stimulation, optimized SCPPC formulation | 0.0026 S/cm | Compressive stress: 21.3 ± 1.5 kPa, modulus: 20.8 ± 1.8 kPa, ~90% recovery | Not reported | 96.46% wound closure at 10 days, enhanced angiogenesis, macrophage polarization, reepithelialization and collagen deposition, real-time strain sensing | Smart conductive wound dressing, wound monitoring | [172] |



23655549, 2026, 45, Downloaded from https://chemistry-europe.onlinelibrary.wiley.com/doi/10.1002/slct.75081 by Esma AHL.ATCIOLU ÖZEROL - Yildiz Technical University , Wiley Online Library on [25/11/2026]. See the Terms and Conditions (https://onlinelibrary.wiley.com/terms-and-conditions) on Wiley Online Library for rules of use; OA articles are governed by the applicable Creative Commons License

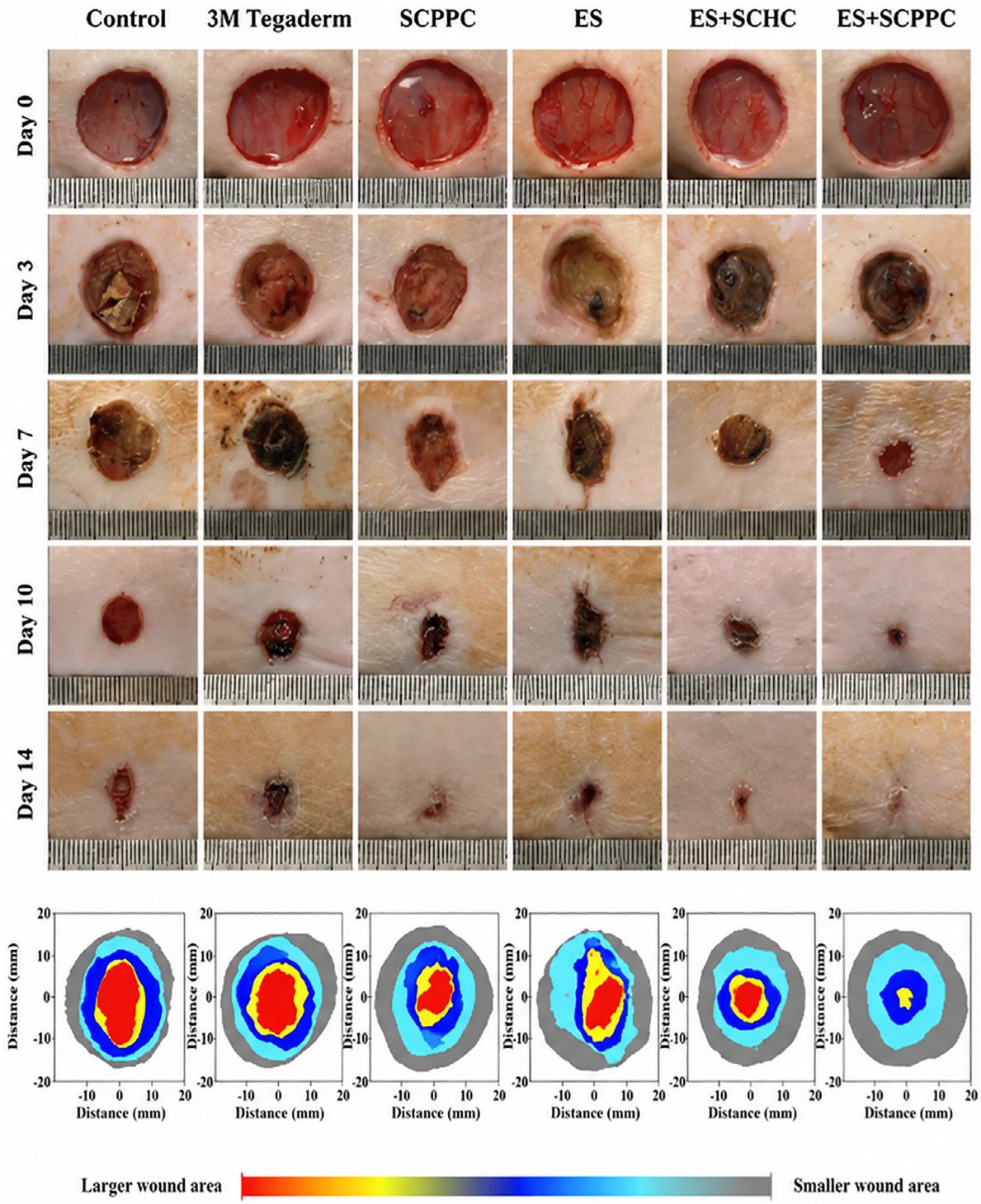


**FIGURE 4** | Enhanced wound regeneration induced by the combination of the conductive SCPPC hydrogel and electrical stimulation. The ES + SCPPC treatment markedly accelerated wound closure compared with the control and other treatment groups, accompanied by increased epidermal thickness and collagen deposition at day 14. These findings demonstrate the potential of integrating conductive hydrogels with electrical stimulation to promote tissue regeneration. Adapted from Liu et al. [172].

### 3.2 | Carbon-Based Materials

Naik et al. developed a CNT-based conductive BSA/cellulose hydrogel for diabetic wound healing by exploiting the electrical conductivity and photothermal properties of CNTs. Increasing CNT concentration significantly enhanced the electrical conductivity of the hydrogel, from $4.4848 \times 10^{-2}$ to $8.7734 \times 10^{-2}$ S/cm, due to the formation of interconnected conductive networks within the hydrogel matrix. The hydrogel also exhibited controlled biodegradability and good biocompatibility, while its tunable electrical and ionic conductivity supported bioelectrical signaling and cell communication at the wound site. In vivo



23656549, 2026, 45, Downloaded from https://chemistry-europe.onlinelibrary.wiley.com/doi/10.1002/slct.75081 by Esma AHLATCIOLU ÖZEROL - Yildiz Technical University , Wiley Online Library on [25/11/2026]. See the Terms and Conditions (https://onlinelibrary.wiley.com/terms-and-conditions) on Wiley Online Library for rules of use; OA articles are governed by the applicable Creative Commons License

studies demonstrated accelerated wound closure, particularly following NIR irradiation, accompanied by reduced inflammation, enhanced collagen deposition, and promoted angiogenesis, as confirmed by CD68, $\alpha$-SMA, and CD31 expression. Furthermore, photoacoustic imaging enabled non-invasive monitoring of vascularity and tissue oxygenation during wound healing. These findings highlight the potential of CNT-based hydrogels as multifunctional wound dressings integrating electrical stimulation, photothermal therapy, and real-time monitoring for chronic diabetic wound management [173].

Elabbasy et al. developed nanocomposite wound dressing films based on a poly(vinyl alcohol)/hyaluronic acid (PVA/HA) matrix incorporating $Sb_2O_3$, $Ca_3(PO_4)_2$, and carbon nanotubes (CNTs) using a solution casting approach. The $Ca_3(PO_4)_2/Sb_2O_3$/CNT-containing film exhibited a porous structure with 48.1% ± 6.1% porosity and pore sizes ranging from 120 to 350 nm, supporting potential cellular infiltration and proliferation. The film demonstrated good mechanical performance, with a tensile strength of 35.94 ± 0.64 MPa and an elongation at break of 168.13% ± 11.29%, together with substantial swelling capacity (450.6% ± 15.9%). In vitro studies demonstrated good cytocompatibility, with approximately 123% cell viability after 3 days, while the composite exhibited antibacterial activity against *Escherichia coli* with an inhibition zone of 25.9 ± 1.1 mm. These findings highlight the potential of PVA/HA-based CNT-containing nanocomposite films as mechanically robust and antibacterial wound dressing materials [174].

Sun et al. developed a multifunctional microneedle patch consisting of an aligned CNT sheet integrated with a HA matrix and VEGF for wound healing. The aligned CNT layer provided an ordered microstructure that promoted fibroblast alignment while its photo- and electrothermal conversion properties enabled externally controlled VEGF release. The released VEGF further facilitated endothelial cell tubular formation, supporting angiogenesis and tissue regeneration. In vivo experiments demonstrated that the aligned CNT-integrated, VEGF-loaded microneedle patch accelerated wound repair. The study highlights the potential of CNT-based intelligent microneedle patches to simultaneously provide cell-guiding topography, controlled therapeutic delivery, and externally responsive functionality for regenerative medicine. However, the authors noted that moisture retention and scalable production remain challenges for practical application [175].

Wu et al. developed a multifunctional photothermal electroactive sponge scaffold (PC1Z2) composed of CNTs, pyrrolidonecarboxylic acid zinc (PC1Z2), and a decellularized dermal matrix for diabetic wound treatment. The CNT-based scaffold exhibited high electrical conductivity and water absorption capacity, enabling the transmission of endogenous electric fields to wound tissues while efficiently absorbing wound exudates. Upon NIR irradiation, the scaffold generated photothermal heat and achieved 98% antibacterial efficacy, while the gradual release of $Zn^{2+}$ contributed to the alleviation of chronic inflammation. In a diabetic wound model, the scaffold promoted hemostasis, granulation tissue formation, angiogenesis, collagen deposition, and re-epithelialization, thereby accelerating tissue repair. These findings demonstrate the potential of CNT-based electroactive sponges as multifunctional wound dressings that integrate bioelectrical signal transmission, photothermal antibacterial activity, exudate management, and inflammatory regulation for chronic diabetic wound healing [176].

Liu et al. developed CS/Gel scaffolds incorporating different concentrations of multi-walled carbon nanotubes (MWCNTs) to overcome the limited electrical conductivity of conventional hydrogel scaffolds for STE. MWCNT incorporation significantly enhanced the electrical conductivity and mechanical strength of the scaffolds, while the 0.3% MWCNT-containing scaffold exhibited superior biocompatibility. Furthermore, fibroblasts seeded on the conductive scaffolds responded positively to electrical stimulation, showing enhanced cell proliferation and increased expression of type I and type III collagen. These findings highlight the potential of CS/Gel/MWCNT scaffolds to enhance fibroblast activity and ECM production through electrical stimulation, supporting their application in conductive wound dressings and skin tissue engineering [177].

Parikh et al. developed biomimetic hierarchical all-carbon scaffolds consisting of CNT carpets covalently bonded to flexible carbon fabric through surface plasma activation followed by CVD. The covalent attachment of CNTs minimized the potential cytotoxicity associated with freely dispersed CNTs while providing a multiscale architecture capable of guiding cellular behavior. The scaffolds exhibited good biocompatibility and supported the migration and proliferation of keratinocytes and fibroblasts, with cells migrating toward and subsequently proliferating within the CNT carpets. Cell growth could be modulated by controlling CNT carpet height and surface wettability, while the scaffolds also provided cytoprotection against UVB-induced environmental stress. Shorter CNTs combined with hydrophilic surfaces demonstrated particularly favorable characteristics for future applications. Overall, these hierarchical carbon scaffolds showed potential as durable, biomimetic platforms for directed cell growth, wound healing, and tissue regeneration [178].

Chen et al. developed electroactive nanofibrous scaffolds to accelerate wound healing by incorporating MWCNTs into a PCL/gelatin matrix. The MWCNTs were dispersed in the PCL/gelatin solution, and the resulting composite scaffolds were fabricated via electrospinning. The biological performance of the scaffolds was evaluated through both in vitro and in vivo studies. Compared with the control scaffolds, the PCL/gelatin/CNT scaffolds significantly enhanced the proliferation of L929 fibroblasts and HUVECs and upregulated wound-healing-related genes, including Col I, Col III, and VEGF. The incorporation of MWCNTs also provided an electrical conductivity of $4.31 \times 10^{-5} \pm 2.28 \times 10^{-5}$ S/c m enabling the scaffolds to effectively respond to electrical stimulation. Consequently, the electroactive PCL/gelatin/CNT scaffolds promoted tissue regeneration and accelerated wound closure, highlighting the potential of CNT-based conductive nanofibers for electrically assisted wound healing [179]. (Figure 5)

Ribeiro et al. developed chitosan films containing GQDs for the treatment of infected wounds. The incorporation of GQDs into the chitosan matrix provided a biocompatible and mechanically stable dressing, while chitosan contributed antibacterial and anti-inflammatory properties. The resulting films exhibited a well-structured and flexible morphology and demonstrated



23656549, 2026, 45, Downloaded from https://chemistry-europe.onlinelibrary.wiley.com/doi/10.1002/slct.75081 by Esma AHLATCIOLU ÖZEROL - Yildiz Technical University , Wiley Online Library on [25/11/2026]. See the Terms and Conditions (https://onlinelibrary.wiley.com/terms-and-conditions) on Wiley Online Library for rules of use; OA articles are governed by the applicable Creative Commons License

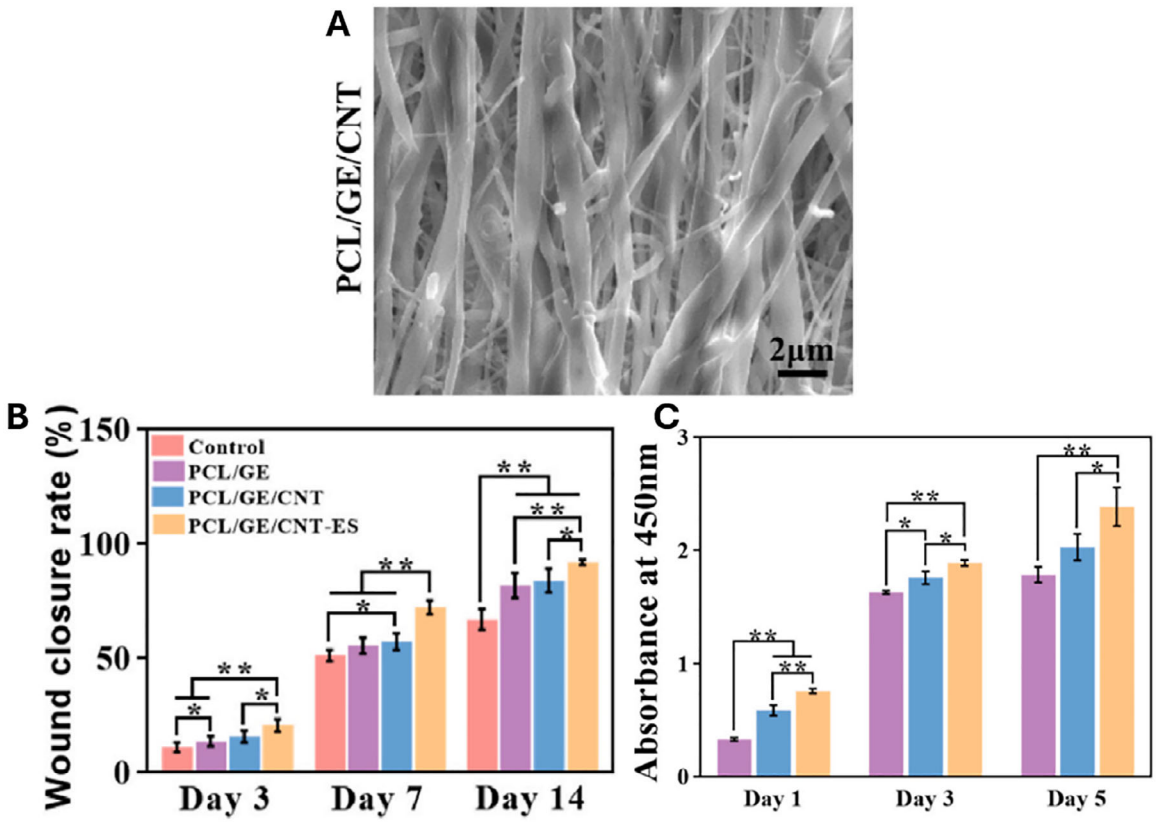


**FIGURE 5** | (A) SEM images of the scaffold. (B) Wound healing process histogram. (C) Cell viability of L929 cells in PCL/GE, PCL/GE/CNT, and PCL/GE/CNT-ES [179].

enhanced cell migration and antibacterial activity, together with low hemolytic activity and favorable moisture-retention capacity. These findings suggest that GQD-containing chitosan films can provide a multifunctional wound-healing platform by combining the biological properties of chitosan with the functional characteristics of GQDs, highlighting their potential for the treatment of infected wounds [180].

Shivam et al. developed a GQD-polyacrylic acid (PAA) hybrid hydrogel as a biomimetic dressing for diabetic wound healing. The incorporation of GQDs into the PAA matrix resulted in a porous, hydrophilic, and water-retentive scaffold with antibacterial and cell-signaling functionalities. In vivo studies using diabetic Wistar albino rats demonstrated that hydrogels containing 0.05%–0.1% GQDs achieved complete wound closure within 13 days, outperforming both natural and standard controls. The optimized GQD-PAA hydrogels also reduced the expression of pro-inflammatory cytokines (IL-6 and TNF-$\alpha$) while increasing the anti-inflammatory cytokine IL-10, indicating improved inflammatory regulation during wound healing. In addition, the hybrid hydrogels exhibited antibacterial activity against *E. coli* and favorable biocompatibility, while their porous structure supported oxygenation, moisture retention, and cell migration. These findings highlight the potential of GQDs as multifunctional nanofillers that can enhance the antibacterial, anti-inflammatory, and wound-healing performance of polymeric hydrogels [181].

Shanmugam et al. developed GO- and rGO-based aloe vera hydrogel formulations for wound healing applications. GO and rGO were uniformly incorporated into aloe vera gel and hydrogel matrices, respectively, and their biological performance was evaluated through in vitro and in vivo assays. The graphene-based formulations exhibited favorable cell viability, attachment, and proliferation, indicating good cytocompatibility. In vivo studies using male Wistar rats further demonstrated enhanced wound contraction and re-epithelialization compared with the untreated control. These findings suggest that the incorporation of GO/rGO into aloe vera-based hydrogels can improve the therapeutic performance of wound dressings and promote tissue regeneration, highlighting their potential as multifunctional graphene-based wound-healing materials [182].

Sanmugam et al. developed chitosan-curcumin-based hybrid nanocomposites incorporating GO and copper oxide (CuO) using a facile one-pot chemical synthesis method. The hybrid nanocomposites exhibited sustained and controlled curcumin release together with pronounced antibacterial activity against *S. aureus* and *E. coli*. In addition, they promoted favorable cytocompatibility with L929 fibroblast cells by enhancing cell adhesion and proliferation. Owing to their high surface area, biocompatibility, and multifunctional antibacterial properties, these chitosan-based hybrid nanocomposites demonstrate considerable potential for wound dressing applications [183].

Xie et al. developed a multifunctional foam gel wound dressing consisting of chitooligosaccharide-modified graphene oxide (CG) nanocomposites incorporated into a calcium alginate foam matrix. The incorporation of CG improved the mechanical prop-



23656549, 2026, 45, Downloaded from https://chemistry-europe.onlinelibrary.wiley.com/doi/10.1002/slct.75081 by Esma AHLATCIOLU ÖZEROL - Yildiz Technical University , Wiley Online Library on [25/11/2026]. See the Terms and Conditions (https://onlinelibrary.wiley.com/terms-and-conditions) on Wiley Online Library for rules of use; OA articles are governed by the applicable Creative Commons License

erties, thermal stability, porosity, water absorption, and water retention of the dressing while providing enhanced antibacterial and hemostatic activities. Owing to the strong interaction between CG and platelets, the dressing achieved rapid hemostasis within 10 s. In a full-thickness wound model, CG-loaded foam gel significantly accelerated wound closure, with wounds nearly completely healed within 12 days. Histological analysis further demonstrated reduced inflammation and enhanced vascular remodeling, indicating the potential of CG-based foam gels as multifunctional wound dressings for promoting tissue regeneration [119].

Luong et al. developed GO-incorporated poly(ethylene glycol) methyl ether methacrylate ($MeO_2MA$) hydrogels for wound-healing applications. GO was incorporated into the $MeO_2MA$ matrix through free-radical polymerization, and increasing GO content significantly enhanced the mechanical performance of the hydrogels, with tensile strength increasing from 223 kPa for the pristine hydrogel to 303, 463, and 626 kPa with increasing GO concentrations. The GO/$MeO_2MA$ hydrogels exhibited favorable swelling behavior and were non-cytotoxic toward human dermal fibroblasts, indicating good biocompatibility. In vivo evaluation using a rat skin wound model demonstrated that the GO-containing hydrogel achieved more than 95% wound closure after 15 days, outperforming the pristine hydrogel. Histopathological analysis further confirmed enhanced tissue regeneration. These findings demonstrate that incorporating GO into MEO2MA hydrogels can improve both the mechanical performance and wound-healing efficacy of the scaffold, highlighting the potential of GO-based hydrogels for advanced wound dressings [118].

Liu et al. developed PVA/GO-CDPC-La films using a solution-based fabrication approach, in which GO was functionalized with citicoline and $La^{3+}$ ions to improve its dispersion and antibacterial performance. The resulting films exhibited enhanced hydrophilicity and water absorption, enabling effective wound exudate management while maintaining a moist environment. Moreover, GO-CDPC-La incorporation improved antibacterial activity without compromising cytocompatibility or cell adhesion. In vivo, the films promoted faster wound closure and mature epidermal regeneration. These findings demonstrate that functionalization of GO with bioactive ionic components can overcome some limitations of pristine GO and provide multifunctional wound dressings combining antibacterial activity with favorable biological compatibility [184].

Jafarkhani et al. employed freeze-drying to fabricate hybrid scaffolds by incorporating GO into decellularized tissue (DT) to address the poor mechanical properties of native DT-derived constructs. Increasing GO content enhanced the mechanical strength of the scaffolds, while the 3 wt% GO formulation exhibited approximately 25% higher cell viability than the pristine DT scaffold. The porous architecture of the DT/GO scaffolds further supported cell adhesion, proliferation, and cellular activity over 7 days. These findings suggest that GO incorporation can simultaneously reinforce decellularized scaffolds and maintain their cytocompatibility, although the optimal GO concentration is important to achieve a balance between mechanical enhancement and biological performance [185].

Pollini et al. developed electrospun nanofibrous scaffolds based on PCL and Col incorporating conductive graphene nanosheets (Gr) to enhance electrically stimulated wound healing. The incorporation of Gr significantly increased the electrical conductivity of the scaffolds, with the PCLCOL-Gr2 formulation exhibiting the highest conductivity. The scaffolds showed adequate mechanical resistance under cyclic loading up to 10 Hz and a slow degradation rate over 28 days, providing sustained structural support during tissue regeneration. In vitro studies demonstrated good biocompatibility, fibroblast adhesion, and proliferation, while the combination of Gr-doped scaffolds with external electrical stimulation promoted oriented fibroblast alignment, in contrast to the randomly organized cells observed without stimulation. In vivo, the PCLCOL-Gr2 scaffold combined with electrical stimulation achieved complete re-epithelialization by day 18, accompanied by enhanced collagen remodeling and restoration of sebaceous glands and hair follicles. Overall, the study demonstrated that graphene-doped PCL/collagen nanofibrous scaffolds can enhance electrically stimulated wound healing by promoting fibroblast alignment, organized collagen deposition, and skin regeneration [186].

Narayanan et al. developed electrospun poly(vinyl alcohol) (PVA) nanofibrous scaffolds reinforced with glucose-reduced graphene oxide (GRGO) for skin tissue engineering. GRGO was incorporated at concentrations of 0–1.0 wt% and the nanofibrous scaffolds were subsequently crosslinked with glutaraldehyde. Increasing GRGO content resulted in thicker nanofibers and enhanced thermal stability, while tensile strength and elongation at break decreased, which was attributed to the nonuniform distribution of GRGO and the formation of rigid acetal bonds during crosslinking. GRGO incorporation also shifted the scaffold surface toward greater hydrophobicity. Importantly, all scaffolds exhibited good hemocompatibility and cytocompatibility, while the 1.0 wt% GRGO-containing scaffold significantly enhanced fibroblast metabolic activity after 21 days. Overall, the results demonstrated that GRGO-doped PVA nanofibrous scaffolds possess promising biocompatibility and cell proliferation-supporting properties for sSTE applications [187].

Sanmugam et al. synthesized rGO/$ZrO_2$-activated ZnO nanocomposite via a one-pot chemical method. The hybrid nanocomposite exhibited excellent thermal stability, significant cytotoxic activity against human lung cancer cells, and potent antibacterial activity against *E. coli* and *S. aureus*, demonstrating its potential for wound dressing applications. The authors also highlighted that the incorporation of rGO into ZnO-based nanocomposites is generally associated with enhanced electrical conductivity, mechanical strength, and multifunctional performance, making these materials promising candidates for advanced biomedical applications [188].

Sellepan et al. developed bioactive chitosan-alginate scaffolds reinforced with nickel oxide-curcumin (NiO-Cur) nanocomposites using sol-gel synthesis, chemical crosslinking, and freeze-drying. The incorporation of NiO-Cur nanocomposites significantly improved the physicochemical, mechanical, and antibacterial properties of the scaffolds while promoting controlled drug release, biomineralization, and osteoconductive potential. The multifunctional scaffold exhibited enhanced antibacterial activity against *S. aureus* and *E. coli*, demonstrating its potential for



23656549, 2026, 45, Downloaded from https://chemistry-europe.onlinelibrary.wiley.com/doi/10.1002/slct.75081 by Esma AHLATCIOLU ÖZEROL - Yildiz Technical University , Wiley Online Library on [25/11/2026]. See the Terms and Conditions (https://onlinelibrary.wiley.com/terms-and-conditions) on Wiley Online Library for rules of use; OA articles are governed by the applicable Creative Commons License

bone tissue engineering and infected bone regeneration. This study highlights the growing interest in incorporating functional nanocomposites into polymeric scaffolds to enhance the biological performance of tissue engineering constructs [189].

Bakadia et al. developed a multifunctional rGO-silk protein hybrid hydrogel in which teicoplanin served as a green reducing agent for GO while simultaneously providing residual antibacterial functionality. Incorporation of 0.2 wt% rGO improved the mechanical and thermal properties of the hydrogel and provided self-healing and shear-thinning behavior without compromising cytocompatibility. Beyond conventional antibacterial activity, the hydrogel effectively eradicated bacterial biofilms and exhibited high penetration into hydroxyapatite-associated biofilms, addressing the challenge of bone-associated infections in diabetic wounds. In vivo, the rGO-SP hydrogel enhanced wound contraction, re-epithelialization, angiogenesis, and M2 macrophage polarization while suppressing inflammatory responses and MMP-9 expression. The hydrogel also promoted bone regeneration in an infected tibial defect model, suggesting potential for preventing diabetic foot osteomyelitis. However, the lack of clinical validation remains an important limitation, and further studies are required to establish its long-term safety and therapeutic efficacy in humans [96].

Narayanan et al. synthesized rGO using *Lysinibacillus sphaericus* as a green reducing and stabilizing agent and incorporated the resulting L-rGO into polyacrylamide hydrogels for STE. The L-rGO-containing hydrogels exhibited good cytocompatibility and supported fibroblast adhesion and proliferation, maintaining approximately 83% cell viability after 28 days. However, L-rGO incorporation at 0.25 mg/mL unexpectedly enhanced biofilm formation by *P. aeruginosa* and *S. aureus*, possibly due to adsorption of organic components onto the carbon nanomaterial surface. These findings demonstrate that although biologically synthesized rGO can improve scaffold biocompatibility, its concentration and potential effects on biofilm formation must be carefully considered [190].

Sun et al. developed an antioxidative active-shrinkage hydrogel (AHF@AS Gel) incorporating amino- and hydroxyl-functionalized C70 fullerene (AHF) into a thermosensitive hydrogel composed of N-isopropylacrylamide (NIPAM) and alginate. The incorporation of AHF provided antioxidant activity by reducing excessive reactive oxygen species (ROS), thereby alleviating inflammation, preventing cellular apoptosis, and promoting fibroblast migration. Meanwhile, the thermoresponsive active-shrinkage network generated mechanical stimulation that promoted skin contraction and activated the epidermal growth factor receptor/Akt (EGFR/Akt) pathway, enhancing cell proliferation. The AHF@AS Gel consequently promoted re-epithelialization and skin contraction, resulting in approximately 2.7-fold and 1.7-fold improvements in re-epithelialization in acute and diabetic chronic wounds, respectively. In vivo studies further demonstrated accelerated wound closure in both acute and diabetic mouse models by regulating the inflammatory, proliferative, and remodeling phases. Overall, this study highlights the potential of functionalized fullerene-based hydrogels to integrate antioxidant biochemical regulation with mechanical stimulation for enhanced wound healing [191].

Li et al. developed antioxidant nanofibrous membranes by electrospinning sodium alginate (SA) with a multi-ether fullerene derivative (mono-C60-O), combining the biocompatibility of SA with the potent antioxidant activity of fullerene. The resulting SA/mono-C60-O nanofibers exhibited a uniform morphology, high hydrophilicity, water absorption capacity, and good cytocompatibility and hemocompatibility. Notably, the SA/mono-C60-O-25 membrane demonstrated strong free-radical scavenging activity, with removal efficiencies of approximately 93.3%, 91.1%, and 92.2% against DPPH, ABTS, and hydroxyl radicals, respectively. In a full-thickness wound model, treatment with the nanofibrous membrane significantly accelerated wound closure compared with SA and control groups. Histological and immunohistochemical analyses indicated that the enhanced healing was associated with reduced oxidative stress and inflammation, increased angiogenesis, collagen deposition, and skin regeneration. These findings demonstrate that the incorporation of fullerene derivatives into electrospun SA nanofibers can provide an effective antioxidant strategy for regulating the oxidative microenvironment and promoting wound healing. However, further evaluation of the long-term biocompatibility and in vivo safety of fullerene derivatives is necessary to clarify their potential for clinical translation [192].

Chen et al. developed a C60@PDA/GelMA hybrid hydrogel as an antioxidative wound dressing by incorporating mussel-inspired C60@PDA nanocomposites into GelMA. The hydrogel exhibited sustained ROS-scavenging activity, good cytocompatibility, hemocompatibility, and antibacterial properties, together with elastic and shear-thinning behavior. In vivo studies demonstrated accelerated wound closure and enhanced re-epithelialization, collagen deposition, and angiogenesis, highlighting the potential of fullerene-based hydrogels for regulating oxidative stress and promoting skin regeneration [124].

Shan et al. developed a multifunctional injectable conductive hydrogel based on a polysaccharide biopolymer, PVA, and hydroxylated graphene, in which dynamic borate ester bonds and supramolecular interactions provided rapid self-healing and mechanical adaptability. The hydrogel exhibited conductivity, injectability, pH responsiveness, and real-time motion monitoring capabilities while enabling in situ bacterial detection through electrical signal variations. Furthermore, its photothermal antibacterial activity effectively eliminated bacteria without relying on antibiotics, thereby reducing the risk of antimicrobial resistance. Owing to its excellent biocompatibility, electromechanical performance, and ability to conform to irregular wound surfaces, the hydrogel successfully promoted infected joint wound healing in vivo, highlighting its potential as a multifunctional bioelectronic wound dressing for integrated wound monitoring and therapy [193] (Table 4).

### 3.3 | Metallic Materials

Dong et al. developed a tensile, self-healing, and biocompatible PAA-CMCS-Au hydrogel containing ultrasmall gold nanoparticles (UsAuNPs, 1–3 nm) for the treatment of infected wounds. Carboxymethyl chitosan (CMCS) stabilized the UsAuNPs and prevented their aggregation, thereby improving their dispersion and antibacterial efficacy within the polyacrylic acid (PAA)



23655549, 2026, 45, Downloaded from https://chemistry-europe.onlinelibrary.wiley.com/doi/10.1002/slct.75081 by Esma AHLATCIOLU ÖZEROL - Yildiz Technical University , Wiley Online Library on [25/11/2026]. See the Terms and Conditions (https://onlinelibrary.wiley.com/terms-and-conditions) on Wiley Online Library for rules of use; OA articles are governed by the applicable Creative Commons License

**TABLE 4** | Recent carbon-based conductive biomaterials for skin tissue engineering and wound healing.

| Material | Fabrication method | Processing parameters | Electrical conductivity | Mechanical properties | Biodegradation | Biological performance | Applications | References |
|---|---|---|---|---|---|---|---|---|
| CNT-based BSA/cellulose hydrogel | Hydrogel fabrication, CNT incorporation | Increasing CNT concentration, NIR irradiation | $4.4848 \times 10^{-2}$–$8.7734 \times 10^{-2}$ S/cm | Adhesive strength increased from 1.5 ± 0.34 to 10.89 ± 1.14 kPa with CNT incorporation | Controlled weight loss over 20 days | Accelerated wound closure, reduced inflammation, enhanced collagen deposition and angiogenesis, photoacoustic monitoring of vascularity and oxygenation | Diabetic wound healing, multifunctional smart wound dressing | [173] |
| PVA/HA/$Sb_2O_3$/$Ca_3(PO_4)_2$/CNT nanocomposite film | Solvent casting | CNT, $Sb_2O_3$ and $Ca_3(PO_4)_2$ incorporation | Not reported | Tensile strength: 35.94 ± 0.64 MPa, elongation at break: 168.13% ± 11.29% | Not reported | ~123% cell viability, antibacterial activity against *E. coli* (25.9 ± 1.1 mm inhibition zone) | Antibacterial wound dressing | [174] |
| Aligned CNT/HA/VEGF microneedle patch | Microneedle patch fabrication with aligned CNT sheet integration | 808 nm NIR irradiation, photo-/electrothermal stimulation for controlled VEGF release | Conductive, numerical value not reported | Flexible, maintained conductivity under bending/stretching | Not reported | Promoted fibroblast alignment, endothelial tube formation and angiogenesis, accelerated wound regeneration | Smart microneedle wound dressing, controlled drug delivery | [175] |
| CNT/PC1Z2/decellularized dermal matrix (PADM) sponge | Sponge scaffold fabrication | NIR irradiation, $Zn^{2+}$ release | High conductivity, numerical value not reported | Young Modulus 0.46 ± 0.03 MPa | Not reported | 98% antibacterial efficacy, promoted hemostasis, granulation tissue formation, angiogenesis, collagen deposition and re-epithelialization | Photothermal and electroactive dressing for diabetic wounds | [176] |
| CS/Gel/MWCNT composite scaffold | Scaffold fabrication, MWCNT incorporation | 0.3–0.5% MWCNTs, electrical stimulation | $2.42 \times 10^{-4}$ S/cm for wet CS/Gel, conductivity increased with MWCNT content | Tensile stress: 13.671 kPa, compressive stress: 54.25 kPa, compressive modulus: 15.2 kPa (0.5% MWCNT) | Not reported | 0.3% MWCNT showed superior biocompatibility, electrical stimulation enhanced fibroblast proliferation and type I/III collagen expression | Conductive wound dressing, skin tissue engineering | [177] |
| CNT-coated carbon fiber fabric | Surface plasma activation followed by CVD | CNT carpet length and surface wettability were varied | Conductive, exact value not reported | Flexible carbon fiber fabric provided mechanical support, strong covalent CNT attachment | Nonbiodegradable / durable scaffold | Good biocompatibility, supported keratinocyte and fibroblast migration and proliferation, Short CNTs showed more favorable cell growth, cytoprotective against UVB | Wound healing, skin regeneration, tissue engineering | [178] |

(Continues)



23655549, 2026, 45, Downloaded from https://chemistry-europe.onlinelibrary.wiley.com/doi/10.1002/slct.75081 by Esma AHL.ATCIOLU ÖZEROL - Yildiz Technical University , Wiley Online Library on [25/11/2026]. See the Terms and Conditions (https://onlinelibrary.wiley.com/terms-and-conditions) on Wiley Online Library for rules of use; OA articles are governed by the applicable Creative Commons License

**TABLE 4** | (Continued)

| Material | Fabrication method | Processing parameters | Electrical conductivity | Mechanical properties | Biodegradation | Biological performance | Applications | References |
|---|---|---|---|---|---|---|---|---|
| PCL/Gelatin/MWCNT | Electrospinning | MWCNT incorporated into PCL/gelatin matrix, combined with electrical stimulation | $4.31 \times 10^{-3}$ S/m | Not reported | In vivo degradation evaluated over 14 days, good biocompatibility with no notable foreign-body or inflammatory reaction | Enhanced L929 fibroblast and HUVEC proliferation, upregulated Col I, Col III, and VEGF, promoted macrophage regulation, angiogenesis, collagen deposition and re-epithelialization | Electroactive wound dressing, electrically assisted skin regeneration | [179] |
| Chitosan/GQD films | Film fabrication, GQDs incorporated into chitosan matrix | GQD incorporation into chitosan | Not reported | Flexible and mechanically stable | Not reported | Enhanced cell migration and antibacterial activity, low hemolytic activity, favorable moisture retention, biocompatible | Infected wound dressing, wound healing | [180] |
| GQD/PAA hybrid hydrogel | Hydrogel fabrication, GQDs incorporated into PAA matrix | 0.05%–0.1% GQD | Not reported | Porous and hydrophilic hydrogel with good water-retention capacity, mechanical values not reported | Not reported | Complete wound closure within 13 days, reduced IL-6 and TNF-$\alpha$ and increased IL-10, antibacterial activity against *E. coli*, non-toxic and biocompatible, supported cell migration and oxygenation | Diabetic wound dressing, wound healing | [181] |
| GO/rGO–*Aloe vera* gel/hydrogel | GO synthesized by modified Hummer's method, GO/rGO uniformly incorporated into aloe vera gel/hydrogel | GO and rGO incorporation into aloe vera matrices | Not reported | Not reported | Not reported | Good cell viability, attachment, and proliferation, enhanced wound contraction and re-epithelialization in vivo | Wound healing, tissue regeneration | [182] |
| Chitosan/CUR/GO/CuO hybrid nanocomposite | Facile one-pot chemical synthesis | Chitosan incorporated with curcumin, GO and CuO | Not reported | Not reported | Not reported | Sustained and controlled curcumin release, strong antibacterial activity against *S. aureus* and *E. coli*, favorable cytocompatibility with L929 fibroblasts, enhanced cell adhesion and proliferation | Antibacterial wound dressing, wound healing | [183] |

(Continues)



23655549, 2026, 45, Downloaded from https://chemistry-europe.onlinelibrary.wiley.com/doi/10.1002/slct.75081 by Esma AHL.ATCIOLU ÖZEROL - Yildiz Technical University , Wiley Online Library on [25/11/2026]. See the Terms and Conditions (https://onlinelibrary.wiley.com/terms-and-conditions) on Wiley Online Library for rules of use; OA articles are governed by the applicable Creative Commons License

**TABLE 4** | (Continued)

| Material | Fabrication method | Processing parameters | Electrical conductivity | Mechanical properties | Biodegradation | Biological performance | Applications | References |
|---|---|---|---|---|---|---|---|---|
| CG/Calcium alginate foam gel (chitooligosaccharide -modified GO) | Foam gel fabrication / incorporation of CG nanocomposite into calcium alginate foam | CG incorporated into calcium alginate foam matrix | Not reported | CG incorporation improved mechanical strength, stress–strain curves indicate maximum stress up to ~470 kPa depending on formulation | Not reported | Enhanced antibacterial and hemostatic activity, rapid hemostasis within 10 s, reduced inflammation, promoted vascular remodeling, accelerated wound closure with near-complete healing within 12 days | Multifunctional wound dressing, hemostatic and antibacterial wound treatment | [119] |
| GO/$MeO_2MA$ hydrogel | Free-radical polymerization | GO incorporated at different concentrations into $MeO_2MA$ matrix | Not reported | Tensile strength increased from 223 kPa (pristine) to 303, 463, and 626 kPa with increasing GO content | Not reported | Noncytotoxic to human dermal fibroblasts, favorable swelling, >95% wound closure after 15 days in rat wound model, enhanced tissue regeneration | Wound healing, advanced conductive/GO-based wound dressing | [118] |
| PVA/GO-CDPC-La film | Solution intercalation method | GO functionalized with citicoline (CDPC) and $La^{3+}$ ions, followed by incorporation into PVA | Not reported | Not reported | Not reported | Enhanced hydrophilicity and water absorption, effective exudate absorption, improved antibacterial activity, good cytocompatibility and cell adhesion, accelerated wound closure and mature epidermal regeneration in vivo | Multifunctional antibacterial wound dressing | [184] |
| DT/GO scaffold | Freeze-drying | GO incorporated into decellularized tissue (DT), GO content varied up to 5 wt% | Not reported | Young's modulus increased from 8.4 ± 1.3 kPa (0% GO) to a maximum elastic modulus of 12.7 ± 2.5 kPa at 5% GO, attributed to partial covalent interactions between DT and GO and pore filling by GO | Not reported | 3 wt% GO showed approximately 25% higher cell viability than pristine DT, porous structure supported cell adhesion, proliferation, and cellular activity over 7 days | Skin tissue engineering | [185] |

(Continues)



23655549, 2026, 45, Downloaded from https://chemistry-europe.onlinelibrary.wiley.com/doi/10.1002/slct.75081 by Esma AHL.ATCIOLU ÖZEROL - Yildiz Technical University , Wiley Online Library on [25/11/2026]. See the Terms and Conditions (https://onlinelibrary.wiley.com/terms-and-conditions) on Wiley Online Library for rules of use; OA articles are governed by the applicable Creative Commons License

**TABLE 4** | (Continued)

| Material | Fabrication method | Processing parameters | Electrical conductivity | Mechanical properties | Biodegradation | Biological performance | Applications | References |
|---|---|---|---|---|---|---|---|---|
| PCL/Col-Gr nanofibrous scaffold | Electrospinning | PCL/Collagen incorporating different graphene nanosheet (Gr) concentrations, PCLCOL-Gr2 showed the highest Gr content | PCLCOL-Gr2: 12.8 ± 3.09 kΩ surface resistance, undoped PCLCOL: 54.5 ± 8.9 kΩ. Higher Gr content increased conductivity | Maximum elongation at break of 159.9% ± 14% for PCLCOL, Young's modulus and tensile strength decreased with increasing Gr content, while elongation remained unchanged. Stable under cyclic loading and hydration | Slow degradation over 28 days, degradation rate decreased with increasing Gr concentration | Good biocompatibility, fibroblast adhesion and proliferation, electrical stimulation promoted oriented fibroblast alignment, enhanced collagen remodeling, complete re-epithelialization by day 18, and restoration of sebaceous glands and hair follicles in vivo | Electrically stimulated wound healing, skin tissue engineering | [186] |
| PVA/GRGO nanofibrous scaffold | Electrospinning followed by chemical crosslinking | PVA containing 0–1.0 wt% glucose-reduced graphene oxide (GRGO), crosslinked with 0.7 wt% glutaraldehyde in acidic acetone medium | Not reported | Tensile strength: 5.96 ± 0.97 MPa (PG-0) → 2.58 ± 0.43 MPa (PG-1.0). Elongation at break: 78.3% ± 3.9% → 11.5%. Increasing GRGO generally decreased tensile strength and elongation, attributed to restricted PVA chain mobility and crosslinking effects | Not reported | Good hemocompatibility and cytocompatibility, no significant hemolysis even at 1 wt% GRGO. All scaffolds supported fibroblast viability and proliferation, PG-1.0 significantly increased fibroblast metabolic activity after 21 days | Skin tissue engineering, wound dressing | [187] |

(Continues)



23655549, 2026, 45, Downloaded from https://chemistry-europe.onlinelibrary.wiley.com/doi/10.1002/slct.75081 by Esma AHL.ATCIOLU ÖZEROL - Yildiz Technical University , Wiley Online Library on [25/11/2026]. See the Terms and Conditions (https://onlinelibrary.wiley.com/terms-and-conditions) on Wiley Online Library for rules of use; OA articles are governed by the applicable Creative Commons License

**TABLE 4** | (Continued)

| Material | Fabrication method | Processing parameters | Electrical conductivity | Mechanical properties | Biodegradation | Biological performance | Applications | References |
|---|---|---|---|---|---|---|---|---|
| rGO-$ZrO_2$/ZnO nanocomposite | One-pot chemical synthesis | rGO incorporated with $ZrO_2$-activated ZnO nanoparticles | NR, the authors state that rGO incorporation can enhance electrical conductivity | NR, enhanced mechanical strength is reported as a general advantage of rGO incorporation, but no quantitative mechanical data were provided | Not reported | Potent antibacterial activity against *E. coli* and *S. aureus*, exhibited high cytotoxic activity against A549 human lung cancer cells, high thermal stability | Antibacterial wound dressing, biomedical applications | [188] |
| Chitosan–alginate/NiO-Cur (CANC) scaffold | Sol–gel synthesis, chemical crosslinking, freeze-drying | NiO-Cur nanocomposites incorporated into chitosan–alginate (CA) matrix, CANC1–CANC3 formulations | Not reported | Compressive strength: 406.1 ± 3.79 kPa, porosity: 85.72 ± 1.01–91.08% ± 1.19%, interconnected pores: 114–132 μm, G′ > G′′, indicating stable viscoelastic structure | Controlled degradation under physiological conditions, quantitative degradation rate not reported | Strong antibacterial activity: inhibition zone 10.78 ± 0.23 mm against *S. aureus* and 8.05 ± 0.20 mm against *E. coli*, dense apatite formation within 14 days in SBF, high hydrophilicity and swelling, Cur release after 72 h: 72.05%–83.95% | Bone tissue engineering, infected bone regeneration | [189] |
| rGO–silk protein (SP) hybrid hydrogel | Green reduction of GO followed by physicochemical crosslinking | 0.2 wt% rGO, teicoplanin used as a green reducing agent and antibacterial component, silk protein crosslinked with genipin | Not reported | Incorporation of 0.2 wt% rGO improved mechanical and thermal properties, hydrogel exhibited self-healing and shear-thinning behavior | Not reported | Good cytocompatibility, enhanced cell proliferation and migration, strong antibiofilm activity, and accelerated wound healing, angiogenesis, M2 macrophage polarization, and bone regeneration. | Diabetic wound healing | [121] |
| L-rGO/ polyacrylamide hydrogel | Microbial synthesis of rGO followed by hydrogel fabrication | *Lysinibacillus sphaericus* used as green reducing/stabilizing agent, L-rGO incorporated into polyacrylamide hydrogel, 0.25 mg/mL L-rGO evaluated | Not reported | Not reported | Not reported | Good cytocompatibility, supported fibroblast proliferation with 83% cell viability after 28 days. However, 0.25 mg/mL L-rGO increased biofilm formation by *P. aeruginosa* and *S. aureus* | Skin tissue engineering | [190] |

(Continues)



23655549, 2026, 45, Downloaded from https://chemistry-europe.onlinelibrary.wiley.com/doi/10.1002/slct.75081 by Esma AHL.ATCIOLU ÖZEROL - Yildiz Technical University , Wiley Online Library on [25/11/2026]. See the Terms and Conditions (https://onlinelibrary.wiley.com/terms-and-conditions) on Wiley Online Library for rules of use; OA articles are governed by the applicable Creative Commons License

**TABLE 4** | (Continued)

| Material | Fabrication method | Processing parameters | Electrical conductivity | Mechanical properties | Biodegradation | Biological performance | Applications | References |
|---|---|---|---|---|---|---|---|---|
| AHF@AS Gel (C70 fullerene/ thermosensitive hydrogel) | Facile solid-liquid derivatization | Amino- and hydroxyl-functionalized C70 fullerene (AHF) incorporated into NIPAM/alginate thermosensitive hydrogel | Not reported | Thermoresponsive active-shrinkage behavior providing mechanical stimulation, activated the EGFR/Akt pathway | Not reported | Antioxidant and anti-inflammatory activity, reduced ROS and apoptosis and promoted fibroblast migration. Enhanced re-epithelialization by approximately 2.7-fold in acute wounds and 1.7-fold in diabetic wounds, accelerated wound closure | Diabetic and acute wound healing | [191] |
| SA/mono-$C_{60}$-O nanofibrous membrane | Electrospinning | Sodium alginate (SA) incorporated with multi-ether fullerene derivative (mono-$C_{60}$-O), increasing mono-$C_{60}$-O increased solution viscosity | Decreased with increasing mono-C60-O content, quantitative conductivity value not reported | Not reported | Not reported | Good cytocompatibility and hemocompatibility, strong antioxidant activity with 93.3% DPPH, 91.1% ABTS, and 92.2% hydroxyl radical scavenging, accelerated wound closure and promoted angiogenesis, collagen deposition, and skin regeneration | Wound healing, antioxidant wound dressing | [192] |
| $C_{60}$@PDA/ GelMA hydrogel | Hydrogel fabrication, in situ gel formation | $C_{60}$@PDA nanocomposites incorporated into GelMA hydrogel | Not reported | Elastic and stable hydrogel, $G' > G''$, storage modulus $>10^4$ Pa, shear-thinning, CPGH remained intact up to 150% strain, compressive strength of control GelMA hydrogel: 3.7 kPa | Not reported | Sustained ROS-scavenging, antioxidant, antibacterial, cytocompatible and hemocompatible. Promoted re-epithelialization, collagen deposition and angiogenesis, accelerated wound closure by 38.5% and 42.9% on days 3 and 7, respectively | Cutaneous wound healing | [124] |



23655549, 2026, 45, Downloaded from https://chemistry-europe.onlinelibrary.wiley.com/doi/10.1002/slct.75081 by Esma AHL.ATCIOLU ÖZEROL - Yildiz Technical University , Wiley Online Library on [25/11/2026]. See the Terms and Conditions (https://onlinelibrary.wiley.com/terms-and-conditions) on Wiley Online Library for rules of use; OA articles are governed by the applicable Creative Commons License

hydrogel network. The resulting hydrogel exhibited enhanced mechanical and self-healing properties, together with strong and sustained antibacterial activity against *S. aureus* and *E. coli*. The antibacterial effect was attributed to the interaction of UsAuNPs with bacterial surfaces, disruption of membrane integrity and potential, and induction of oxidative stress through reactive oxygen species generation. In vivo studies further demonstrated accelerated healing of *S. aureus*-infected wounds, accompanied by reduced inflammation and improved skin tissue reconstruction. Overall, the PAA-CMCS-Au hydrogel combined mechanical robustness, biocompatibility, antibacterial activity, and wound-healing functionality, highlighting the potential of ultrasmall AuNPs as effective antibacterial nanofillers for multifunctional wound dressings. However, the authors noted that the current system has limitations in achieving sustained and controlled nanoparticle release, which may need to be addressed for clinical translation [128].

Kolarijani et al. developed electrospun PCL/gelatin nanofibrous scaffolds incorporating gold nanoparticles (AuNPs) at concentrations of 200, 400, and 800 ppm for full-thickness wound treatment. The resulting scaffolds exhibited suitable mechanical properties, porosity, wettability, water uptake, and blood compatibility. Among the tested formulations, the scaffold containing 400 ppm AuNPs demonstrated the highest L929 fibroblast proliferation. Furthermore, in vivo evaluation using a rat full-thickness wound model showed that the AuNP-containing scaffold significantly promoted wound healing compared with sterile gauze. These findings highlight the potential of AuNP-incorporated nanofibrous scaffolds as multifunctional wound dressings, with an optimized AuNP concentration being important for maximizing cellular responses and tissue regeneration [129].

Salama et al. developed curcumin-loaded gold nanoparticles (Cur-AuNPs) incorporated into Pluronic F127 gel as a topical delivery system for diabetic wound healing. The optimized AuNP formulation exhibited a particle size of $41.77 \pm 6.8$ nm and a high curcumin entrapment efficiency of $94.43\% \pm 0.25\%$. Incorporation of curcumin into AuNPs followed by integration into the F127 gel enhanced drug release and skin permeation compared with free curcumin. Moreover, Cur-AuNPs exhibited enhanced antibacterial activity against both Gram-positive and Gram-negative bacteria, as evidenced by reduced minimum inhibitory concentrations and improved antibiofilm activity. In a diabetic wound model, the Cur-AuNP formulation promoted wound closure, reduced oxidative stress and inflammation, and enhanced collagen deposition, cellular proliferation, and angiogenesis compared with free curcumin. These findings demonstrate the potential of AuNPs not only as functional nanomaterials but also as effective nanocarriers for improving the delivery and therapeutic efficacy of poorly soluble bioactive compounds in diabetic wound treatment [194].

Hong et al. developed multifunctional gold-based nanoflowers (PAu@C/B) incorporating chlorin e6 (Ce6) and bromfenac sodium (BS) to combine mild photothermal therapy (mPTT), photodynamic therapy (PDT), and controlled anti-inflammatory drug delivery for infected skin wound healing. Upon NIR irradiation, the nanoflowers generated a mild temperature of approximately 45°C and reactive oxygen species through PDT, while simultaneously triggering the controlled release of BS. This synergistic approach achieved approximately 99% antibacterial efficiency and effective biofilm inhibition in vitro. In vivo, the nanoflowers exhibited good biocompatibility and significantly accelerated healing of wounds infected with drug-resistant bacteria. Furthermore, BS-mediated inflammation control promoted growth factor production, collagen deposition, and angiogenesis, thereby enhancing tissue regeneration. Overall, the study demonstrates the potential of combining mild photothermal and photodynamic antibacterial effects with controlled anti-inflammatory drug delivery for the treatment of infected wounds [195].

Amiri et al. developed a collagen-based silver nanoparticle (AgNP)-hydrogel composite as a multifunctional wound dressing designed to simultaneously prevent bacterial infection and support tissue regeneration. AgNPs were incorporated into the hydrogel at concentrations of 200, 400, and 600 ppm, and the resulting composites exhibited significant antibacterial activity both in vitro and in vivo, whereas the hydrogel alone showed no antibacterial effect. In a rat splinted wound model, AgNP-hydrogel treatment accelerated wound healing without causing adverse effects. The composites also demonstrated favorable biocompatibility, as indicated by MTT assays and in vivo histological evaluation, with no significant alterations in hematological or biochemical parameters. These findings highlight the potential of AgNP-containing hydrogels as multifunctional wound dressings that combine effective antibacterial activity with a supportive three-dimensional scaffold for tissue repair [196].

Chen et al. developed lysozyme (LYZ)-stabilized silver nanoparticles (LYZ/AgNPs) through a facile and green one-step synthesis under visible-light irradiation. In this approach, LYZ acted as both a reducing and stabilizing agent, enabling the rapid and stable formation of AgNPs in an aqueous environment. The resulting LYZ/AgNPs exhibited broad-spectrum and efficient antibacterial activity, attributed to the synergistic antibacterial effects of AgNPs and lysozyme. Furthermore, a LYZ/AgNPs-loaded cream demonstrated effective antibacterial activity in vitro and in vivo and significantly promoted scald wound healing. The composite also showed good stability and could be readily redispersed after lyophilization, supporting its practical storage and application. These findings highlight LYZ-mediated AgNP synthesis as an environmentally friendly strategy for producing multifunctional antibacterial nanomaterials with potential applications in wound infection control and tissue repair [197].

Sharma et al. developed a biocompatible AgNP-based hydrogel using '*Cyperus rotundus*' extract as a green reducing and stabilizing agent for wound-healing applications. The synthesized AgNPs exhibited good stability and potent antibacterial activity against '*E. coli*' and '*Staphylococcus epidermidis*', together with antioxidant and anti-inflammatory properties. The AgNPs were subsequently incorporated into a Carbopol 974P hydrogel, which demonstrated significant antibacterial activity and promoted wound contraction in an excision wound model, with performance comparable to the standard treatment. In vitro cytotoxicity assays further confirmed favorable biocompatibility, suggesting that the hydrogel may mitigate some of the toxicity concerns associated with conventional AgNP-based formulations. Overall, the study highlights green-synthesized AgNPs as promising mul-



23656549, 2026, 45, Downloaded from https://chemistry-europe.onlinelibrary.wiley.com/doi/10.1002/slct.75081 by Esma AHLATCIOLU ÖZEROL - Yildiz Technical University , Wiley Online Library on [25/11/2026]. See the Terms and Conditions (https://onlinelibrary.wiley.com/terms-and-conditions) on Wiley Online Library for rules of use; OA articles are governed by the applicable Creative Commons License

tifunctional components for antibacterial and anti-inflammatory wound dressings [134].

Wang et al. developed a flexible electrical patch (ePatch) based on a conductive hydrogel composed of silver nanowires (AgNWs) and methacrylated alginate (MAA) to overcome the poor conformability of conventional electrical stimulation devices to wound surfaces. AgNWs provided electrical conductivity and antibacterial activity, while alginate contributed to biocompatibility and printability. A double-crosslinked hydrogel network further improved the mechanical stability of the patch in the wound environment. Electrical stimulation delivered by the ePatch enhanced fibroblast proliferation and migration and growth factor secretion, while in vivo studies demonstrated accelerated re-epithelialization, angiogenesis, immune regulation, and infection prevention. In a Sprague–Dawley rat wound model, the ePatch reduced wound closure time to approximately 7 days compared with 20 days in untreated wounds, highlighting its potential as a flexible and multifunctional platform for electrically stimulated wound healing [198].

Arumugam et al. developed silk fibroin/gelatin nanofibrous scaffolds incorporating silver and gold nanoparticles (Ag–Au) via electrospinning for wound dressing applications. The resulting composite nanofibers exhibited a well-defined fibrous morphology and favorable structural characteristics, while the incorporation of Ag and Au nanoparticles provided a multifunctional platform for wound treatment. In vitro evaluation using L929 fibroblasts confirmed favorable cellular viability with limited apoptosis. Furthermore, in vivo studies in Sprague-Dawley rats demonstrated that the SF/gelatin/Ag–Au nanofibrous scaffolds significantly accelerated wound closure, achieving a 99.58% wound healing rate after 21 days compared with the control groups. These findings highlight the potential of combining bimetallic Ag–Au nanoparticles with protein-based nanofibrous scaffolds to enhance the biological performance of wound dressings and promote tissue regeneration [199].

Najafian-Najafabadi et al. developed a biomimetic multilayered skin regeneration system combining a PCL–gelatin electrospun scaffold containing bromelain–silver nanoparticles (Bro-AgNPs) with an alginate hydrogel incorporating bioglass (BGPs) and selenium-doped bioglass particles (SeBGPs), together with mesenchymal stem cell (MSC) injection. Bro-AgNPs provided strong antibacterial activity and increased the yield strength of the PCL–gelatin scaffold from 1.30 ± 0.12 to 1.59 ± 0.20 MPa while maintaining comparable stiffness. Incorporation of BGPs and SeBGPs into the alginate hydrogel reduced swelling and porosity while supporting cell viability and proliferation. In vivo, the SeBGPs + MSCs treatment achieved the highest wound closure throughout the experimental period, with histological analysis demonstrating enhanced epithelialization and well-organized collagen deposition without significant inflammation by day 21. Overall, the composite scaffold provided a combination of antibacterial protection, improved mechanical performance, cellular support, and enhanced tissue regeneration, highlighting its potential for skin tissue engineering applications (Figure 6) [200].

Ragothaman et al. developed a bio-hybrid hydrogel composed of collagen, aminated xanthan gum (AXG), bio-capped silver nanoparticles (AgNPs), and melatonin for the treatment of infected chronic wounds. Collagen was used as a green reducing and stabilizing agent for the synthesis of highly stable AgNPs with an average particle size of 16 ± 3 nm, while AXG provided a biodegradable polymeric and gel-forming matrix. The resulting hydrogel exhibited favorable gelation, rheological, morphological, and degelation properties and showed strong antibacterial activity against both Gram-positive and Gram-negative bacteria, including multidrug-resistant *K. pneumoniae*. The hydrogel also demonstrated excellent cytocompatibility with NIH 3T3 fibroblasts. In vivo, the synergistic effects of AgNPs and melatonin enhanced re-epithelialization, collagen deposition, and angiogenesis, attributed to their combined antimicrobial, antioxidant, and anti-inflammatory activities. Overall, the study highlights the potential of multifunctional AgNP- and melatonin-loaded hydrogels for infected chronic wounds, burns, and diabetic wound treatment [201].

Srivastava et al. developed silver nanoparticle (AgNP)-coated tasar fibroin nanofibrous mats for skin tissue engineering and wound dressing applications. Tasar fibroin nanofibers were fabricated using an ionic liquid, 1-butyl-3-methylimidazolium acetate, and subsequently coated in situ with AgNPs synthesized using Tridax procumbens leaf extract as a green reducing agent. The successful incorporation of AgNPs was confirmed by XRD, TEM, EDX, and EDX mapping analyses. AgNP coating enhanced the therapeutic potential of the nanofibrous mats while maintaining good mechanical strength, water absorption, and adequate porosity, together with antimicrobial and biological activity. Overall, the AgNP-coated tasar fibroin nanofibrous mats demonstrated potential as antimicrobial wound dressings, drug delivery vehicles, and tissue-engineered scaffolds, although further in vivo and clinical studies are required to establish their practical applicability [202].

Afghah et al. developed 3D-printed polycaprolactone-block-poly(1,3-propylene succinate) (PCL-PPSu) scaffolds incorporating silver nitrate for STE and wound healing. Incorporation of PPSu into PCL enabled lower processing temperatures, improved hydrophilicity, and enhanced hydrolytic and enzymatic degradation compared with neat PCL. The optimized 3D-printing parameters produced porous scaffolds with well-defined interconnected structures, supporting nutrient and oxygen transport. Incorporation of 1 wt% silver nitrate provided antimicrobial activity by significantly reducing microbial adhesion without inducing cytotoxicity in human dermal fibroblasts. Silver nitrate was particularly effective against *E. coli* and *C. albicans*, while its activity against *P. aeruginosa* and *S. aureus* was comparatively lower. Overall, the combination of controlled degradation, low-temperature processability, interconnected porosity, hydrophilicity, and antimicrobial activity makes PCL-PPSu/silver composites promising candidates for 3D-printed skin regenerative scaffolds [203].

Kumari et al. investigated the effect of copper nanoparticles (CuNPs) on the physicochemical and biological properties of chitosan–gelatin composite scaffolds for STE. The CuNP-doped scaffolds were fabricated by freeze-drying with CuNP concentrations of 0.01%, 0.02%, and 0.03%. The scaffolds exhibited interconnected porous structures, with the average pore size increasing from 25–40 μm to approximately 95 μm following CuNP incorporation, while overall porosity ranged from 65% to



23656549, 2026, 45, Downloaded from https://chemistry-europe.onlinelibrary.wiley.com/doi/10.1002/slct.75081 by Esma AHLATCIOLU ÖZEROL - Yildiz Technical University , Wiley Online Library on [25/11/2026]. See the Terms and Conditions (https://onlinelibrary.wiley.com/terms-and-conditions) on Wiley Online Library for rules of use; OA articles are governed by the applicable Creative Commons License

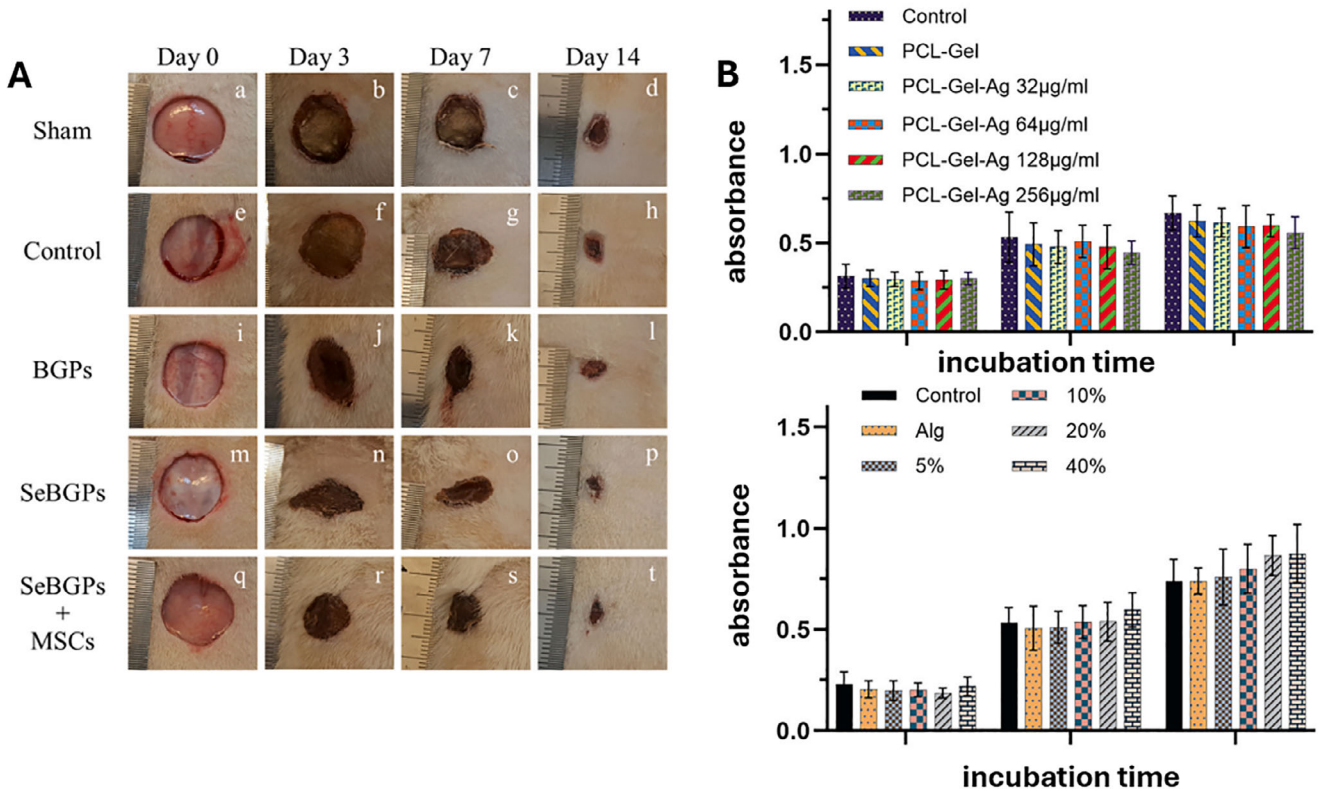


**FIGURE 6** | (A) macroscopic views of wound closure under different treatment groups. (B) cell viability results performed with MSCs [200].

88%. The incorporation of 0.03% CuNPs decreased the scaffold degradation rate but did not adversely affect cell adhesion or proliferation. Importantly, the CuNP-containing scaffolds showed good hemocompatibility and cytocompatibility without significant reactive oxygen species (ROS) generation, indicating limited oxidative stress. Overall, CuNP incorporation improved selected structural and degradation characteristics while maintaining the biological compatibility of chitosan–gelatin scaffolds, demonstrating their potential for STE applications [204].

Ghosh et al. developed copper-loaded alginate fibers as bioactive surgical sutures for accelerating incisional wound healing. Copper ions were selected due to their roles in angiogenesis, growth factor induction, and extracellular matrix remodeling. Approximately 95% of the loaded copper was released within the first 24 h, providing localized and rapid copper delivery at the wound site. In a mouse incisional wound model, copper-eluting sutures significantly improved tissue biomechanical strength compared with conventional nylon and calcium alginate sutures during the early healing period. Histological and immunohistochemical analyses demonstrated reduced epithelial gaps and increased $CD31^+$ cells, indicating enhanced angiogenesis. Although the copper alginate fibers also exhibited a strong photothermal response upon NIR irradiation, comparable healing efficacy was observed without irradiation. Importantly, copper delivery did not induce significant toxicity under the tested conditions. Overall, the study highlights the potential of copper-ion-releasing fibers as bioactive sutures for promoting angiogenesis and accelerating surgical and trauma wound repair [205].

Xu et al. developed an antibiotic-free multifunctional hydrogel (PulMA/CuS@PC) by incorporating phycocyanin-functionalized copper sulfide (CuS@PC) nanoparticles into a photocrosslinkable methacrylated pullulan (PulMA) matrix for infected wound treatment. The resulting hydrogel exhibited favorable mechanical properties, swelling capacity, and biocompatibility, while CuS@PC nanoparticles significantly enhanced its photothermal antibacterial activity against *E. coli* and *S. aureus*. In vivo studies using a full-thickness infected wound model demonstrated accelerated wound healing, accompanied by reduced inflammatory responses, enhanced collagen deposition, tissue regeneration, and increased angiogenesis. These findings indicate that CuS-based nanocomposites can provide multifunctional antibacterial and regenerative properties when integrated into hydrogel wound dressings, highlighting their potential as antibiotic-free strategies for infected wound management [206].

Fan et al. developed 3D-printed copper-doped 1393-2B bioglass/chitosan (Cu-BG/CS) wound dressings to promote skin regeneration and functional repair. Compared with BG/CS dressings, Cu-BG/CS exhibited enhanced antibacterial activity and vascularization, highlighting the contribution of Cu ions to wound repair. The Cu-BG/CS scaffold was further loaded with SB216763, a bioactive compound targeting the Wnt/$\beta$-catenin pathway. The resulting Cu-BG/CS@SB dressing enhanced fibroblast proliferation and upregulated $\beta$-catenin expression in vitro. In vivo, Cu-BG/CS@SB significantly accelerated wound closure, reaching approximately 85% closure by day 10, and promoted hair follicle regeneration and func-



23656549, 2026, 45, Downloaded from https://chemistry-europe.onlinelibrary.wiley.com/doi/10.1002/slct.75081 by Esma AHLATCIOLU ÖZEROL - Yildiz Technical University , Wiley Online Library on [25/11/2026]. See the Terms and Conditions (https://onlinelibrary.wiley.com/terms-and-conditions) on Wiley Online Library for rules of use; OA articles are governed by the applicable Creative Commons License

**TABLE 5** | Recent metallic conductive biomaterials for skin tissue engineering and wound healing.

| Material | Fabrication method | Processing parameters | Electrical conductivity | Mechanical properties | Biodegradation | Biological performance | Applications | References |
|---|---|---|---|---|---|---|---|---|
| PAA-CMCS-Au hydrogel | One pot method | UsAuNPs (1–3 nm) stabilized with CMCS and incorporated into PAA hydrogel network | Not reported | High tensile strength, self-healing ability, enhanced mechanical stability | Not reported | Strong and sustained antibacterial activity against *S. aureus* and *E. coli*, good biocompatibility, accelerated healing of infected wounds, reduced inflammation, and improved tissue reconstruction | Infected wound healing, antibacterial wound dressing | [128] |
| PCL/Gel/AuNPs nanofibrous scaffold | Electrospinning | AuNPs incorporated at 200, 400, and 800 ppm | Not reported | Elastic modulus: 48.55 ± 5.2 MPa (PCL/Gel) and 35.79 ± 4.85 MPa (800 ppm AuNPs), elongation at break: 13.6% ± 1.1% and 9.4% ± 2.4%, respectively. Mechanical properties decreased with increasing AuNP content, but differences were not significant | Weight loss after 7/14 days decreased with increasing AuNP content. For 800 ppm AuNPs: 7.93% ± 0.93% / 13.94% ± 1.54%, indicating slower degradation | Suitable porosity, wettability, water uptake, and blood compatibility, 400 ppm AuNPs showed the highest L929 fibroblast proliferation. In vivo, AuNP-containing scaffolds significantly enhanced wound healing compared with sterile gauze | Full-thickness wound healing, multifunctional wound dressing | [129] |
| Cur-AuNPs/F127 gel | Nanoparticle synthesis followed by incorporation into Pluronic F127 gel | Curcumin-loaded AuNPs, particle size 41.77 ± 6.8 nm, curcumin entrapment efficiency 94.43% ± 0.25% | Not reported | Not reported | Not reported | Enhanced antibacterial and antibiofilm activity, improved curcumin release and skin permeation, promoted wound closure, reduced oxidative stress and inflammation, and enhanced collagen deposition, cell proliferation, and angiogenesis in diabetic wounds | Diabetic wound healing, topical drug delivery | [194] |
| PAu@C/B nanoflowers (Ce6/BS-loaded gold-based nanoflowers) | Chemical synthesis of multifunctional gold-based nanoflowers | NIR irradiation, mild photothermal temperature ≈45°C, Ce6-mediated PDT and BS-controlled release | Not reported | Not reported | Not reported | ≈99% antibacterial efficiency, effective biofilm inhibition, good biocompatibility, enhanced growth factor production, collagen deposition, angiogenesis, and wound healing against drug-resistant bacterial infection | Infected skin wound healing, antibacterial and anti-inflammatory wound therapy | [195] |

(Continues)



23655549, 2026, 45, Downloaded from https://chemistry-europe.onlinelibrary.wiley.com/doi/10.1002/slct.75081 by Esma AHL.ATCIOLU ÖZEROL - Yildiz Technical University , Wiley Online Library on [25/11/2026]. See the Terms and Conditions (https://onlinelibrary.wiley.com/terms-and-conditions) on Wiley Online Library for rules of use; OA articles are governed by the applicable Creative Commons License

**TABLE 5** | (Continued)

| Material | Fabrication method | Processing parameters | Electrical conductivity | Mechanical properties | Biodegradation | Biological performance | Applications | References |
|---|---|---|---|---|---|---|---|---|
| AgNP–collagen hydrogel composite | Chemical reduction of Ag | AgNP concentrations: 200, 400, and 600 ppm | Not reported | Not reported | Not reported | Significant in vitro and in vivo antibacterial activity, favorable biocompatibility, accelerated wound healing, no significant hematological or biochemical alterations, no adverse effects | Infected wound healing, antibacterial and tissue-regenerative wound dressing | [196] |
| LYZ-stabilized AgNPs (LYZ/AgNPs) | Green one-step synthesis under visible-light irradiation | Lysozyme (LYZ) served as both reducing and stabilizing agent, aqueous synthesis, visible-light irradiation, lyophiliza-tion/redispersion | Not reported | Not reported | Not reported | Broad-spectrum and efficient antibacterial activity, synergistic antibacterial effect of AgNPs and LYZ, promoted scald wound healing in vitro and in vivo, good stability | Wound infection control, antibacterial wound dressing/cream, tissue repair | [197] |
| AgNP–Carbopol 974P hydrogel | Green synthesis of AgNPs using *Cyperus rotundus* extract, followed by incorporation into Carbopol 974P hydrogel | *C. rotundus* extract served as reducing and stabilizing agent, AgNPs incorporated into Carbopol 974P hydrogel | Not reported | Not reported | Not reported | Potent antibacterial activity against *E. coli* and *S. epidermidis*, antioxidant and anti-inflammatory activity, favorable cytocompatibility, enhanced wound contraction | Antibacterial, anti-inflammatory, and wound-healing applications | [134] |
| AgNW–MAA conductive hydrogel (ePatch) | Mask-based printing of AgNW/MAA hydrogel onto a silicone substrate, double-crosslinked hydrogel network | Electrode thickness ≈5 μm, AgNWs uniformly distributed within hydrogel | $1.54 \times 10^5$ S/m | Enhanced mechanical stability due to double-crosslinked hydrogel network, flexible and conformable to wound surfaces | Not reported | Enhanced fibroblast proliferation, migration, and growth-factor secretion, accelerated re-epithelialization and angiogenesis, immune regulation and infection prevention, wound closure ≈7 days versus 20 days in untreated wounds | Flexible electrical stimulation patch for wound healing, infection prevention, electrically stimulated tissue regeneration | [198] |

(Continues)



23655549, 2026, 45, Downloaded from https://chemistry-europe.onlinelibrary.wiley.com/doi/10.1002/slct.75081 by Esma AHL.ATCIOLU ÖZEROL - Yildiz Technical University , Wiley Online Library on [25/11/2026]. See the Terms and Conditions (https://onlinelibrary.wiley.com/terms-and-conditions) on Wiley Online Library for rules of use; OA articles are governed by the applicable Creative Commons License

**TABLE 5** | (Continued)

| Material | Fabrication method | Processing parameters | Electrical conductivity | Mechanical properties | Biodegradation | Biological performance | Applications | References |
|---|---|---|---|---|---|---|---|---|
| SF/gelatin/Ag-Au composite nanofibers | Electrospinning of silk fibroin (SF)/gelatin containing Ag and Au nanoparticles | Electrospinning, nanofiber roughness ≈777 nm, thickness ≈292.71 nm, Ag/Au NPs characterized by FE-SEM and HR-TEM | Not reported | Not reported | Not reported | High cell viability and limited apoptosis in L929 fibroblasts, enhanced cell differentiation, migration, proliferation, and regeneration, high biocompatibility and cellular uptake, reduced inflammation, 99.58% wound healing after 21 days in Sprague–Dawley rats | Wound dressing, tissue regeneration and skin repair | [199] |
| PCL–gelatin/Bro-AgNPs electrospun scaffold + Alg/BGPs or SeBGPs hydrogel | Electrospinning of PCL–gelatin scaffold containing bromelain–silver nanoparticles (Bro-AgNPs), combined with alginate hydrogel incorporating bioglass (BGPs) or selenium-doped bioglass (SeBGPs), MSC injection | Bro-AgNP incorporation, multilayered biomimetic skin regeneration system, BGPs/SeBGPs incorporated into alginate hydrogel | Not reported | Bro-AgNPs increased yield strength from 1.30 ± 0.12 to 1.59 ± 0.20 MPa, elastic modulus remained comparable, increased UTS and slightly increased elongation at break, indicating improved structural integrity, ductility, and flexibility | PCL-Gel-Bro-AgNPs: 63.68% ± 5.08% degradation after 21 days versus 68.31% ± 5.93% for PCL-Gel, BGP/SeBGP hydrogels also showed reduced weight loss (68.31% ± 5.93% and 69.73 ± 5.89%, respectively) compared with Alg hydrogel (76.18% ± 7.42%) | Strong antibacterial activity, reduced swelling and porosity, supported cell viability and proliferation, SeBGPs + MSCs produced the highest wound closure, enhanced epithelialization and organized collagen deposition without significant inflammation at day 21 | Skin tissue engineering, multilayered wound dressing, antibacterial and regenerative skin repair | [200] |

(Continues)



23655549, 2026, 45, Downloaded from https://chemistry-europe.onlinelibrary.wiley.com/doi/10.1002/slct.75081 by Esma AHL.ATCIOLU ÖZEROL - Yildiz Technical University , Wiley Online Library on [25/11/2026]. See the Terms and Conditions (https://onlinelibrary.wiley.com/terms-and-conditions) on Wiley Online Library for rules of use; OA articles are governed by the applicable Creative Commons License

**TABLE 5** | (Continued)

| Material | Fabrication method | Processing parameters | Electrical conductivity | Mechanical properties | Biodegradation | Biological performance | Applications | References |
|---|---|---|---|---|---|---|---|---|
| Collagen/AXG/AgNPs/melatonin bio-hybrid hydrogel | Green synthesis of AgNPs using collagen as reducing and stabilizing agent, followed by incorporation into collagen/aminated xanthan gum (AXG) hydrogel with melatonin | AgNP size: 16 ± 3 nm, freeze-dried hydrogel, non-covalently cross-linked hydrogel system | Not reported | Not reported | Not directly reported, hydrogel underwent rapid degelation/weight loss, with AgNP- and/or melatonin-containing hydrogels showing >93% weight loss after 4 days. This represents hydrogel-to-liquid transformation rather than degradation | Strong antibacterial activity against Gram-positive and Gram-negative bacteria, including multidrug-resistant *K. pneumoniae*, excellent cytocompatibility with NIH 3T3 fibroblasts, enhanced re-epithelialization, collagen deposition, and angiogenesis through antimicrobial, antioxidant, and anti-inflammatory effects | Infected chronic wounds, burns, diabetic wound healing, tissue regeneration | [201] |
| AgNP-coated tasar fibroin nanofibrous mats | Electrospinning using ionic liquid 1-butyl-3-methylimidazolium acetate, followed by in situ coating with green-synthesized AgNPs | AgNPs synthesized using *Tridax procumbens* leaf extract as reducing agent, AgNP incorporation confirmed by XRD, TEM, EDX and EDX mapping | Not reported | Tensile strength: 12 MPa, Young's modulus: 35 MPa, elongation at break: 28 mm, good extensibility and flexibility suitable for load-bearing areas | 6% mass loss after 30 days in PBS, 48% mass loss after 30 days in PBS with trypsin, indicating controlled degradation under non-enzymatic conditions and accelerated enzymatic degradation | Antimicrobial activity, favorable biological activity, good water absorption and adequate porosity, maintained mechanical integrity, potential for supporting tissue regeneration | Antimicrobial wound dressing, drug delivery, skin tissue engineering scaffold, applications in load-bearing wound areas such as knees and joints | [202] |

(Continues)



23655549, 2026, 45, Downloaded from https://chemistry-europe.onlinelibrary.wiley.com/doi/10.1002/slct.75081 by Esma AHL.ATCIOLU ÖZEROL - Yildiz Technical University , Wiley Online Library on [25/11/2026]. See the Terms and Conditions (https://onlinelibrary.wiley.com/terms-and-conditions) on Wiley Online Library for rules of use; OA articles are governed by the applicable Creative Commons License

**TABLE 5** | (Continued)

| Material | Fabrication method | Processing parameters | Electrical conductivity | Mechanical properties | Biodegradation | Biological performance | Applications | References |
|---|---|---|---|---|---|---|---|---|
| 3D-printed PCL-PPSu/silver composite scaffold | 3D printing of polycaprolactone-block-poly(1,3-propylene succinate) (PCL-PPSu) copolymer containing antimicrobial silver particles | Lower processing temperature than neat PCL, incorporation of temperature-sensitive bioactive agents possible, silver nitrate incorporated into polymer matrix | Not reported | Not reported | Enhanced hydrolytic and enzymatic degradation compared with conventional PCL | No significant cytotoxicity toward human dermal fibroblasts (HDFs), significantly reduced adhesion of different microorganisms, antimicrobial activity without compromising cell viability | Skin regeneration, wound healing, 3D-printed antimicrobial scaffold for skin tissue engineering | [203] |
| CuNP-doped chitosan–gelatin composite scaffold | Green-chemical reduction, freeze-drying | CuNP concentrations: 0.01%, 0.02%, and 0.03%, interconnected porous structure, pore size increased from 25–40 μm to ≈95 μm, overall porosity: 65%–88% | Not reported | Not reported | 0.03% CuNPs decreased the scaffold degradation rate | Good cell adhesion and proliferation, good hemocompatibility and cytocompatibility, no significant ROS generation, indicating limited oxidative stress | Skin tissue engineering, regenerative wound dressing/scaffold | [204] |
| Cu-alginate fibers/sutures | Calcium-mediated gelation | ≈95% Cu release within 24 h, optional NIR irradiation, sutures removed after 3 days | Not reported | Tensile strength of healed tissue: 102 ± 7 kPa (Cu-alginate, without NIR) and 95 ± 15 kPa (Cu-alginate, with NIR), intact skin: 188 ± 22 kPa, tensile-strength recovery: 50.5 ± 6.5% and 54.4 ± 1.3%, respectively | Not reported | Enhanced wound closure and angiogenesis, reduced epithelial gaps, increased $CD31^{+}$ cells, no significant toxicity, Cu-alginate sutures showed superior biomechanical recovery compared with nylon (75 ± 7 kPa) and Ca-alginate (72 ± 15 kPa) sutures | Bioactive surgical sutures, incisional wound healing, trauma and surgical wound repair | [205] |

(Continues)



23655549, 2026, 45, Downloaded from https://chemistry-europe.onlinelibrary.wiley.com/doi/10.1002/slct.75081 by Esma AHL.ATCIOLU ÖZEROL - Yildiz Technical University , Wiley Online Library on [25/11/2026]. See the Terms and Conditions (https://onlinelibrary.wiley.com/terms-and-conditions) on Wiley Online Library for rules of use; OA articles are governed by the applicable Creative Commons License

**TABLE 5** | (Continued)

| Material | Fabrication method | Processing parameters | Electrical conductivity | Mechanical properties | Biodegradation | Biological performance | Applications | References |
|---|---|---|---|---|---|---|---|---|
| PulMA/CuS@PC multifunctional hydrogel | Photocross-linking of methacrylated pullulan (PulMA) hydrogel incorporating phycocyanin-functionalized CuS (CuS@PC) nanoparticles | CuS@PC NPs incorporated into PulMA matrix, equilibrium swelling >400%, increasing CuS@PC content slightly decreased swelling, NIR irradiation for photothermal antibacterial activity | Not reported | CuS@PC incorporation caused a slight, statistically insignificant increase in compression modulus and Young's modulus, hydrogel retained the mechanical strength and elasticity of PulMA, $\mathbf{G' > G''}$, indicating elastic solid-like behavior | Not reported | Strong photothermal antibacterial activity against *E. coli* and *S. aureus*, favorable biocompatibility, reduced inflammation, enhanced collagen deposition, tissue regeneration, and angiogenesis, accelerated healing of infected full-thickness wounds | Antibiotic-free infected wound dressing, photothermal antibacterial therapy, tissue regeneration | [206] |
| BG/CS and Cu-BG/CS scaffolds | Melting method / 3D freeze printing | Increasing BG concentration (BG1–BG5), tensile testing | Not reported | Tensile strength increased with increasing BG concentration, approximately 0.20–0.52 MPa for BG1/CS–BG5/CS, BG and Cu-BG scaffolds showed comparable mechanical properties | Not reported | Cu-BG4/CS@SB and Cu-BG5/CS@SB significantly accelerated wound healing, wound closure at day 5: 48.37% ± 0.99% and 50.71% ± 1.89%, respectively, versus22.09% ± 3.25% for blank, at day 10: 84.70% ± 2.08% and 85.64% ± 2.25%, continuous epidermal layer formed by day 10, increased hair follicle formation and newly formed blood vessels, enhanced HUVEC-related angiogenic response and $\beta$-catenin expression | Skin tissue engineering | [207] |



23655549, 2026, 45, Downloaded from https://chemistry-europe.onlinelibrary.wiley.com/doi/10.1002/slct.75081 by Esma AHL.ATCIOLU ÖZEROL - Yildiz Technical University , Wiley Online Library on [25/11/2026]. See the Terms and Conditions (https://onlinelibrary.wiley.com/terms-and-conditions) on Wiley Online Library for rules of use; OA articles are governed by the applicable Creative Commons License

tional tissue repair. Overall, the study demonstrates that the combination of 3D-printed Cu-doped bioglass, chitosan, and controlled bioactive molecule delivery can provide antibacterial, pro-angiogenic, and appendage-regenerative effects, offering a promising strategy for comprehensive skin regeneration [207].

Yang et al. developed a multifunctional conductive hydrogel composed of quaternized carboxyl-functionalized chitosan (QCCS), ε-polylysine (ε-PL), PVA, and polydopamine-modified $Ti_3C_2$ MXene (PDA-MXene) for the treatment of bacterially infected wounds. $Ti_3C_2$ MXene served as the conductive component, while the PDA coating enhanced its antioxidant activity, photothermal conversion efficiency, and stability. The hydrogel exhibited excellent mechanical properties, efficient ROS scavenging, strong antibacterial activity, good hemocompatibility, and significantly accelerated the healing of infected wounds, demonstrating its potential as a multifunctional conductive wound dressing (Table 5).

## 4 | Conclusion

Conductive biomaterials have gained increasing attention as promising platforms for advanced wound management due to their ability to provide both structural support and electrical cues to the regenerating tissue. Unlike conventional wound dressings, these materials can interact with the bioelectrical microenvironment of injured skin and influence key processes involved in wound healing, including cell migration, proliferation, differentiation, angiogenesis, inflammatory regulation, and extracellular matrix remodeling. Conductive polymers, carbon-based materials, and metallic materials each provide distinct advantages, while their combination with hydrogels, nanofibers, and other biomimetic matrices has enabled the development of multifunctional wound dressings with improved physicochemical and biological properties. Recent studies further demonstrate that conductivity can be integrated with additional functionalities, such as antibacterial activity, drug delivery, self-healing, stretchability, sensing, and electrical stimulation, highlighting the potential of conductive biomaterials for personalized and smart wound care.

At the same time, the advantages of conductive materials must be considered alongside their limitations. Although high electrical conductivity may enhance bioelectrical interactions, increasing the concentration of conductive components can adversely affect cytocompatibility, degradation, mechanical properties, or long-term safety. In particular, the potential toxicity and persistence of some carbon-based and metallic components remain important concerns, whereas conductive polymers may present challenges related to degradation and processing. Therefore, the selection of conductive components should not be based solely on electrical conductivity, but rather on a balance between conductivity, biocompatibility, biodegradability, mechanical performance, antibacterial activity, and clinical applicability. Furthermore, advances in electrospinning, 3D printing, 4D printing, microfluidic fabrication, and other emerging manufacturing strategies are providing new opportunities to precisely control scaffold architecture, composition, and dynamic behavior. Overall, the field is moving from simple conductive wound coverings toward multifunctional and bio-responsive systems capable of actively participating in the healing process. Nevertheless, substantial challenges remain before these systems can achieve widespread clinical translation, particularly regarding long-term safety, reproducibility, manufacturing scalability, standardized evaluation, and validation in clinically relevant wound models.

### 4.1 | Future Perspectives

Future research should increasingly focus on the development of multifunctional, biodegradable, and biomimetic conductive wound dressings that can simultaneously address the diverse requirements of complex and chronic wounds. Rather than maximizing electrical conductivity alone, future material design should aim to establish an optimal balance between electrical properties and biological performance. The development of intrinsically conductive and biodegradable materials, as well as the use of naturally derived polymers and carefully engineered nanocomposites, may help reduce concerns regarding toxicity and long-term accumulation. In parallel, hybrid systems combining conductive materials with therapeutic agents, antimicrobial components, growth factors, or bioactive molecules could provide synergistic effects throughout different stages of wound healing.

Advanced fabrication technologies are also expected to play an increasingly important role. 3D and 4D printing may enable the fabrication of patient-specific scaffolds with precisely controlled architectures and stimulus-responsive properties, while microfluidic approaches can facilitate spatially controlled incorporation of multiple materials or therapeutic agents. These technologies could ultimately support the fabrication of wound dressings that more closely reproduce the heterogeneous and dynamic nature of native skin tissue. Furthermore, integration of conductive scaffolds with self-powered sensors, wireless communication, and closed-loop therapeutic systems could enable continuous monitoring of parameters such as electrical signals, temperature, moisture, pH, or wound status and allow treatment to be adjusted according to the changing healing environment.

Another important direction is the transition from proof-of-concept studies toward clinically relevant validation. Future studies should employ standardized methods for evaluating electrical conductivity, degradation, cytotoxicity, immune responses, antibacterial efficacy, and mechanical performance to facilitate meaningful comparison between different conductive biomaterials. Long-term in vivo studies, particularly in diabetic, infected, and other chronic wound models, will be essential for determining whether the beneficial effects observed in vitro can be maintained under clinically relevant conditions. Finally, considerations of large-scale manufacturing, sterilization, storage stability, cost, regulatory requirements, and patient-specific treatment should be incorporated at earlier stages of material development. Addressing these challenges will be critical for translating conductive biomaterials from experimental platforms into safe, reliable, and clinically applicable next-generation wound-healing technologies.



23656549, 2026, 45, Downloaded from https://chemistry-europe.onlinelibrary.wiley.com/doi/10.1002/slct.75081 by Esma AHLATCIOLU ÖZEROL - Yildiz Technical University , Wiley Online Library on [25/11/2026]. See the Terms and Conditions (https://onlinelibrary.wiley.com/terms-and-conditions) on Wiley Online Library for rules of use; OA articles are governed by the applicable Creative Commons License

## Author Contributions

**Zeynep SÜNBÜL**: conceptualization of the review, comprehensive literature search, analysis and interpretation of the published studies, drafting of the manuscript, and critical revision of the manuscript for important intellectual content. **Cem Bülent ÜSTÜNDAĞ**: conceptualization of the review, comprehensive literature search, analysis and interpretation of the published studies, drafting of the manuscript, and critical revision of the manuscript for important intellectual content. Both authors approved the final version of the manuscript and agree to be accountable for all aspects of the work. **Esma AHLATCIOĞLU ÖZEROL**: conceptualization of the review, comprehensive literature search, analysis and interpretation of the published studies, drafting of the manuscript, and critical revision of the manuscript for important intellectual content. All authors approved the final version of the manuscript and agree to be accountable for all aspects of the work.

## Conflicts of Interest

The authors declare no conflicts of interest.

## Data Availability Statement

Data sharing is not applicable to this article as no new datasets were generated or analyzed during the current study.

## References


1. K. Vig, A. Chaudhari, S. Tripathi, et al., "Advances in Skin Regeneration Using Tissue Engineering," *International Journal of Molecular Sciences* 18, no. 4 (2017): 789, https://doi.org/10.3390/ijms18040789.

2. A. Guo, B. Song, B. Reid, et al., "Effects of Physiological Electric Fields on Migration of Human Dermal Fibroblasts," *Journal of Investigative Dermatology* 130, no. 9 (2010): 2320–2327, https://doi.org/10.1038/jid.2010.96.

3. S. D. Bhoyar, K. Malhotra, and B. Madke, "Dressing Materials: A Comprehensive Review," *Journal of Cutaneous & Aesthetic Surgery* 16, no. 2 (2023): 81–89, https://doi.org/10.4103/JCAS.JCAS_163_22.

4. R. Dong and B. Guo, "Smart Wound Dressings for Wound Healing," *Nano Today* 41 (2021): 101290, https://doi.org/10.1016/j.nantod.2021.101290.

5. V. N. V. A. Uppuluri, S. Thukani Sathanantham, S. K. Bhimavarapu, and L. Elumalai, "Polymeric Hydrogel Scaffolds: Skin Tissue Engineering and Regeneration," *Advanced Pharmaceutical Bulletin* 12, no. 3 (2022): 437–448, https://doi.org/10.34172/apb.2022.069.

6. J. X. Law, L. L. Liau, A. Saim, Y. Yang, and R. Idrus, "Electrospun Collagen Nanofibers and Their Applications in Skin Tissue Engineering," *Tissue Engineering & Regenerative Medicine* 14, no. 6 (2017): 699–718, https://doi.org/10.1007/s13770-017-0075-9.

7. R. Yu, H. Zhang, and B. Guo, "Conductive Biomaterials as Bioactive Wound Dressing for Wound Healing and Skin Tissue Engineering," *Nano-Micro Letters* 14, no. 1 (2022): 1–46, https://doi.org/10.1007/s40820-021-00751-y.

8. J. Wu, F. Yu, M. Shao, et al., "Electrospun Nanofiber Scaffold for Skin Tissue Engineering: A Review," *ACS Applied Bio Materials* 7, no. 6 (2024): 3556–3567, https://doi.org/10.1021/acsabm.4c00318.

9. R. Cai, N. Gimenez-Camino, M. Xiao, S. Bi, and K. A. DiVito, "Technological Advances in Three-Dimensional Skin Tissue Engineering," *Reviews on Advanced Materials Sciences* 62, no. 1 (2023): 1–22, https://doi.org/10.1515/rams-2022-0289.

10. D. Li, Y. Wang, S. Zhu, X. Hu, and R. Liang, "Recombinant Fibrous Protein Biomaterials Meet Skin Tissue Engineering," *Frontiers in Bioengineering and Biotechnology* 12 (2024): 1–21, https://doi.org/10.3389/fbioe.2024.1411550.

11. X. Zhang, Y. Liang, S. Huang, and B. Guo, "Chitosan-Based Self-Healing Hydrogel Dressing for Wound Healing," *Advances in Colloid and Interface Science* 332 (2024): 103267, https://doi.org/10.1016/j.cis.2024.103267.

12. M. Kaviani and B. Geramizadeh, "Basic Aspects of Skin Tissue Engineering: Cells, Biomaterials, Scaffold Fabrication Techniques, and Signaling Factors," *Journal of Medicine Biology & Engineering* 43, no. 5 (2023): 508–521, https://doi.org/10.1007/s40846-023-00822-y.

13. J. Ye and Y. Lai, "Keratinocytes: New Perspectives in Inflammatory Skin Diseases," *Trends in Molecular Medicine* (2025): 1103–1113, https://doi.org/10.1016/j.molmed.2025.03.012.

14. E. Korkmaz, S. C. Balmert, T. L. Sumpter, C. D. Carey, G. Erdos, and L. D. Falo, "Microarray Patches Enable the Development of Skin-Targeted Vaccines Against COVID-19," *Advanced Drug Delivery Reviews* 171 (2021): 164–186, https://doi.org/10.1016/j.addr.2021.01.022.

15. F. Boraldi, F. D. Lofaro, S. Bonacorsi, A. Mazzilli, M. Garcia-Fernandez, and D. Quaglino, "The Role of Fibroblasts in Skin Homeostasis and Repair," *Biomedicines* 12, no. 7 (2024): 1586, https://doi.org/10.3390/biomedicines12071586.

16. S. M. Riha, M. Maarof, and M. B. Fauzi, "Synergistic Effect of Biomaterial and Stem Cell for Skin Tissue Engineering in Cutaneous Wound Healing: A Concise Review," *Polymers* 13, no. 10 (2021): 1546, https://doi.org/10.3390/polym13101546.

17. K. Sindhi, R. B. Pingili, V. Beldar, S. Bhattacharya, J. Rahaman, and D. Mukherjee, "The Role of Biomaterials-Based Scaffolds in Advancing Skin Tissue Construct," *Journal of Tissue Viability* 34, no. 2 (2025): 100858, https://doi.org/10.1016/j.jtv.2025.100858.

18. M. Rahmati, D. K. Mills, A. M. Urbanska, et al., "Electrospinning for Tissue Engineering Applications," *Progress in Materials Science* 117 (2021): 100721, https://doi.org/10.1016/j.pmatsci.2020.100721.

19. F. Topuz, B. Satilmis, and T. Uyar, "Electrospinning of Uniform Nanofibers of Polymers of Intrinsic Microporosity (PIM-1): The Influence of Solution Conductivity and Relative Humidity," *Polymer* 178 (2019): 121610, https://doi.org/10.1016/j.polymer.2019.121610.

20. J. J. Chung, H. Im, S. H. Kim, J. W. Park, and Y. Jung, "Toward Biomimetic Scaffolds for Tissue Engineering: 3D Printing Techniques in Regenerative Medicine," *Frontiers in Bioengineering and Biotechnology* 8 (2020): 1–12, https://doi.org/10.3389/fbioe.2020.586406.

21. T. L. D. A. Montanheiro, V. M. Schatkoski, B. R. C. Menezes, et al., "Recent Progress on Polymer Scaffolds Production: Methods, Main Results, Advantages and Disadvantages," *eXPRESS Polymers Letters* 16, no. 2 (2022): 197–219, https://doi.org/10.3144/expresspolymlett.2022.16.

22. C. M. Brougham, T. J. Levingstone, N. Shen, et al., "Freeze-Drying as a Novel Biofabrication Method for Achieving a Controlled Microarchitecture Within Large, Complex Natural Biomaterial Scaffolds," *Advance Healthcare Materials* 6, no. 21 (2017): 1–7, https://doi.org/10.1002/adhm.201700598.

23. M. R. I. Shishir, L. Xie, C. Sun, X. Zheng, and W. Chen, "Advances in Micro and Nano-Encapsulation of Bioactive Compounds Using Biopolymer and Lipid-Based Transporters," *Trends in Food Science & Technology* 78 (2018): 34–60, https://doi.org/10.1016/j.tifs.2018.05.018.

24. M. Aguado, L. Saldaña, E. P. D. Río, et al., "Polylactide, Processed by a Foaming Method Using Compressed Freon R134a, for Tissue Engineering," *Polymers* 13, no. 20 (2021): 3453, https://doi.org/10.3390/polym13203453.

25. T. Garg, O. Singh, S. Arora, and R. S. R. Murthy, "Scaffold: A Novel Carrier for Cell and Drug Delivery," *Critical Reviews in Therapeutic Drug Carrier Systems* 29, no. 1 (2012): 1–63, https://doi.org/10.1615/critrevtherdrugcarriersyst.v29.i1.10.

26. L. A. Damiati, S. A. Alsudir, R. Y. Mohammed, et al., "4D Printing in Skin Tissue Engineering: A Revolutionary Approach to Enhance Wound Healing and Combat Infections," *Bioprinting* 45 (2025): e00386, https://doi.org/10.1016/j.bprint.2025.e00386.




23656549, 2026, 45, Downloaded from https://chemistry-europe.onlinelibrary.wiley.com/doi/10.1002/slct.75081 by Esma AHLATCIOLU ÖZEROL - Yildiz Technical University , Wiley Online Library on [25/11/2026]. See the Terms and Conditions (https://onlinelibrary.wiley.com/terms-and-conditions) on Wiley Online Library for rules of use; OA articles are governed by the applicable Creative Commons License

27. B. Xie, J. Lin, L. Cui, X. Shi, and S. Wu, "Microfluidic Biomaterials for Next-Generation Biomedical Platforms: Advances in Fabrication, Functionality, and Applications," *Journal of Biomedical Materials Research: Part A* 114, no. 2 (2026): e70032, https://doi.org/10.1002/jbma.70032.

28. Z. Sun, J. Zhou, L. Sheng, et al., "Microfluidic Engineering of Microgels: Fabrication Methods, Structural Design, Assembly Strategies, and Biomedical Applications," *Acta Biomaterialia* 207 (2025): 142–173, https://doi.org/10.1016/j.actbio.2025.10.017.

29. M. Geiger, J. Frank, F. Schmitz, et al., "Microfluidic Spinning of PEDOT:PSS Microfibers for Nerve Guidance Conduits," *Advanced Materials & Technology* 10, no. 12 (2025): 2401996, https://doi.org/10.1002/admt.202401996.

30. H. Esmaeili, Y. Zhang, K. Ravi, et al., "Development of an Electroconductive Heart-on-a-Chip Model to Investigate Cellular and Molecular Response of Human Cardiac Tissue to Gold Nanomaterials," *Biomaterials* 320 (2025): 123275, https://doi.org/10.1016/j.biomaterials.2025.123275.

31. E. Yarali, M. J. Mirzaali, A. Ghalayaniesfahani, A. Accardo, P. J. Diaz-Payno, and A. A. Zadpoor, "4D Printing for Biomedical Applications," *Advanced Materials* 36, no. 31 (2024): 2402301, https://doi.org/10.1002/adma.202402301.

32. M. Sathishkumar, M. M. Dhorajiwala, M. S. Kumar, S. Gaba, M. Vignesh, and G. Anbuchezhiyan, "Smart Materials for 4D Printing: Emerging Biomedical Applications, Stimuli, Techniques, and Future Directions," *Materials Today Communications* 50 (2026): 114490, https://doi.org/10.1016/j.mtcomm.2025.114490.

33. K. Kumar and A. Nain, "Emerging 4D Fabrication of Tubular Structures and Clinical Challenges: Critical Perspective," *ACS Mater Au* 5, no. 6 (2025): 886–895, https://doi.org/10.1021/acsmaterialsau.5c00101.

34. X. Liu, H. Xu, M. Zhang, and D.-G. Yu, "Electrospun Medicated Nanofibers for Wound Healing: Review," *Membranes* 11, no. 10 (2021): 770, https://doi.org/10.3390/membranes11100770.

35. Q. Zheng, Y. Xi, and Y. Weng, "Functional Electrospun Nanofibers: Fabrication, Properties, and Applications in Wound-Healing Process," *RSC Advances* 14, no. 5 (2024): 3359–3378, https://doi.org/10.1039/D3RA07075A.

36. V. Perez-Puyana, M. Jiménez-Rosado, A. Romero, and A. Guerrero, "Polymer-Based Scaffolds for Soft-Tissue Engineering," *Polymers* 12, no. 7 (2020): 1566, https://doi.org/10.3390/polym12071566.

37. E. Capuana, F. Lopresti, F. Carfì Pavia, V. Brucato, and V. L. Carrubba, "Solution-Based Processing for Scaffold Fabrication in Tissue Engineering Applications: A Brief Review," *Polymers* 13, no. 13 (2021): 2041, https://doi.org/10.3390/polym13132041.

38. R. A. Sachdeo, C. Khanwelkar, and A. Shete, "3D Printing in Wound Healing: Innovations, Applications, and Future Directions," *Cureus* (2024): 1–12, https://doi.org/10.7759/cureus.75331.

39. A. Sadeghianmaryan, N. Ahmadian, S. Wheatley, et al., "Advancements in 3D-printable Polysaccharides, Proteins, and Synthetic Polymers for Wound Dressing and Skin Scaffolding—A Review," *International Journal of Biological Macromolecules* 266 (2024): 131207, https://doi.org/10.1016/j.ijbiomac.2024.131207.

40. L. Bonetti and G. Scalet, "4D fabrication of Shape-changing Systems for Tissue Engineering: State of the Art and Perspectives," *Progress in Additive Manufacturing* 10, no. 4 (2025): 1913–1943, https://doi.org/10.1007/s40964-024-00743-5.

41. S. Bhushan, S. Singh, T. K. Maiti, et al., "Scaffold Fabrication Techniques of Biomaterials for Bone Tissue Engineering: A Critical Review," *Bioengineering* 9, no. 12 (2022): 728, https://doi.org/10.3390/bioengineering9120728.

42. Z. U. Arif, M. Y. Khalid, W. Ahmed, and H. Arshad, "A Review on Four-Dimensional (4D) Bioprinting in Pursuit of Advanced Tissue Engineering Applications," *Bioprinting* 27 (2022): e00203, https://doi.org/10.1016/j.bprint.2022.e00203.

43. C. Fang, J. Zhang, X. Chen, and G. J. Weng, "Calculating the Electrical Conductivity of Graphene Nanoplatelet Polymer Composites by a Monte Carlo Method," *Nanomaterials* 10, no. 6 (2020): 1129, https://doi.org/10.3390/nano10061129.

44. J. Zhu, Y. He, J. Wang, et al., "Clog-Free all-Aqueous Microfluidic Fabrication of Hydrogel Microfibers Governed by a Universal Scaling Law," *Lab on A Chip* 26, no. 2 (2026): 345–352, https://doi.org/10.1039/D5LC01007A.

45. S. Alven and B. A. Aderibigbe, "Hyaluronic Acid-Based Scaffolds as Potential Bioactive Wound Dressings," *Polymers* 13, no. 13 (2021): 2102, https://doi.org/10.3390/polym13132102.

46. Y. Wang, Z. Wang, and Y. Dong, "Collagen-Based Biomaterials for Tissue Engineering," *ACS Biomaterials & Science Engineering* 9, no. 3 (2023): 1132–1150, https://doi.org/10.1021/acsbiomaterials.2c00730.

47. S. S. Mathew-Steiner, S. Roy, and C. K. Sen, "Collagen in Wound Healing," *Bioengineering* 8, no. 5 (2021): 63, https://doi.org/10.3390/bioengineering8050063.

48. T. T. Ho, H. A. Tran, V. K. Doan, et al., "Natural Polymer-Based Materials for Wound Healing Applications," *Advanced NanoBiomedical Research* 4, no. 5 (2024): 2300131, https://doi.org/10.1002/anbr.202300131.

49. Y. Chen, Y. Lv, W. Su, G. Wu, and P. Li, "A Gelatin-chitosan-based Film Containing Berberine Hydrochloride/Polypyrrole That Promotes Infectious Wound Healing Through Antibacterial and Antioxidant Properties, and Electrical Conductivity," *International Journal of Biological Macromolecules* 305 (2025): 141228, https://doi.org/10.1016/j.ijbiomac.2025.141228.

50. S. Y. Sonaye, E. G. Ertugral, C. R. Kothapalli, and P. Sikder, "Extrusion 3D (Bio)Printing of Alginate-Gelatin-Based Composite Scaffolds for Skeletal Muscle Tissue Engineering," *Materials* 15, no. 22 (2022): 7945, https://doi.org/10.3390/ma15227945.

51. M. F. P. Graça, S. P. Miguel, C. S. D. Cabral, and I. J. Correia, "Hyaluronic Acid—Based Wound Dressings: A Review," *Carbohydrate Polymers* 241 (2020): 116364, https://doi.org/10.1016/j.carbpol.2020.116364.

52. F. P. Hajipour, A. Feyzbakhsh, L. Maleknia, and I. Ahanian, "Electrospun Scaffold With Bioactive Polyurethane Shell Infused With Propolis and Starch-Hyaluronic Acid Core: An Advanced Therapeutic Platform for Skin Tissue Engineering," *International Journal of Biological Macromolecules* 288 (2025): 138745, https://doi.org/10.1016/j.ijbiomac.2024.138745.

53. K. Saravanakumar, S. Park, S. S. Santosh, et al., "Application of Hyaluronic Acid in Tissue Engineering, Regenerative Medicine, and Nanomedicine: A Review," *International Journal of Biological Macromolecules* 222 (2022): 2744–2760, https://doi.org/10.1016/j.ijbiomac.2022.10.055.

54. X. Wang, R. Song, M. Johnson, et al., "Chitosan-Based Hydrogels for Infected Wound Treatment," *Macromolecular Bioscience* 23, no. 9 (2023): 2300094, https://doi.org/10.1002/mabi.202300094.

55. A. Madni, R. Kousar, N. Naeem, and F. Wahid, "Recent Advancements in Applications of Chitosan-Based Biomaterials for Skin Tissue Engineering," *Journal of Bioresources & Bioproduction* 6, no. 1 (2021): 11–25, https://doi.org/10.1016/j.jobab.2021.01.002.

56. H. L. Loo, B. H. Goh, L.-H. Lee, and L. H. Chuah, "Application of Chitosan-Based Nanoparticles in Skin Wound Healing," *Asian Journal of Pharmaceutical Sciences* 17, no. 3 (2022): 299–332, https://doi.org/10.1016/j.ajps.2022.04.001.

57. M. Zhang and X. Zhao, "Alginate Hydrogel Dressings for Advanced Wound Management," *International Journal of Biological Macromolecules* 162 (2020): 1414–1428, https://doi.org/10.1016/j.ijbiomac.2020.07.311.

58. A. Froelich, E. Jakubowska, M. Wojtyłko, et al., "Alginate-Based Materials Loaded With Nanoparticles in Wound Healing," *Pharmaceutics* 15, no. 4 (2023): 1142, https://doi.org/10.3390/pharmaceutics15041142.



23656549, 2026, 45, Downloaded from https://chemistry-europe.onlinelibrary.wiley.com/doi/10.1002/slct.75081 by Esma AHLATCIOLU ÖZEROL - Yildiz Technical University , Wiley Online Library on [25/11/2026]. See the Terms and Conditions (https://onlinelibrary.wiley.com/terms-and-conditions) on Wiley Online Library for rules of use; OA articles are governed by the applicable Creative Commons License

59. T. Lehmann, A. E. Vaughn, S. Seal, K. W. Liechty, and C. Zgheib, "Silk Fibroin-Based Therapeutics for Impaired Wound Healing," *Pharmaceutics* 14, no. 3 (2022): 651, https://doi.org/10.3390/pharmaceutics14030651.

60. W. Shi, Y. Jiang, T. Wu, Y. Zhang, and T. Li, "Advancements in Drug-Loaded Hydrogel Systems for Bone Defect Repair," *Regenative Therapeutics* 25 (2024): 174–185, https://doi.org/10.1016/j.reth.2023.12.010.

61. W. Daamen, J. Veerkamp, J. Vanhest, and T. Vankuppevelt, "Elastin as a Biomaterial for Tissue Engineering," *Biomaterials* 28, no. 30 (2007): 4378–4398, https://doi.org/10.1016/j.biomaterials.2007.06.025.

62. J. Bhoopathy, L. Prabakaran, W. V. Sathyaraj, R. Karthikeyan, and R. Senthil, "A Comprehensive Review on Natural Therapeutics for Wound Treatment," *Regenrative Engineering & Translational Medicine* 10, no. 1 (2024): 34–45, https://doi.org/10.1007/s40883-023-00314-0.

63. C. Wei, Y. Feng, D. Che, et al., "Biomaterials in Skin Tissue Engineering," *International Journal of Polymer Materials & Polymer Biomaterials* 71, no. 13 (2022): 993–1011, https://doi.org/10.1080/00914037.2021.1933977.

64. E. Özdilek, S. Samatya Yilmaz, H. Uzuner, and A. Aytac, "Nanofibrous Biomaterial Containing Raw-Propolis Particles Encapsulated by PLA/PBS for Wound Dressing Application," *Macromolecular Materials and Engineering* 310, no. 4 (2025): 2400321, https://doi.org/10.1002/mame.202400321.

65. S. Castañeda-Rodríguez, M. G. Torres, R. M. R. Aparicio, et al., "Recent Advances in Modified Poly (lactic acid) as Tissue Engineering Materials," *Journal of Biological Engineering* 17, no. 1 (2023): 1–20, https://doi.org/10.1186/s13036-023-00338-8.

66. A. Kouketsu, Y. Shimizu, S. Nogami, et al., "Wound Healing Effect of Autologous Fibrin Glue and Polyglycolic Acid Sheets in a Rat Back Skin Defect Model," *Transfusion & Apheresis Science* 60, no. 4 (2021): 103144, https://doi.org/10.1016/j.transci.2021.103144.

67. J. Zhang, S. Yang, X. Yang, et al., "Novel Fabricating Process for Porous Polyglycolic Acid Scaffolds by Melt-Foaming Using Supercritical Carbon Dioxide," *ACS Biomaterials & Science Engineering* 4, no. 2 (2018): 694–706, https://doi.org/10.1021/acsbiomaterials.7b00692.

68. E. Göktürk and H. Erdal, "Poliglikolik Asit' in (PGA) Biyomedikal Uygulamaları," *SAÜ Fen Bilim Enstitüsü Derg* (2017): 1–1, https://doi.org/10.16984/saufenbilder.283156.

69. Y. C. Teo, A. Abbas, E. Park, et al., "3D Printed Bioactive PLGA Dermal Scaffold for Burn Wound Treatment," *ACS Mater Au* 3, no. 3 (2023): 265–272, https://doi.org/10.1021/acsmaterialsau.2c00079.

70. A. Guzmán-Soria, V. Moreno-Serna, D. A. Canales, C. García-Herrera, P. A. Zapata, and P. A. Orihuela, "Effect of Electrospun PLGA/Collagen Scaffolds on Cell Adhesion, Viability, and Collagen Release: Potential Applications in Tissue Engineering," *Polymers* 15, no. 5 (2023): 1079, https://doi.org/10.3390/polym15051079.

71. H. S. Mergen, S. Duzyer Gebizli, E. Ermis, M. Cansev, S. Isik Dokuzoglu, and G. Goktalay, "Uridine-Loaded Polycaprolactone Nanofiber Mats as a Novel Wound Dressing," *Fibers and Polymers* 25, no. 7 (2024): 2471–2484, https://doi.org/10.1007/s12221-024-00615-3.

72. M. S. El-Okaily, A. A. Mostafa, J. Dulnik, et al., "Nanofibrous Polycaprolactone Membrane With Bioactive Glass and Atorvastatin for Wound Healing: Preparation and Characterization," *Pharmaceutics* 15, no. 7 (2023): 1990, https://doi.org/10.3390/pharmaceutics15071990.

73. Y. Dong, Z. Liu, F. Qi, L. Jin, L. Zhang, and N. Zhu, "Polyethylene-Glycol-Ornamented Small Intestinal Submucosa Biosponge for Skin Tissue Engineering," *ACS Biomaterials & Science Engineering* 5, no. 5 (2019): 2457–2465, https://doi.org/10.1021/acsbiomaterials.8b01592.

74. M. Liu, W. Chen, X. Zhang, et al., "Improved Surface Adhesion and Wound Healing Effect of Madecassoside Liposomes Modified by Temperature-Responsive PEG-PCL-PEG Copolymers," *European Journal of Pharmaceutical Sciences* 151 (2020): 105373, https://doi.org/10.1016/j.ejps.2020.105373.

75. S. Piluso, G. A. Skvortsov, M. Altunbek, et al., "3D bioprinting of Molecularly Engineered PEG-Based Hydrogels Utilizing Gelatin Fragments," *Biofabrication* 13, no. 4 (2021): 045008, https://doi.org/10.1088/1758-5090/ac0ff0.

76. P. Mousavi, H. Yeganeh, I. Omrani, and M. Babaahmadi, "Gelatin Modified Nonisocyanate Polyurethane/Siloxane Functionalized With Quaternary Ammonium Groups as Antibacterial Wound Dressing Membrane," *Journal of Biomaterials Science, Polymer Edition* (2025): 1–20, https://doi.org/10.1080/09205063.2025.2518305.

77. M. Morales-González, L. E. Díaz, C. Dominguez-Paz, and M. F. Valero, "Insights Into the Design of Polyurethane Dressings Suitable for the Stages of Skin Wound-Healing: A Systematic Review," *Polymers* 14, no. 15 (2022): 2990, https://doi.org/10.3390/polym14152990.

78. V. Ken Hiytesh, D. Sivalingam, J. Prakash, et al., "Accelerated Wound Healing by PrO2 Incorporated PVA/SA Fibers," *Journal of Industrial and Engineering Chemistry* 137 (2024): 301–316, https://doi.org/10.1016/j.jiec.2024.03.017.

79. M. M. Nemati, R. Heidari, A. Keshavarzi, et al., "In Vitro and In Vivo Evaluation of Electrospun PVA Nanofiber Containing ZnO/Curcumin for Wound Healing Application," *Applied Biochemistry and Biotechnology* 197, no. 1 (2025): 194–215, https://doi.org/10.1007/s12010-024-05018-x.

80. S. Jadbabaei, M. Kolahdoozan, F. Naeimi, and H. Ebadi-Dehaghani, "Preparation and Characterization of Sodium Alginate–PVA Polymeric Scaffolds by Electrospinning Method for Skin Tissue Engineering Applications," *RSC Advances* 11, no. 49 (2021): 30674–30688, https://doi.org/10.1039/d1ra04176b.

81. Y. Li, W. Peng, Y. Dong, et al., "Mussel-Inspired PEDOT-Incorporated Gelatin-Based Conductive Hydrogel With Flexibility and Electroactivity to Accelerate Wound Healing In Vitro," *ACS Applied Polymer Materials* 5, no. 6 (2023): 4233–4243, https://doi.org/10.1021/acsapm.3c00445.

82. X. Bi, X. Chen, Z. Pang, et al., "Advances in Electrical Stimulation for Wound Healing," *Frontiers in Bioengineering and Biotechnology* 13 (2025): 1662900, https://doi.org/10.3389/fbioe.2025.1662900.

83. Y. Jiang, Y. Zhou, Y. Tian, et al., "Conductive Polymers in Smart Wound Healing: From Bioelectric Stimulation to Regenerative Therapies," *Materials Today Bio* 34 (2025): 102114, https://doi.org/10.1016/j.mtbio.2025.102114.

84. Y. Zhang, Y. Tang, B. Lu, F. Li, and K. Yu, "Electroactive Electrospun Nanoplatform Combined With Electrical Stimulation Modulates Anti-Inflammatory Macrophage Polarization for Enhanced Wound Healing," *Frontiers in Bioengineering and Biotechnology* 13 (2026): 1739989, https://doi.org/10.3389/fbioe.2025.1739989.

85. M. Gao, Y. Luo, L. Zheng, W. Li, and Y. Pei, "Biomimetic Electric Interface-Mediated Cellular Activation Promotes Diabetic Wound Healing via Self-Powered Wearable Thermoelectric Patch," *Materials Today Bio* 35 (2025): 102520, https://doi.org/10.1016/j.mtbio.2025.102520.

86. Y. Ma, T. Lei, X. Yang, et al., "Electrically Conductive Polypyrrole@Keratin Nanofiber Membranes With Potential for Tissue Restoration," *Fibers and Polymers* 25, no. 3 (2024): 751–763, https://doi.org/10.1007/s12221-023-00439-7.

87. H.-J. Jang, D. M. Tiruneh, H. Ryu, and J.-K. Yoon, "Piezoelectric and Triboelectric Nanogenerators for Enhanced Wound Healing," *Biomimetics* 8, no. 7 (2023): 517, https://doi.org/10.3390/biomimetics8070517.

88. P. V. Palanisamy, W. V. Sathyaraj, and Y. R. Pravin, "Role of Electrospun Conductive Polymeric Nanofibers for Inducing Neuronal Tissue Regeneration—A Novel Strategy for Targeting Neurodegenerative Disorders," *Regenrative Engineering & Translational Medicine* (2025): 377–390, https://doi.org/10.1007/s40883-025-00405-0.

89. A. H. Majeed, L. A. Mohammed, O. H. Hamoodi, et al., "A Review on Polyaniline: Synthesis, Properties, Nanocomposites, and Electrochemical Applications," *International Journal of Polymer Science* 2022 (2022): 1–19, https://doi.org/10.1155/2022/9047554.

90. C. D. Pina and E. Falletta, "Advances in Polyaniline for Biomedical Applications," *Current Medicinal Chemistry* 29, no. 2 (2022): 329–357, https://doi.org/10.2174/0929867328666210419135519.



23656549, 2026, 45, Downloaded from https://chemistry-europe.onlinelibrary.wiley.com/doi/10.1002/slct.75081 by Esma AHLATCIOLU ÖZEROL - Yildiz Technical University , Wiley Online Library on [25/11/2026]. See the Terms and Conditions (https://onlinelibrary.wiley.com/terms-and-conditions) on Wiley Online Library for rules of use; OA articles are governed by the applicable Creative Commons License

91. R. Rajasekaran, A. K. Ojha, V. S. Seesla, et al., "Polyaniline Doped Silk Fibroin-PCL Electrospunfiber: An Electroactive Fibrous Sheet for Full-Thickness Wound Healing Study," *Chemistry- AnEngineering Journal* 475 (2023): 146245, https://doi.org/10.1016/j.cej.2023.146245.

92. M. Beygisangchin, S. A. Rashid, S. Shafie, A. R. Sadrolhosseini, and H. N. Lim, "Preparations, Properties, and Applications of Polyaniline and Polyaniline Thin Films—A Review," *Polymers* 13, no. 12 (2021): 2003, https://doi.org/10.3390/polym13122003.

93. M. A. Marsudi, R. T. Ariski, A. Wibowo, et al., "Conductive Polymeric-Based Electroactive Scaffolds for Tissue Engineering Applications: Current Progress and Challenges From Biomaterials and Manufacturing Perspectives," *International Journal of Molecular Sciences* 22, no. 21 (2021): 11543, https://doi.org/10.3390/ijms222111543.

94. B. Guo, J. Zhao, C. Wu, et al., "One-Pot Synthesis of Polypyrrole Nanoparticles With Tunable Photothermal Conversion and Drug Loading Capacity," *Colloids and Surfaces B: Biointerfaces* 177 (2019): 346–355, https://doi.org/10.1016/j.colsurfb.2019.02.016.

95. L. Hao, C. Dong, and D. Yu, "Polypyrrole Derivatives: Preparation, Properties and Application," *Polymers* 16, no. 16 (2024): 2233, https://doi.org/10.3390/polym16162233.

96. Q. Peng, Q. Yang, Z. Yan, et al., "Nanofiber-Reinforced Chitosan/Gelatine Hydrogel With Photothermal, Antioxidant and Conductive Capabilities Promotes Healing of Infected Wounds," *International Journal of Biological Macromolecules* 279 (2024): 134625, https://doi.org/10.1016/j.ijbiomac.2024.134625.

97. L. Hao, C. Dong, L. Zhang, K. Zhu, and D. Yu, "Polypyrrole Nanomaterials: Structure, Preparation and Application," *Polymers* 14, no. 23 (2022): 5139, https://doi.org/10.3390/polym14235139.

98. T. P. Kaloni, P. K. Giesbrecht, G. Schreckenbach, and M. S. Freund, "Polythiophene: From Fundamental Perspectives to Applications," *Chemistry Materials* 29, no. 24 (2017): 10248–10283, https://doi.org/10.1021/acs.chemmater.7b03035.

99. H. Zhao, J. Xu, E. Zhang, et al., "3D Bioprinting of Polythiophene Materials for Promoting Stem Cell Proliferation in a Nutritionally Deficient Environment," *ACS Applied Materials Interfaces* 13, no. 22 (2021): 25759–25770, https://doi.org/10.1021/acsami.1c04967.

100. S. M. Mousavi, S. A. Hashemi, S. Bahrani, et al., "Recent Advancements in Polythiophene-Based Materials and Their Biomedical, Geno Sensor and DNA Detection," *International Journal of Molecular Sciences* 22, no. 13 (2021): 6850, https://doi.org/10.3390/ijms22136850.

101. M. Jaymand, M. Hatamzadeh, and Y. Omidi, "Modification of Polythiophene by the Incorporation of Processable Polymeric Chains: Recent Progress in Synthesis and Applications," *Progress in Polymer Science* 47 (2015): 26–69, https://doi.org/10.1016/j.progpolymsci.2014.11.004.

102. F. Fu, J. Wang, and J. Yu, "Interpenetrating PAA-PEDOT Conductive Hydrogels for Flexible Skin Sensors," *Journal of Materials Chemistry C* 9, no. 35 (2021): 11794–11800, https://doi.org/10.1039/D1TC01578H.

103. S. M. A. Mokhtar, N. J. Nataren, D. R. Evans, et al., "Molecular and Histological Evidence for the Biocompatibility of PEDOT-Coated Microneedles in Human Skin," *Journal ofMaterials in Chemistry B* 13, no. 22 (2025): 6393–6401, https://doi.org/10.1039/D4TB02281E.

104. L. J. Del Valle, D. Aradilla, R. Oliver, et al., "Cellular Adhesion and Proliferation on Poly(3,4-ethylenedioxythiophene): Benefits in the Electroactivity of the Conducting Polymer," *European Polymer Journal* 43, no. 6 (2007): 2342–2349, https://doi.org/10.1016/j.eurpolymj.2007.03.050.

105. Y. Chung, P. Chou, and M. Sheu, "The Wound-Healing Activity of PEDOT-PSS in Animals," *International Journal of Molecular Sciences* 24, no. 16 (2023): 12539, https://doi.org/10.3390/ijms241612539.

106. G. Rajakumar, X. Zhang, T. Gomathi, et al., "Current Use of Carbon-Based Materials for Biomedical Applications—A Prospective and Review," *Processes* 8, no. 3 (2020): 355, https://doi.org/10.3390/pr8030355.

107. A. Thakur, R. Bharti, and R. Sharma, "Carbon Nanotubes: Types, Synthesis, Cytotoxicity and Applications in Biomedical," *Materials Today Proceedings* 50 (2022): 2256–2268, https://doi.org/10.1016/j.matpr.2021.10.002.

108. S. Singh, S. Vardharajula, P. Tiwari, et al., "Functionalized Carbon Nanotubes: Biomedical Applications," *International Journal of Nanomedicine* (2012): 5361, https://doi.org/10.2147/ijn.s35832.

109. T. V. Patil, D. K. Patel, S. D. Dutta, K. Ganguly, A. Randhawa, and K. Lim, "Carbon Nanotubes-Based Hydrogels for Bacterial Eradiation and Wound-Healing Applications," *Applied Sciences* 11, no. 20 (2021): 9550, https://doi.org/10.3390/app11209550.

110. A. Shariati, S. M. Hosseini, Z. Chegini, A. Seifalian, and M. R. Arabestani, "Graphene-Based Materials for Inhibition of Wound Infection and Accelerating Wound Healing," *Biomedicine & Pharmacotherapy* 158 (2023): 114184, https://doi.org/10.1016/j.biopha.2022.114184.

111. M. Handayani, Hendrik, A. Abbas, et al., "Development of Graphene and Graphene Quantum Dots Toward Biomedical Engineering Applications: A Review," *Nanotechnology Reviews* 12, no. 1 (2023): 1–42, https://doi.org/10.1515/ntrev-2023-0168.

112. S. Zhang, T. Jiang, M. Li, et al., "Graphene-Based Wound Dressings for Wound Healing: Mechanism, Technical Analysis, and Application Status," *ACS Biomaterials Science Engineering* 10, no. 11 (2024): 6790–6813, https://doi.org/10.1021/acsbiomaterials.4c01142.

113. R. Chandrasekaran, U. Uthirakrishnan, G. Sankar, K. Natarajan, J. Joseph, and S. Sagadevan, "Recent Progress and Challenges in Graphene Quantum Dots as Multifunctional Nanoplatforms for Biomedical Applications," *BioNanoScience* 14, no. 3 (2024): 3401–3429, https://doi.org/10.1007/s12668-024-01531-9.

114. E. Haque, J. Kim, V. Malgras, et al., "Recent Advances in Graphene Quantum Dots: Synthesis, Properties, and Applications," *Small Methods* 2, no. 10 (2018): 1800050, https://doi.org/10.1002/smtd.201800050.

115. B. Mansuriya and Z. Altintas, "Applications of Graphene Quantum Dots in Biomedical Sensors," *Sensors* 20, no. 4 (2020): 1072, https://doi.org/10.3390/s20041072.

116. J. J. Grant, S. C. Pillai, S. Hehir, M. McAfee, and A. Breen, "Biomedical Applications of Electrospun Graphene Oxide," *ACS Biomaterials Science Engineering* 7, no. 4 (2021): 1278–1301, https://doi.org/10.1021/acsbiomaterials.0c01663.

117. A. Raslan, L. Saenz Del Burgo, J. Ciriza, and J. L. Pedraz, "Graphene Oxide and Reduced Graphene Oxide-Based Scaffolds in Regenerative Medicine," *International Journal of Pharmaceutics* 580 (2020): 119226, https://doi.org/10.1016/j.ijpharm.2020.119226.

118. A. H. Luong, D. Istiqomah, and W. Lin, "Study of Mechanical Property and Biocompatibility of Graphene Oxide/MEO2MA Hydrogel Scaffold for Wound Healing Application," *Biomedical Engineering Letters* 14, no. 3 (2024): 537–548, https://doi.org/10.1007/s13534-024-00349-4.

119. F. Xie, L. Zou, Z. Xu, et al., "Alginate Foam Gel Modified by Graphene Oxide for Wound Dressing," *International Journal of Biological Macromolecules* 223 (2022): 391–403, https://doi.org/10.1016/j.ijbiomac.2022.11.013.

120. D. Perumal, E. L. Albert, and C. A. C. Abdullah, "Green Reduction of Graphene Oxide Involving Extracts of Plants From Different Taxonomy Groups," *Journal of Composite Science* 6, no. 2 (2022): 58, https://doi.org/10.3390/jcs6020058.

121. B. M. Bakadia, R. Zheng, A. A. Qaed Ahmed, et al., "Teicoplanin-Decorated Reduced Graphene Oxide Incorporated Silk Protein Hybrid Hydrogel for Accelerating Infectious Diabetic Wound Healing and Preventing Diabetic Foot Osteomyelitis," *Advanced Healthcare Materials* 13, no. 20 (2024): 2304572, https://doi.org/10.1002/adhm.202304572.

122. M. Nasrollahzadeh, Z. Issaabadi, M. Sajjadi, S. M. Sajadi, and M. Atarod, "Types of Nanostructures", in *Interface Science and Technology*, 28, (Elsevier, 2019), pp. 29–80, https://doi.org/10.1016/B978-0-12-813586-0.00002-X.



23656549, 2026, 45, Downloaded from https://chemistry-europe.onlinelibrary.wiley.com/doi/10.1002/slct.75081 by Esma AHLATCIOLU ÖZEROL - Yildiz Technical University , Wiley Online Library on [25/11/2026]. See the Terms and Conditions (https://onlinelibrary.wiley.com/terms-and-conditions) on Wiley Online Library for rules of use; OA articles are governed by the applicable Creative Commons License

123. A. Kausar, "Potential of Polymer/Fullerene Nanocomposites for Anticorrosion Applications in the Biomedical Field," *Journal of Composite Science* 6, no. 12 (2022): 394, https://doi.org/10.3390/jcs6120394.

124. X. Chen, Y. Zhang, W. Yu, W. Zhang, H. Tang, and W. Yuan, "In Situ Forming ROS-Scavenging Hybrid Hydrogel Loaded With Polydopamine-Modified Fullerene Nanocomposites for Promoting Skin Wound Healing," *Journal of Nanobiotechnology* 21, no. 1 (2023): 129, https://doi.org/10.1186/s12951-023-01879-2.

125. Y. Pan, Y. Qi, C. Fei, et al., "Novel Sprayable Antioxidative Dressing Based on Fullerene and Curdlan for Accelerating Chronic Wound Healing," *Macromolecular Rapid Communications* 45, no. 17 (2024): 2400240, https://doi.org/10.1002/marc.202400240.

126. M. Godoy-Gallardo, U. Eckhard, L. M. Delgado, et al., "Antibacterial Approaches in Tissue Engineering Using Metal Ions and Nanoparticles: From Mechanisms to Applications," *Bioactive Materials* 6, no. 12 (2021): 4470–4490, https://doi.org/10.1016/j.bioactmat.2021.04.033.

127. A. Kwiatkowska, M. Drabik, A. Lipko, et al., "Composite Membrane Dressings System With Metallic Nanoparticles as an Antibacterial Factor in Wound Healing," *Membranes* 12, no. 2 (2022): 215, https://doi.org/10.3390/membranes12020215.

128. H. Dong, C. Feng, J. Zhu, et al., "Ultrasmall Gold Nanoparticles/Carboxymethyl Chitosan Composite Hydrogel: Tough, Restorable, Biocompatible Antimicrobial Dressing for Wound Healing," *Applied Materials Today* 38 (2024): 102206, https://doi.org/10.1016/j.apmt.2024.102206.

129. N. Rezaei Kolarijani, D. Cheraghali, H. Khastar, et al., "Nanofibrous Polycaprolactone/Gelatin Scaffold Containing Gold Nanoparticles: Physicochemical and Biological Characterization for Wound Healing," *Wound Repair and Regeneration* 31, no. 6 (2023): 804–815, https://doi.org/10.1111/wrr.13126.

130. M. M. Ghobashy, S. A. Alkhursani, H. A. Alqahtani, et al., "Gold Nanoparticles in Microelectronics Advancements and Biomedical Applications," *Materials Science and Engineering: B* 301 (2024): 117191.

131. M. I. Anik, N. Mahmud, A. Al Masud, and M. Hasan, "Gold Nanoparticles (GNPs) in Biomedical and Clinical Applications: A Review," *Nano Select* 3, no. 4 (2022): 792–828, https://doi.org/10.1002/nano.202100255.

132. M. Rybka, Ł. Mazurek, and M. Konop, "Beneficial Effect of Wound Dressings Containing Silver and Silver Nanoparticles in Wound Healing—From Experimental Studies to Clinical Practice," *Life* 13, no. 1 (2022): 69, https://doi.org/10.3390/life13010069.

133. A. Choudhary, S. Singh, and V. Ravichandiran, "Toxicity, Preparation Methods and Applications of Silver Nanoparticles: An Update," *Toxicology Mechanisms and Methods* 32, no. 9 (2022): 650–661, https://doi.org/10.1080/15376516.2022.2064257.

134. S. Sharma, A. Bose, S. Biswas, S. Sen, and I. Roy, "*Cyperus rotundus* Mediated Green Synthesis of Silver Nanoparticles for Antibacterial Wound Dressing Applications," *Scientific Reports* 15, no. 1 (2025): 18394, https://doi.org/10.1038/s41598-025-03555-x.

135. Q. Wei, Y. Pan, Z. Zhang, S. Yan, and Z. Li, "Copper-Based Nanomaterials for Biomedical Applications," *Chemistry– An Engineering Journal* 483 (2024): 149040, https://doi.org/10.1016/j.cej.2024.149040.

136. Y. Wang, W. Zhang, and Q. Yao, "Copper-based Biomaterials for Bone and Cartilage Tissue Engineering," *Journal of Orthop aedic Translation* 29 (2021): 60–71, https://doi.org/10.1016/j.jot.2021.03.003.

137. T. Cheng, Y. Xiang, X. He, et al., "Nanostructured Conductive Polymers: Synthesis and Application in Biomedicine," *Journal of Materials Chemistry B* 13, no. 16 (2025): 4739–4769, https://doi.org/10.1039/D4TB02513J.

138. J. Aboagye, M. Edwards, J. Ge, Y. Hong, and H. Yang, "Evaluating and Improving Biocompatibility of Conductive Polymers for Cardiac Tissue Engineering," *Journal ofMaterials Chemistry B* 14, no. 3 (2026): 775–798, https://doi.org/10.1039/D5TB01523E.

139. V. Agarwal and P. B. Zetterlund, "Strategies for Reduction of Graphene Oxide—A Comprehensive Review," *Chemistry– An Engineering Journal* 405 (2021): 127018, https://doi.org/10.1016/j.cej.2020.127018.

140. K. Staszak, M. Rzelewska-Piekut, and M. Regel-Rosocka, "Role of Noble and Rare Earth Metals in Bioactive Materials for Medical Applications in Tissue Engineering," *RSC Advances* 15, no. 48 (2025): 40709–40729, https://doi.org/10.1039/D5RA04036A.

141. S. Stoukatch, M. Debliquy, F. Dupont, and J. Redouté, "Low-Cost Optical pH Sensor With a Polyaniline (PANI)-Sensitive Layer Based on Commercial off-the-Shelf (COTS) Components," *Micromachines* 14, no. 12 (2023): 2197, https://doi.org/10.3390/mi14122197.

142. Y. Ma, T. Lei, X. Yang, et al., "Electrically Conductive Polypyrrole@Keratin Nanofiber Membranes With Potential for Tissue Restoration," *Fibers and Polymers* 25, no. 3 (2024): 751–763, https://doi.org/10.1007/s12221-023-00439-7.

143. D. Switha, S. K. Basha, and V. S. Kumari, "Fabrication of Conductive Hybrid Scaffold Based on Polyaniline/Polyvinyl Alcohol–Chitosan Nanoparticles for Skin Tissue Engineering Application," *Polymer Bulletin* 80, no. 10 (2023): 11439–11467, https://doi.org/10.1007/s00289-022-04616-1.

144. Y. Jiang, T. Liu, and Y. Zhou, "Recent Advances of Synthesis, Properties, Film Fabrication Methods, Modifications of Poly(3,4-ethylenedioxythiophene), and Applications in Solution-Processed Photovoltaics," *Advanced Functional Materials* 30, no. 51 (2020): 2006213, https://doi.org/10.1002/adfm.202006213.

145. G. Li and C. F. Ghuo, "PEDOT:PSS-Based Intrinsically Soft and Stretchable Bioelectronics," *Soft Sciences* 2, no. 2 (2022): 7, https://doi.org/10.20517/ss.2022.07.

146. M. A. Al Faruque, M. Syduzzaman, J. Sarkar, K. Bilisik, and M. Naebe, "A Review on the Production Methods and Applications of Graphene-Based Materials," *Nanomaterials* 11, no. 9 (2021): 2414, https://doi.org/10.3390/nano11092414.

147. U. R, A. KA, G. Munusamy-Ramanujam, and S. S, "Biological Applications of Graphene: Exploring the Role of Nonmetal Functionalization," *Total Chemistry* 1 (2025): 100007, https://doi.org/10.1016/j.totche.2025.100007.

148. N. M. Mubarak, E. C. Abdullah, N. S. Jayakumar, and J. N. Sahu, "An Overview on Methods for the Production of Carbon Nanotubes," *Journal of Industrial and Engineering Chemistry* 20, no. 4 (2014): 1186–1197, https://doi.org/10.1016/j.jiec.2013.09.001.

149. Y. Wang and G. J. Weng, "Electrical Conductivity of Carbon Nanotube- and Graphene-Based Nanocomposites," in *Micromechanics and Nanomechanics of Composite Solids*, eds. S. A. Meguid and G. J. Weng, (Springer International Publishing, 2018), 123–156, https://doi.org/10.1007/978-3-319-52794-9_4.

150. M. Aminul Islam, M. Hasan, M. Rahman, M. Hosne Mobarak, M. Akter Mimona, and N. Hossain, "Advances and Significances of Carbon Nanotube Applications: A Comprehensive Review," *European Polymer Journal* 220 (2024): 113443, https://doi.org/10.1016/j.eurpolymj.2024.113443.

151. H. Hassan, P. Sharma, M. R. Hasan, S. Singh, D. Thakur, and J. Narang, "Gold Nanomaterials—The Golden Approach From Synthesis to Applications," *Materials Sci ence Energy Technology* 5 (2022): 375–390, https://doi.org/10.1016/j.mset.2022.09.004.

152. M. Zahdeh and R. Karaman, "Gold Nanoparticles in Biomedical Applications: Synthesis, Functionalization, and Recent Advances," *Molecules* 31, no. 1 (2025): 17, https://doi.org/10.3390/molecules31010017.

153. H. Liu, L. Jin, S. Zhu, et al., "Interfacial Electronic Modulation on Polyaniline/Curcumin fiber for Photo-Powered Rapid Wound Healing," *Nano Today* 57 (2024): 102397, https://doi.org/10.1016/j.nantod.2024.102397.

154. S. Najafian, M. Eskandani, H. Derakhshankhah, M. Jaymand, and B. Massoumi, "Extracellular Matrix-Mimetic Electrically Conductive Nanofibrous Scaffolds Based on Polyaniline-Grafted Tragacanth Gum and Poly(vinyl alcohol) for Skin Tissue Engineering Application," *Interna-*



23656549, 2026, 45, Downloaded from https://chemistry-europe.onlinelibrary.wiley.com/doi/10.1002/slct.75081 by Esma AHLATCIOLU ÖZEROL - Yildiz Technical University , Wiley Online Library on [25/11/2026]. See the Terms and Conditions (https://onlinelibrary.wiley.com/terms-and-conditions) on Wiley Online Library for rules of use; OA articles are governed by the applicable Creative Commons License

*tional Journal of Biological Macromolecules* 249 (2023): 126041, https://doi.org/10.1016/j.ijbiomac.2023.126041.

155. Q. Pang, K. Wu, Z. Jiang, et al., "A Polyaniline Nanoparticles Crosslinked Hydrogel With Excellent Photothermal Antibacterial and Mechanical Properties for Wound Dressing," *Macromolecular Bioscience* 22, no. 3 (2022): 2100386, https://doi.org/10.1002/mabi.202100386.

156. M. Javid, M. Eskandani, M. Jaymand, and B. Massoumi, "Nanofibrous Electroconductive Scaffolds Composed of Poly(vinyl alcohol) and Modified Polyaniline for Skin Tissue Engineering Application," *Journal of Applied Polymer Science* 141, no. 34 (2024): 1–16, https://doi.org/10.1002/app.55871.

157. S. A. H. Shah, S. F. B. Farukh, H. S. U. B. Farukh, et al., "Nickel Selenide-Loaded PANI/PEO Fibers for Boosted Wound Healing Response in Rabbits," *Polymers for Advanced Technologies* 36, no. 3 (2025): 1–12, https://doi.org/10.1002/pat.70156.

158. Z. Akbari Kheirabadi, Z. Nazemi, M. Janmohammadi, F. Radmanesh, H. R. Moslemi, and M. S. Nourbakhsh, "Biocompatible and Antibacterial co-electrospun Tragacanth Gum and Polyaniline Nanofibers for Skin Tissue Engineering," *Scientific Reports* 15, no. 1 (2025): 38647, https://doi.org/10.1038/s41598-025-22553-7.

159. S. Wu, H. Lu, H. T. Nguyen, P. Lin, W. Pan, and A. E. Chuang, "Microwave-Orchestrated Phototherapeutic Polypyrrole/Soy Extraction Micro-Complex for Burn Wound Healing in a Rodent Model," *J Drug Deliv Sci Technol* 108 (2025): 106911, https://doi.org/10.1016/j.jddst.2025.106911.

160. Z. Chu, X. Liu, T. Zhao, et al., "Self-Healing Ppy-Hydrogel Promotes Diabetic Skin Wound Healing Through Enhanced Sterilization and Macrophage Orchestration Triggered by NIR," *Biomaterials* 315 (2025): 122964, https://doi.org/10.1016/j.biomaterials.2024.122964.

161. M. Zarei, A. Samimi, M. Khorram, M. M. Abdi, and S. I. Golestaneh, "Fabrication and Characterization of Conductive Polypyrrole/Chitosan/Collagen Electrospun Nanofiber Scaffold for Tissue Engineering Application," *International Journal of Biological Macromolecules* 168 (2021): 175–186, https://doi.org/10.1016/j.ijbiomac.2020.12.031.

162. H. Wang, "A capacitive polypyrrole-wrapped carbon cloth/bacterial cellulose antibacterial dressing with electrical stimulation for infected wound healing," .

163. K. Zhou, D. Chigan, L. Xu, et al., "Anti-Sandwich Structured Photo-Electronic Wound Dressing for Highly Efficient Bacterial Infection Therapy," *Small* 17, no. 33 (2021): 2101858–2101868, https://doi.org/10.1002/smll.202101858.

164. S. Najafian, M. Eskandani, H. Derakhshankhah, M. Jaymand, and B. Massoumi, "Biomimetic Electroactive Nanofibrous Hydrogel Scaffolds Based on Polythiophene-Grafted Tragacanth Gum and Poly(vinyl alcohol) for Skin Tissue Engineering Application," *Materials Today Communications* 37 (2023): 107532, https://doi.org/10.1016/j.mtcomm.2023.107532.

165. X. Chai, Y. Lou, L. Nie, et al., "A Three-dimensional Printable Conductive Composite Dressing for Accelerating Wound Healing Under Electrical Stimulation," *Colloids and Surfaces B: Biointerfaces* 245 (2025): 114264, https://doi.org/10.1016/j.colsurfb.2024.114264.

166. A. Lari, N. Sultana, and C. F. Soon, "Biocomposite conductive scaffold based on PEDOT:PSS/nHA/chitosan/PCL: Fabrication and characterization," 15, no. 2 (2019).

167. K. Hu, Z. Huang, Q. Tang, et al., "Green Tea Carbon Dots-Based Electrically Active Hydrogel Dressing for Promoting Wound Healing," *Advances in Therapy* 7, no. 8 (2024): 2400016, https://doi.org/10.1002/adtp.202400016.

168. J. Lee, H. Y. Ng, Y. Lin, et al., "The 3D Printed Conductive Grooved Topography Hydrogel Combined With Electrical Stimulation for Synergistically Enhancing Wound Healing of Dermal Fibroblast Cells," *Biomaterials Advances* 142 (2022): 213132, https://doi.org/10.1016/j.bioadv.2022.213132.

169. A. I. F. Alves, N. M. Alves, and J. R. Dias, "Electrospun PEDOT-Based Meshes for Skin Regeneration," *Polymers* 17, no. 16 (2025): 2227, https://doi.org/10.3390/polym17162227.

170. Y. Jiang, A. A. Trotsyuk, S. Niu, et al., "Wireless, Closed-loop, Smart Bandage With Integrated Sensors and Stimulators for Advanced Wound Care and Accelerated Healing," *Nature Biotechnology* 41, no. 5 (2023): 652–662, https://doi.org/10.1038/s41587-022-01528-3.

171. E. Shirzaei Sani, C. Xu, C. Wang, et al., "A Stretchable Wireless Wearable Bioelectronic System for Multiplexed Monitoring and Combination Treatment of Infected Chronic Wounds," *Science Advances* 9, no. 12 (2023): eadf7388, https://doi.org/10.1126/sciadv.adf7388.

172. X. Liu, F. Chen, Y. Zhang, et al., "Self-Healing Sodium Alginate-PEDOT:PSS Conductive Hydrogel for Accelerated Burn Wound Healing and Real-Time Monitoring," *Chemistry – An Engineering Journal* 522 (2025): 167411, https://doi.org/10.1016/j.cej.2025.167411.

173. K. Naik, S. Tripathi, R. Ranjan, et al., "Conductive Hybrid Hydrogel of Carbon Nanotubes-Protein-Cellulose: In Vivo Treatment of Diabetic Wound via Photothermal Therapy and Tracking Real-Time Wound Assessment via Photoacoustic Imaging," *ACS Applied Bio Materials* 8, no. 3 (2025): 2229–2241, https://doi.org/10.1021/acsabm.4c01755.

174. M. T. Elabbasy, F. A. Almarshadi, M. H. Alshammari, et al., "Antimony (III) Oxide and Calcium Phosphate Doped With Carbon Nanotubes in PVA/HA Matrix for Wound Dressing Applications," *Materials Chemistry and Physics* 341 (2025): 130933, https://doi.org/10.1016/j.matchemphys.2025.130933.

175. L. Sun, Y. Wang, L. Fan, and Y. Zhao, "Multifunctional Microneedle Patches With Aligned Carbon Nanotube Sheet Basement for Promoting Wound Healing," *Chemistry - An Engineering Journal* 457 (2023): 141206, https://doi.org/10.1016/j.cej.2022.141206.

176. C. Wu, B. Liu, Q. Wen, and Q. Zhai, "A Carbon Nanotube/Pyrrolidonecarboxylic Acid Zinc Sponge for Programmed Management of Diabetic Wounds: Hemostatic, Antibacterial, Anti-inflammatory, and Healing Properties," *Materials Today Bio* 32 (2025): 101769, https://doi.org/10.1016/j.mtbio.2025.101769.

177. Z. Liu, Z. Ma, N. Li, et al., "CS/Gel/MWCNTs Conductive Scaffolds Assisted by Electrical Stimulus for Skin Tissue Engineering," *Biotechnology and Bioengineering* 122, no. 8 (2025): 2259–2272, https://doi.org/10.1002/bit.29025.

178. S. D. Parikh, W. Wang, M. T. Nelson, C. E. W. Sulentic, and S. M. Mukhopadhyay, "Bioinspired Hierarchical Carbon Structures as Potential Scaffolds for Wound Healing and Tissue Regeneration Applications," *Nanomaterials* 13, no. 11 (2023): 1791, https://doi.org/10.3390/nano13111791.

179. W. Chen, Y. Wei, J. Chang, et al., "Electrostimulation Combined With Biodegradable Electroactive Oriented Nanofiber Polycaprolactone/Gelatin/Carbon Nanotube to Accelerate Wound Healing," *Materials Today Bio* 31 (2025): 101490, https://doi.org/10.1016/j.mtbio.2025.101490.

180. E. R. F. R. Ribeiro, L. B. Correa, E. Ricci-Junior, et al., "Chitosan-Graphene Quantum Dot Based Active Film as Smart Wound Dressing," *Journal of Drug Delivery Science & Technology* 80 (2023): 104093, https://doi.org/10.1016/j.jddst.2022.104093.

181. K. Shivam, A. Selvam, S. Sangam, et al., "Graphene Quantum Dots-hybrid Hydrogel as an Avant-Garde Biomimetic Scaffold for Diabetic Wound Healing," *Biomaterials Advances* 149 (2023): 213395, https://doi.org/10.1016/j.bioadv.2023.213395.

182. D. K. Shanmugam, Y. Madhavan, A. Manimaran, et al., "Efficacy of Graphene-Based Nanocomposite Gels as a Promising Wound Healing Biomaterial," *Gels* 9, no. 1 (2022): 22, https://doi.org/10.3390/gels9010022.

183. A. Sanmugam, L. K. Sellappan, A. Sridharan, et al., "Chitosan-Integrated Curcumin–Graphene Oxide/Copper Oxide Hybrid Nanocomposites for Antibacterial and Cytotoxicity Applications," *Antibiotics* 13, no. 7 (2024): 620, https://doi.org/10.3390/antibiotics13070620.

184. Y. Liu, Q. Zhang, N. Zhou, et al., "Study on a Novel Poly (vinyl alcohol)/Graphene Oxide-Citicoline Sodium-Lanthanum Wound Dressing: Biocompatibility, Bioactivity, Antimicrobial Activity, and Wound Healing Effect," *Chemistry- An Engineering Journal* 395 (2020): 125059, https://doi.org/10.1016/j.cej.2020.125059.



23656549, 2026, 45, Downloaded from https://chemistry-europe.onlinelibrary.wiley.com/doi/10.1002/slct.75081 by Esma AHLATCIOLU ÖZEROL - Yildiz Technical University , Wiley Online Library on [25/11/2026]. See the Terms and Conditions (https://onlinelibrary.wiley.com/terms-and-conditions) on Wiley Online Library for rules of use; OA articles are governed by the applicable Creative Commons License

185. M. Jafarkhani, Z. Salehi, Z. Bagheri, et al., "Graphene Functionalized Decellularized Scaffold Promotes Skin Cell Proliferation," *Canadian Journal of Chemical Engineering* 98, no. 1 (2020): 62–68, https://doi.org/10.1002/cjce.23588.

186. M. Pollini, M. Ruggeri, E. Bianchi, et al., "Smart Conductive Nanofibers Integrating Electrical Stimulation for Enhanced Fibroblast Alignment and Collagen Deposition in Chronic Wound Repair," *Results in Engineering* 29 (2026): 108824, https://doi.org/10.1016/j.rineng.2025.108824.

187. K. B. Narayanan, G. T. Park, and S. S. Han, "Electrospun Poly(vinyl alcohol)/Reduced Graphene Oxide Nanofibrous Scaffolds for Skin Tissue Engineering," *Colloids and Surfaces B: Biointerfaces* 191 (2020): 110994, https://doi.org/10.1016/j.colsurfb.2020.110994.

188. A. Sanmugam, L. K. Sellappan, R. Almeer, et al., "Facile Synthesis of Reduced Graphene Oxide-Zirconium Oxide/Zinc Oxide Nanocomposites for Effective Antimicrobial and Cytotoxic Applications," *Surfaces & Interfaces* 53 (2024): 105026, https://doi.org/10.1016/j.surfin.2024.105026.

189. L. K. Sellappan, S. Mishra, S. Sundaresan, T. Rathinavelan, and S. Majumdar, "Multifunctional NiO-Curcumin Nanocomposite-Loaded Chitosan-Alginate Scaffolds for Enhanced Bone Tissue Regeneration and Antibacterial Activity," *Journal of Drug Delivery Science & Technology* 110 (2025): 107114, https://doi.org/10.1016/j.jddst.2025.107114.

190. K. B. Narayanan, S. M. Choi, and S. S. Han, "Biofabrication of *Lysinibacillus sphaericus*-Reduced Graphene Oxide in Three-Dimensional Polyacrylamide/Carbon Nanocomposite Hydrogels for Skin Tissue Engineering," *Colloids and Surfaces B: Biointerfaces* 181 (2019): 539–548, https://doi.org/10.1016/j.colsurfb.2019.06.007.

191. J. Sun, W. Jia, H. Qi, et al., "An Antioxidative and Active Shrinkage Hydrogel Integratedly Promotes Re-Epithelization and Skin Constriction for Enhancing Wound Closure," *Advanced Materials* 36, no. 21 (2024): 2112440–21124455, https://doi.org/10.1002/adma.202312440.

192. X. Li, Y. Dong, Z. Guo, X. Huang, and X. Zhang, "Electrospun Nanofiber Membranes Based on Sodium Alginate and Multi-Ether Fullerene Derivative as Wound Dressings With the Antioxidant Property," *ACS Applied Polymer Materials* (2025): 8558–8569, https://doi.org/10.1021/acsapm.5c01098.

193. M. Shan, X. Chen, X. Zhang, et al., "Injectable Conductive Hydrogel With Self-Healing, Motion Monitoring, and Bacteria Theranostics for Bioelectronic Wound Dressing," *Advanced Healthcare Materials* 13, no. 11 (2024): 2303876, https://doi.org/10.1002/adhm.202303876.

194. A. Salama, N. Elsherbiny, H. F. Hetta, et al., "Curcumin-loaded Gold Nanoparticles With Enhanced Antibacterial Efficacy and Wound Healing Properties in Diabetic Rats," *International Journal of Pharmaceutics* 666 (2024): 124761, https://doi.org/10.1016/j.ijpharm.2024.124761.

195. J. Hong, J. Zhu, X. Cao, et al., "Photo-Triggered Multifunctional Gold-Based Hybrid Nanoflowers Promote Infectious Skin Regeneration," *Chemistry -An Engineering Journal* 482 (2024): 148937, https://doi.org/10.1016/j.cej.2024.148937.

196. N. Amiri, S. Ghaffari, I. Hassanpour, et al., "Antibacterial Thermosensitive Silver–Hydrogel Nanocomposite Improves Wound Healing," *Gels* 9, no. 7 (2023): 542, https://doi.org/10.3390/gels9070542.

197. L. Chen, W. Shi, T. Zhang, et al., "Synthesis of Silver Nanoparticles Using Lysozyme for Scald-Wound Healing," *ACS Applied Nano Materials* 6, no. 19 (2023): 17778–17791, https://doi.org/10.1021/acsanm.3c03009.

198. C. Wang, X. Jiang, H. Kim, et al., "Flexible Patch With Printable and Antibacterial Conductive Hydrogel Electrodes for Accelerated Wound Healing," *Biomaterials* 285 (2022): 121479, https://doi.org/10.1016/j.biomaterials.2022.121479.

199. M. Arumugam, B. Murugesan, P. Balasekar, et al., "Silk Fibroin and Gelatin Composite Nanofiber Combined With Silver and Gold Nanoparticles for Wound Healing Accelerated by Reducing the Inflammatory Response," *Process Biochemistry* 134 (2023): 1–16, https://doi.org/10.1016/j.procbio.2023.10.017.

200. A. Najafian-Najafabadi, M. Salehi, A. M. Amani, et al., "Biomimetic Skin Regeneration Using a Dual-Layer Scaffold/Hydrogel: Polycaprolactone-Gelatin Electrospun Scaffold Incorporated With Bromelain-Silver Nanoparticles and Alginate Hydrogel Enriched With Selenium-Doped Bioglass," *International Journal of Biological Macromolecules* 311 (2025): 143733, https://doi.org/10.1016/j.ijbiomac.2025.143733.

201. M. Ragothaman, A. Kannan Villalan, A. Dhanasekaran, and T. Palanisamy, "Bio-Hybrid Hydrogel Comprising Collagen-capped Silver Nanoparticles and Melatonin for Accelerated Tissue Regeneration in Skin Defects," *Materials Science & Engineering C* 128 (2021): 112328, https://doi.org/10.1016/j.msec.2021.112328.

202. C. M. Srivastava, R. Purwar, and A. P. Gupta, "Enhanced Potential of Biomimetic, Silver Nanoparticles Functionalized *Antheraea mylitta* (tasar) Silk Fibroin Nanofibrous Mats for Skin Tissue Engineering," *International Journal of Biological Macromolecules* 130 (2019): 437–453, https://doi.org/10.1016/j.ijbiomac.2018.12.255.

203. F. Afghah, M. Ullah, J. Seyyed Monfared Zanjani, et al., "3D printing of Silver-Doped Polycaprolactone-Poly(propylene succinate) Composite Scaffolds for Skin Tissue Engineering," *Biomedical Materials* 15, no. 3 (2020): 035015, https://doi.org/10.1088/1748-605X/ab7417.

204. S. Kumari, B. N. Singh, and P. Srivastava, "Effect of Copper Nanoparticles on Physico-Chemical Properties of Chitosan and Gelatin-Based Scaffold Developed for Skin Tissue Engineering Application," *BioTechniques* 9, no. 3 (2019): 1–14, https://doi.org/10.1007/s13205-019-1624-9.

205. D. Ghosh, S. Godeshala, R. Nitiyanandan, et al., "Copper-Eluting Fibers for Enhanced Tissue Sealing and Repair," *ACS Applied Materials & Interfaces* 12, no. 25 (2020): 27951–27960, https://doi.org/10.1021/acsami.0c04755.

206. Z. Xu, Y. Jin, C. Zhang, et al., "A Methacrylated Pullulan Hydrogel Incorporating Phycocyanin-Functionalized Copper Sulfide Nanoparticles for Photothermal Antibacterial Therapy and Improved Wound Healing," *International Journal of Biological Macromolecules* 315 (2025): 144446, https://doi.org/10.1016/j.ijbiomac.2025.144446.

207. S. Fan, Z. Fang, L. Zeng, et al., "SB216763-Loaded Multifunctional Copper-Doped Bioglass 3D Printed Scaffold Promotes Wound Healing and Functional Skin Regeneration," *Ceramics International* 49, no. 9 (2023): 13310–13320, https://doi.org/10.1016/j.ceramint.2022.12.090.



23656549, 2026, 45, Downloaded from https://chemistry-europe.onlinelibrary.wiley.com/doi/10.1002/slct.75081 by Esma AHLATCIOLU ÖZEROL - Yildiz Technical University , Wiley Online Library on [25/11/2026]. See the Terms and Conditions (https://onlinelibrary.wiley.com/terms-and-conditions) on Wiley Online Library for rules of use; OA articles are governed by the applicable Creative Commons License